# The Papers of Independent Authors

## Aviation and Cosmonautics
## Chemistry and Physics
## Physics and Astronomy

# The Papers of Independent Authors

## Volume 43

Israel
2018

ISBN 978-1-387-87164-3

9 781387 871643

90000

**Israel**
**2018**

**Truth - the daughter of time, instead of authority**

Frensis Bacon

Everyone has the right to freedom of opinion and expression; this right includes freedom to hold opinions without interference and to seek, receive and impart information and ideas through any media and regardless of frontiers.

United Nations OrganizationUniversal. Declaration of Human Rights. Article 19.

**From the Publisher**

"The Papers of Independent Authors" is a multidisciplinary scientific and technical printed journal in Russian and English. The journal accepts articles for publication from all countries. The following rules are observed:

- articles are not reviewed and the publisher is not responsible for the content and style of publications,
- the author pays for the publication,
- the journal is registered in the iInternational classifications of books (ISBN) and journals (ISSN), identified by the DOI code, transmitted and registered in the national libraries of Russia, Israel, the United States. This ensures the priority and copyrights of the author of the article.
- the commercial rights of the author of the article are reserved for the author,
- the magazine is published in the USA,
- printed magazine is sold, and in electronic form is distributed free of charge.

This magazine is for those authors who are self-confident and do not need approval of the reviewer. We are often reproached for not reviewing the articles. But the review institute is not an ideal filter - misses the failed articles and delays original works. Without analyzing the numerous reasons for this, we only note that if readers can filter out bad articles, then outstanding ideas may remain unknown. Therefore, we - for the fact that scientists and engineers had the right (like writers and artists) to publish without reviewing and not spend years on "punching" their ideas.

*Solomon I. Khmelnik.*

# Contents

## Aviation and Cosmonautics \ 5

## Chemistry and Physics \ 19

## Physics and Astronomy \ 93

## Authors \ 185

# Series: AVIATION and COSMONAUTICS

**Triger V., Khmelnik S., Leshinsky-Altshuller A, Sherbaum V.**

# A Method and System for Braking of Flying Objects

## Abstract

A patent presentation is proposed, details of which are given in Appendix 1. The basis of the device is a stub (made in the form of a cable with a metal sheath), released at the time of braking. The stub develops the force of aerodynamic drag in dense layers of the atmosphere. This force is created due to the interaction of atmospheric ions with a charged stub. The strength of this interaction is regulated in depending on the speed of the satellite and the altitude of the flight. Thus, this alows maintaining the permissible overload from impact when entering the dense layers of the atmosphere. The design is such that the kinetic energy of the satellite is converted into the kinetic energy of the interaction of atmospheric ions with a charged stub. In addition, a description of a ground-based experiment that can prove the existence of the physical effect on which the invention is based is described. The authors of the patent invite firms with the appropriate capabilities to participate in this experiment for a certain share of patent rights.

## Contents

# 1. Introduction

The following is a brief description of the patent. The requisites of the patent are indicated in Appendix 1

The present invention relates in general, to the field of aviation and in particular, to a method and system that supports air vehicle braking for supporting safe landing. In addition, a description of a ground-based experiment that can prove the existence of the physical effect on which the invention is based is described.

# 2. Composition of the project

As such, it is proposed
- patented device,
- physico-mathematical justification of its efficiency,
- programs for calculating various device options,
- programs for calculating the trajectories of the aircraft during the braking process.

# 3. Main advantages:

- A significant reduction in the mass of the satellite due to:
  - reduction of thermal protection weight.,
  - a significant fuel reduction for the brake jet engines,
- Safety:
  - Entrance to the dense layers of the atmosphere without creation of a shock wave.
  - Without additional heating of the satellite
  - Without loss of communication
  - Overload does not exceed 5G, where G = 9.81 m/s². This is relevant for private future flights.
  - As a consequence, probability of a destruction during landing is negligible and
    - the experimental results on the satellite are preserved,
    - crew's health is preserved.

## 4. Some economic assessments

For reusable space vehicles, the application of the proposed system can significantly reduce the amount of fuel for the operation of brake motors. This means that the payload mass increases. On average, it can be assumed that the payload mass increases by 35% (see, for example, Elon Musk, Max performance numbers are for expendable launches. Subtract 30% to 40% for reusable booster payload, [2]). Thus, an increase in the payload by 10% due to the installation of the proposed system allows to increase the total payload by 35%. It can be assumed that **the installation of the proposed system allows increasing the payload by 25%**. The cost of sending a payload into space is currently estimated at $ 50,000-80,000 per 1kg (according to to [3]).

## 5. Operating principle

The method based on THE GENERATION OF combined Electrodynamics and Aerodynamic braking forces BY THE SAME STRUCTURE (STUB).

The basis of the device is a stub released at the time of braking. The stub develops
- the force of electrodynamics inhibition in a rarefied atmosphere,
- the force of aerodynamic drag in dense layers of the atmosphere

Electrodynamics braking force is created due to the interaction of atmospheric ions with a charged stub. The strength of this interaction is regulated by the special design of stub (see Appendix 2), depending on the speed of the satellite and the altitude of the flight. Thus maintaining the permissible overload from impact when entering the dense layers of the atmosphere. The design is such that the kinetic energy of the satellite is converted into the kinetic energy of the interaction of atmospheric ions with a charged stub.

Electrodynamics braking force is generated by interaction between stub charges and atmospheric charges due to the kinetic energy of the satellite – see Appendix 3.

### 6. Method and program of calculation

Essentially, an integral part of the invention is the method and program of calculation

- the forces of electromagnetic braking necessary to keep the acceleration within the given limits at a known speed (in magnitude and direction) and the altitude of the satellite,
- the value of the capacitor charging current, depending on the known electromagnetic braking force.

An example of the result of such a calculation is given in Appendix 4.

# 7. Composition of the device

The device contains:

- o Brake stub – see Appendices 2 and 3,
- o Battery,
- o Source of constant high voltage (by about 1,000 V),
- o Control unit.

The total weight of the device is not more than 5% of the weight of light satellites and decreases with an increase in the weight of the satellite.

For example, Appendix 4 shows the calculation for a satellite weighing 5 kg. In this case the braking device must have the following mass of elements:

Braking stub ≈ 0.15kg,

Battery ≈ 0.05 kg,

High voltage converter ≈0.05kg.

Thus, total weight of the device is equal approximately 5% of the satellite weight

# 8. Control

To control the device, height and speed meters must be installed. Based on these measurements, the control unit calculates the charging current of the stub, on which the electrodynamic braking force depends. This supports the permissible overload and hit when entering the dense layers of the atmosphere. Appendix 4 shows the trajectory of a certain satellite, obtained with a certain control of the braking device.

# 9. Proof of operability and conclusion

The physical effect underlying the invention was found theoretically and substantiated mathematically. However, an undeniable proof can only be an experiment. The experiment in space is very expensive and it can stop a potential investor. Howerer, it is possible to offer an **inexpensive ground-based experiment** that proves the existence of this effect. Such an experiment can be performed

**independently of the authors of the patent**. This experiment is described in Appendix 5.

The authors of the patent invite firms with the appropriate capabilities to participate in this experiment for a certain share of patent rights.

# References

1. A.A. Eichenwald. Electricity, M.L. 1933, paragraph 282,
   http://books.e-heritage.ru/book/10074637
2. Elon Musk,
   https://twitter.com/elonmusk/status/726559990480150528
3. SpacePharma, www.space4p.com.
4. S.I. Khmelnik, 2013. A capacitor engine for an aircraft, Israel patent application number 200435, 2013.
5. S.I. Khmelnik. 2017. Inconsistency solution of Maxwell's equations. Publishing "MiC", Israel, Printed in USA, Lulu Inc., ID 19043222. pp190. ISBN 978-1-365-23941-0, 2017.

# Appendix 1. The requisites of the patent.
A METHOD AND SYSTEM FOR BRAKING OF FLYING OBJECTS

**PCT/IL2017/050671**
**PATENT PENDING**

*Receiving Office:*                    Israel Patent Office
*International Filing Date:*           18/06/2017
*International Searching Athourity:*   Israel Patent Office
*ISA Received Date:*                   05/07/2017
*Sent to IB:*                          25/06/2017
**ISRAEL PATENT**
*Israel Received Date:*                19/07/2017
*Applicantes*
    TRIGER Vitaly                      Israel, Ashdod
    LESHINSKY-ALTSHULLER Anya          Israel, Kiriat Byalik
    KHMELNIK Solomon                   Israel, Bene-Ayish
*Agent*
    ROSENTHAL Ytzhak                   Israel, 21, Hapninim, St
                                       Yaud-Monoson, 6019000

# Appendix 2. Dielectric stub.

Dielectric stub negatively charged is attached to the satellite. It receives its charge from an electric generator installed on the satellite. The stub during the flight stretches and flies with great speed after the satellite. The stub is a flat wire with a metal coating and high-voltage insulation, coiled - see details in Appendix 3. The stub is connected to an internal high-voltage generator - see Fig. 1, where

                    S - Shell of the satellite,
                    G – Generator,
                    L - Stub (material – dielectric),
                    W –Wire (material – metal),
                    **M – Metal coating,**
                    e - Electrons on the stub surface,
                    p – Positive ions.
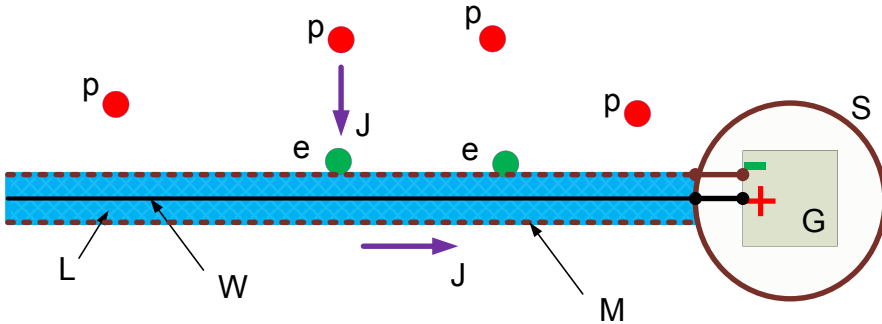
Fig. 1. The stub is connection to the generator.

**Let us consider in more detail the principle of electromagnetic braking**

The stub is a long condenser moving at high speed. The stub is a long condenser moving at high speed. The existence of moving electric charges can create a convection electric current. This current was shown was shown at the beginning of the last century by Eichenwald [1]. In [5] other applications of this effect were found. The electric current creates a magnetic field around the stub. Negative charges on the surface of the stub create a negative electric field in the vicinity of the stub. This field repels negative ions and attracts positive ions. Falling from all sides on the stub positive ions create an electric current directed to stub. This current interacts with the magnetic field of stub directed perpendicular to this current (around stub). The current of the ions is shifted by the Ampere force that arises with this (as in a DC motor). The ions move as move of stube. The energy of this motion is the kinetic energy of stub.

Spending energy on the motion of ions, the stub along with the satellite loses kinetic energy, i.e. is inhibited. Calculations show that the braking force is proportional to the speed of the satellite plume.

Positive ions, incident on the capacitor, discharge it. The constant high voltage generator set on the satellite generates the capacitor charge current. Thus, the force of electromagnetic braking depends on the current of the recharging.

Note that another method of slow decline of satellite can be implemented on the basis of a patent [4].

## Appendix 3. The stub is aerodynamic brake.

Figure 2 shows the stub as an aerodynamic brake. Figure 2a shows the stub in assembled form and figure 2b shows the stub in the half-opened form. The form of a fully-opened spiral for the stub is shown in figure 2c.
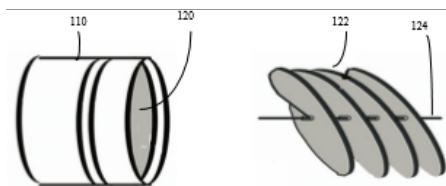


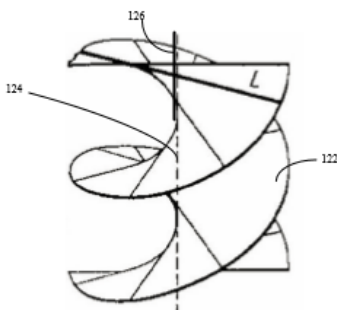FIG 1a                    FIG 1b



FIG 1c

## Appendix 4. Flight trajectories

For illustration, the results of calculating the trajectory for a satellite with the following characteristics are shown here:

- mass – 5 kg,
- initial velocity – 8,000 m\sec,
- initial altitude – 500 km.

The following trajectory characteristics are obtained:

  • deceleration <50 m\s,
  • landing velocity < 5 m\s,
  • speed of entry into the dense layers of the
       atmosphere <160 m\s at an altitude of
       ≈100 km

The following notations are used:

  V(t) is the absolute total velocity,
  W(t) is the vertical velocity (dotted line),
  a(t) is the absolute acceleration,
  F(t)  is the total force,
  Fad(t) is the aerodynamic force
  H(t) is the height,
  L(t) is the distance.

In **Fig. 1** shows the entire trajectory of *H(L)*.
In **Fig. 2** shows the initial segment of the trajectory (first 2000 sec),
  in the upper right window 2 are shown V (t), W (t) (dotted line),
  in the right lower window 4  a (t) is shown,
  in the upper left window 1 are  shown F (t), Fad (t) (dotted line),
  in the lower left window 3 are shown H (t), L (t) (dashed).
In **Fig. 3** shows the final segment of the trajectory (from 2,000 seconds
to 12,000 sec)
  in the left window 1 are shown V (t), W (t) (dotted line),
  in the left window 2, H (t) is shown,
  in the left window 3 are shown F (t), Fad (t) - (dotted line),
  in the right window the trajectory H (L) is shown.
In **Fig. 4** shows the last section of the trajectory (last 400 seconds),
  in the left window 1 are shown V (t), W (t) (dotted line),
  in the left window 2, H (t) is shown,
  in the left window 3 are shown F (t), Fad (t) (dotted line),
  in the right window the trajectory H (L) is shown.
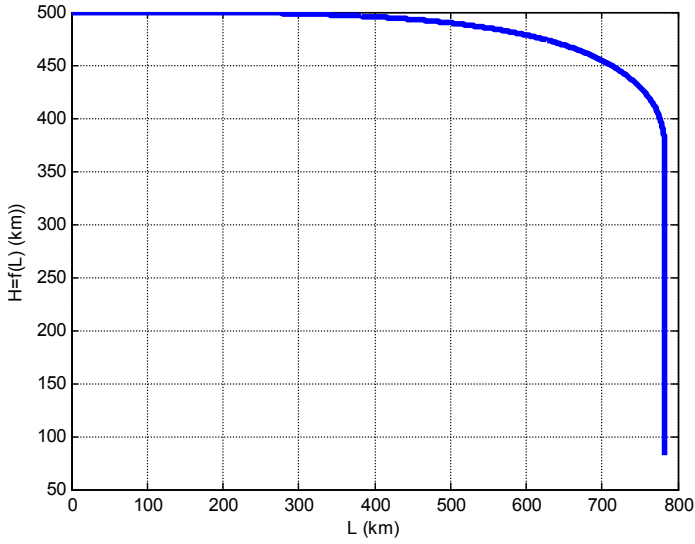
Figure 1
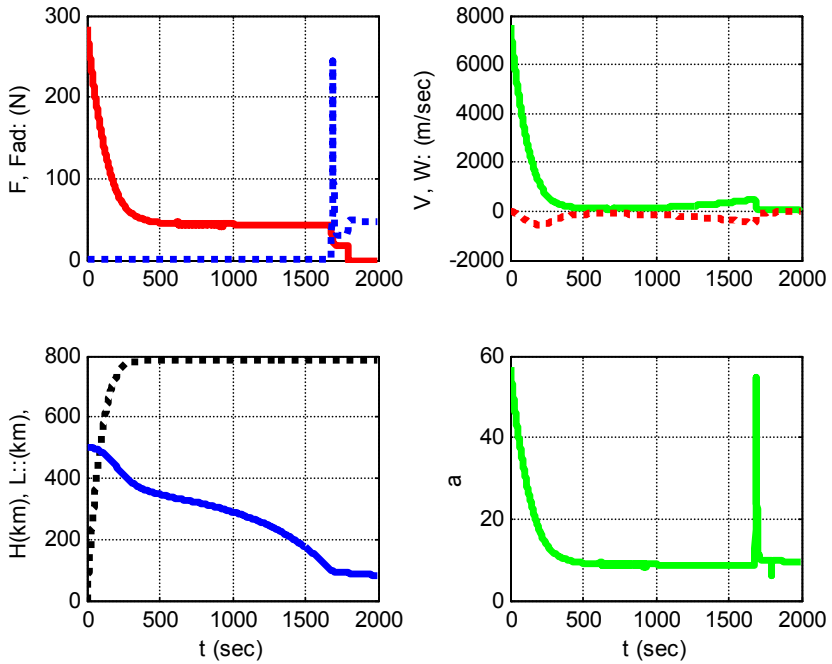


Figure 2
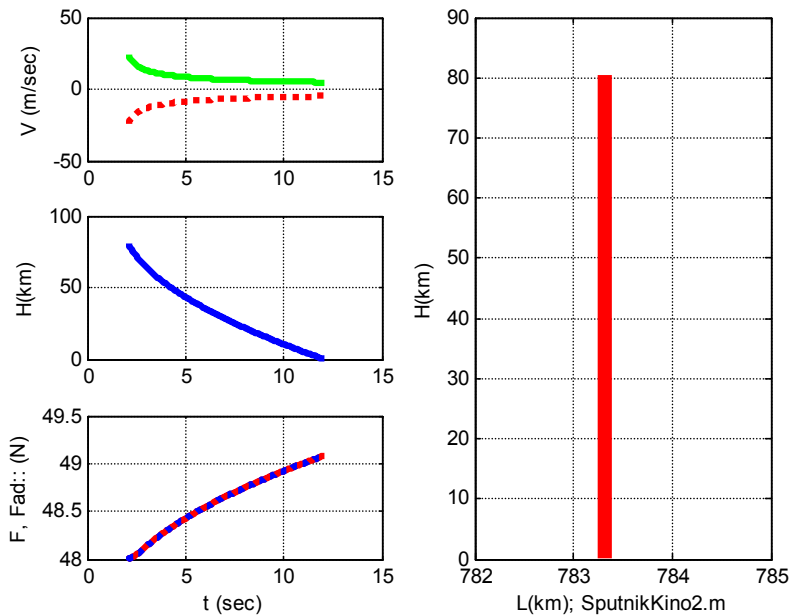
Figure 3
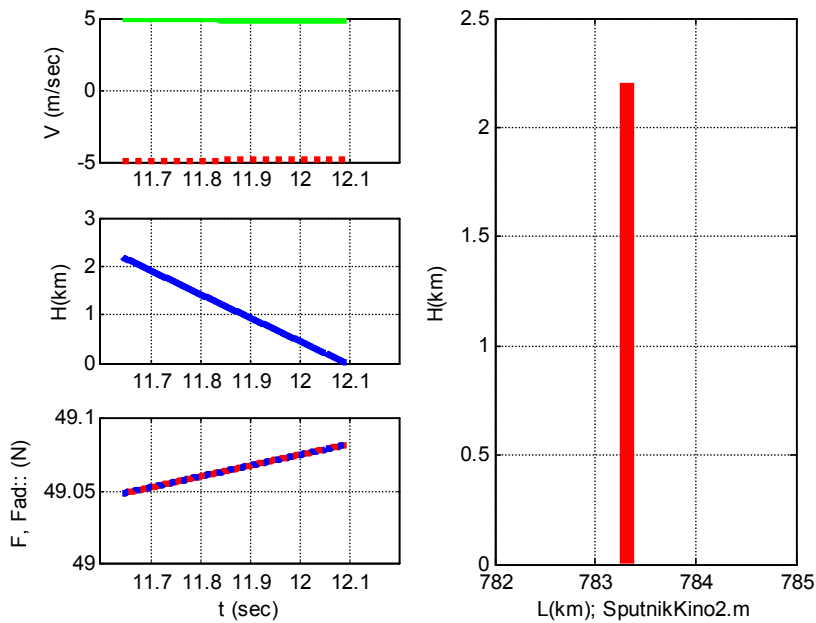


Figure 4

# Appendix 5. Ionic brake

## Content
1. Description of the physical effect.
2. Experiment.
3. Conditions of the experiment.
4. Required measurements and range of parameters.

## 1. Description of the physical effect

Let's consider the scheme which is shown in Fig. 1, where the wire 1, covered with insulation 2, and the insulation is covered with a metal sheath 3. A current 'J' flows along the wire 1, and a constant voltage 'U' is between the wire 1 and the sheath 3. Thus, the wire 1, the insulation 2, and the sheath 3 form a capacitor.
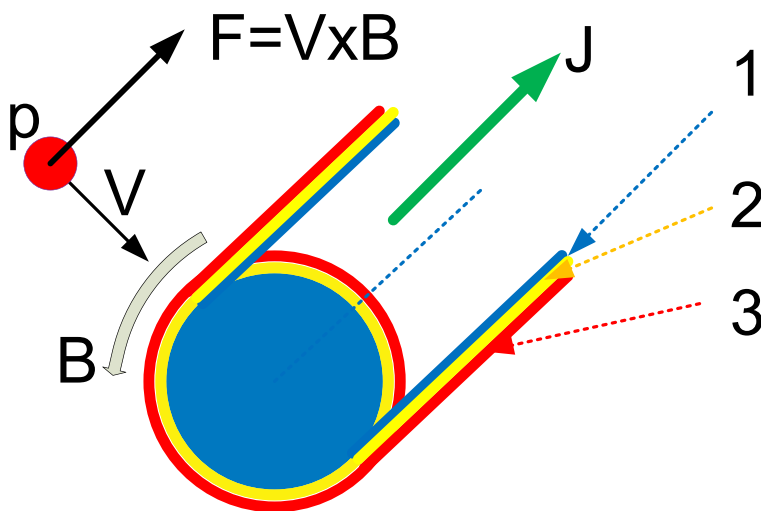


Fig. 1. Schematic of a device.

Let's assume that the negative charges (electrons) are on the sheath 3 of this capacitor, and the wire as a whole is in a cloud of positive ions 'p'. Then the ions will be attracted to the negatively charged sheath and move perpendicular to the wire axis with a certain (not constant) velocity 'V'. Around the wire with a current 'J' there is a magnetic field in which the induction vector 'B' is tangential to the wire circumference. Consequently, the ion 'p' is acted upon by the Lorentz force

$$F = V \times B .$$                                    (1)

The force 'F' is directed towards the current 'J', i.e. <u>the current 'J' by the Lorentz force 'F' pulls the ion 'p' in the direction of motion of current 'J'</u>. In other words, a pulse is applied to the ion 'p' on the side of the wire with current J'. This impulse is directed towards the current 'J'. According to the law of conservation of momentum, from the side of the ion 'p' at the wire acts the same impulse directed towards the current 'J'. If the wire is not fixed, then it will start moving towards the current J.

This effect can be called as **an ion brake**.

## 2. Experiment

Now we consider an experiment to check the existence of this effect and its quantitative estimation. Scheme of the experiment is shown in Figure 2.
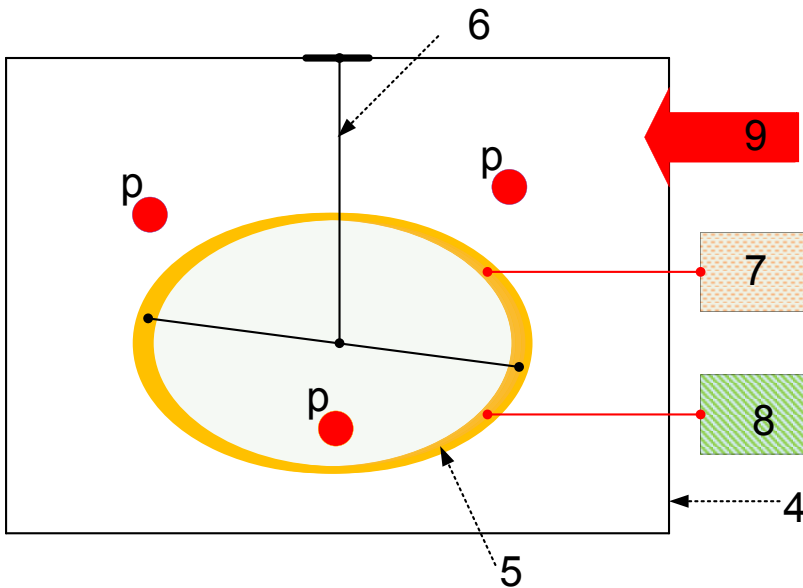


Fig. 2. Scheme of a proposed test rig.

Here:

4 - a vacuum chamber,
5 - folded by a ring wire,
6 – a torsion balance on which the wire 5 hangs,
7 - current source 'J',
8 - voltage source 'U'
9 - injector of positive ions 'p'.

Measuring instruments of current, voltage, pressure, ion density, and torque must also be provided. The design of the wire and its connection to the current and the voltage sources are shown in Figure 3**.**
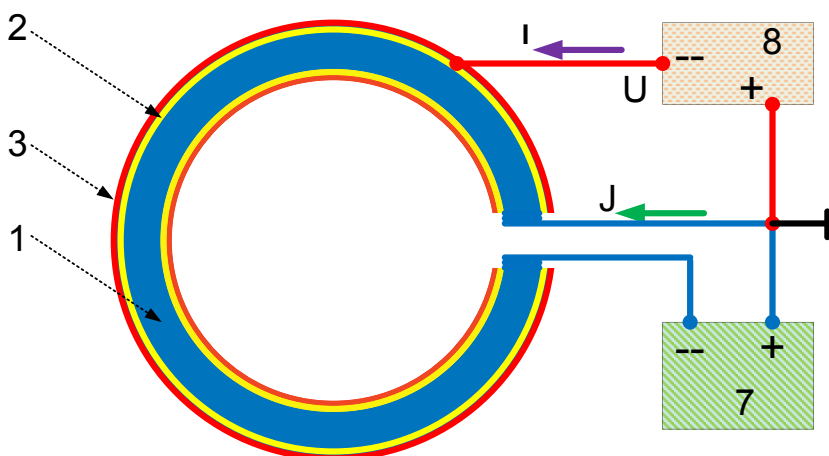
Fig. 3. Wire design.

It follows from a section 1 that the ring of wire 5 must turn under these conditions. This effect must be fixed by the torsion balance 6.

## 3. Conditions of the experiment.

The following conditions should be carried out:

1. Pressure in the vacuum chamber $P \approx 2 \cdot 10^{-9}$ N/m$^2$
2. Strength of current J=200 A
3. The density of ions $\eta \approx 10^{11}/m^3$. The density should be kept constant as the ions are neutralized when they come into contact with the sheath.
4. Surface charge density on the sheath $Q = 5 \cdot 10^{-4} C/m^2$
5. First, the high-voltage source should charge the capacitor to the specified density $Q$, and then to add the charge value till initial value as it will decreases due to the discharge by the current of the ions. This process is observed as the capacitor charge current $I$ - see Figure 3.

## 4. Required measurements and range of parameters.

It should be possible to change the values of x={D, J, $\eta$, Q} within the range

$$x = (0.1 \div 3) \cdot x_o.$$  (2)

where $x_o$ relates to the initial conditions specified above.

It is necessary to receive the following measurements values
- **force 'F'** acting on the wire - by the torsion balance
- **charging current 'I'** from the voltage source U as functions of the parameters (2).

# Series: Chemistry and Physics

**Shatov V.V.**

# Elementary electric charge, ions with multiple charges, atomic spectroscopy and atomic model

The full versions of V.V. Shatov's papers in Russian are published in the DNA journal (dna.izdatelstwo.com) and on the website (shatov.org).

The role of non-atomic ("unquantized") factors in atomic processes and effects is shown in the digest.

The investigation proposed consists of two series which are related to the following topics:

### 1 – Elementary electric charge

Part A: Elementary electric charge, Millikan's experiments and the nature of ions with multiple charges [A0].

Part B: About the discreteness of electric charges in Chemistry [B0].

Part C: The role of cluster fragmentation in the mass-spectrometry of ions with multiple charges [C0].

### 2 – Atomic spectroscopy

Part D: Clusters in radiation sources. Part I. Traditional excitation sources of optical atomic spectrum: flame, electric arc, spark, plasma, laser [D0].

Part E: Clusters in radiation sources. Part II. Atomic and ionic beams, ionic traps, beam-foil spectroscopy [E0].

Part F: Atomic spectroscopy of plasma which is in a magnetic field. Causal relationship between Doppler's and Zeeman's effects [F0].

Part G: The interpretation of the Moseley's law and atomic model. "Cluster quantization" in atomic spectroscopy [G0].

References to the full versions of the papers under consideration published in Russian are marked with the proper letter with null [A0...G0]. Each part of the digest has its own numeration of parts and references which corresponds with the numeration given in Russian papers.

# References

[A0] V.V. Shatov, Elementary charge, Millikan's experiments and the nature of ions with multiple charges, The Papers of independent Authors, «DNA», printed in USA, ISSN 2225-6717, Lulu Inc., ID № 15080253, Russia-Israel, 2014, issue 30, pp.175 – 199, ISBN: ISBN: 978-1-312-39693-7. 43 references; 26 in English. Online at (accessed May 9, 2018): http://izdatelstwo.com/clicks/clicks.php?uri=dna.izdatelstwo.com/volum/15080253.pdf; http://www.shatov.org/articles/Elementary%20electric%20charge%20&%20the%20nature%20of%20multiply%20charged%20ions.docx

[B0] V.V. Shatov, About the discreteness of electric charges in Chemistry, The Papers of independent Authors, «DNA», printed in USA, ISSN 2225-6717, Lulu Inc., ID № 14407999, Russia-Israel, 2014, issue 25, pp.188 – 211, ISBN: 978-1-304-86256-3. 16 references; 0 in English. Online at (accessed May 9, 2018): http://izdatelstwo.com/clicks/clicks.php?uri=dna.izdatelstwo.com/volum/14407999.pdf; http://shatov.org/articles/O_Diskretnosti_EL_Zarjada_v_Himii.docx

[C0] V.V. Shatov, The role of cluster fragmentation in the mass-spectrometry of ions with multiple charges, The Papers of independent Authors, «DNA», printed in USA, ISSN 2225-6717, Lulu Inc., ID № 14407999, Russia-Israel, 2014, issue 25, pp.134 – 187, ISBN: 978-1-304-86256-3. 168 references; 111 in English. Online at (accessed May 9, 2018): http://izdatelstwo.com/clicks/clicks.php?uri=dna.izdatelstwo.com/volum/14407999.pdf; http://shatov.org/articles/Clusters_v_MS_MZI_.doc

[D0] V.V. Shatov, Clusters in radiation sources. Part I. Traditional excitation sources of visible atomic spectrum: flame, electric arc, spark, plasma, laser. The Papers of independent Authors, «DNA», printed in USA, ISSN 2225-6717, Lulu Inc., ID № 14407999, Russia-Israel, 2014, issue 25, pp. 84 – 110, ISBN: 978-1-304-86256-3. 52 references; 14 in English. Online at (accessed May 9, 2018): http://izdatelstwo.com/clicks/clicks.php?uri=dna.izdatelstwo.com/volum/14407999.pdf; http://shatov.org/articles/Clusters_&_Spectry_Part%20I_.docx

[E0] V.V. Shatov, Clusters in radiation sources. Part II. Atomic and ionic beams, ionic traps, beam-foil-spectroscopy, The Papers of

independent Authors, «DNA», printed in USA, ISSN 2225-6717, Lulu Inc., ID № 14407999, Russia-Israel, 2014, issue 25, pp.111 – 133, ISBN: 978-1-304-86256-3. 88 references; 47 in English. Online at (accessed May 9, 2018): http://izdatelstwo.com/clicks/clicks.php?uri=dna.izdatelstwo.com/volum/14407999.pdf; http://shatov.org/articles/Clusters_&_Spectry_Part%20II_Beams_.docx

[F0] V.V. Shatov, Atomic spectroscopy of plasma which is in a magnetic field. Causal relationship between Doppler's and Zeeman's effects, The Papers of independent Authors, «DNA», printed in USA, ISSN 2225-6717, Lulu Inc., ID № 14407999, Russia-Israel, 2016, issue 35, pp.125 – 190, ISBN: 978-1-329-86675-1. 107 of references; 58 in English. Online at (accessed May 9, 2018): http://izdatelstwo.com/clicks/clicks.php?uri=dna.izdatelstwo.com/volum/18374540.pdf; http://www.shatov.org/articles/Spectroscopy_plasma_in_magnetic%20field_Eff_Zeeman_=_Doppler%E2%80%99s%20eff.docx

[G0] V.V. Shatov, The interpretation of the Moseley's law and atomic model. "Cluster quantization" in atomic spectroscopy, The Papers of independent Authors, «DNA», printed in USA, ISSN 2225-6717, Lulu Inc., ID № 14407999, Russia-Israel, 2017, issue 40, pp.204 – 227, ISBN 978-1-387-00793-6. 34 references; 8 in English. Online at (accessed May 9, 2018): http://izdatelstwo.com/clicks/clicks.php?uri=dna.izdatelstwo.com/volum/21006645.pdf; http://shatov.org/articles/St_zakon_Mozli_.doc

# A: The elementary electric charge, Millikan's experiments and the nature of ions with multiple charges

The paper considers criticism of classical Millikan's experiments in measuring the elementary electric chargein oil droplets. The discreteness of the electric charge in the field of Chemistry is discussed.

The hypothesis concerning the nature of ions with multiple charges is formulated and methods of its confirmation are suggested. The given description of mass-spectrometry experiment allows one to validate the present atomic model.

## 1. Introduction

The methods which are used to determine the elementary electric charge (EC) can be divided into two groups. The first group studies the behavior of free electrons under electric and magnetic fields. The second one is applied to electrons bound in atomic shells. These methods are based on the atomic model (MA) as well as the theory of atomic spectrum and use the emission of light by the electrons or an interaction between the electrons and light.

The EC was directly measured only in the classical Millikan's experiment with oil droplets [4 – 6] and its further modifications. Therefore, the special attention is devoted here to this experiment. The Millikan's experiments were based on the results of Faraday [4, p. 21], because the concept of discreteness of electricity stems from electrochemical experiments.

This concept was introduced to science basing on the number of elementary electric charges which were transported by ions in electrolytes. Electric forces were involved to explain chemical interactions and elementary electric charged particles were included into the MA.

This work is the continuation of the research which was started in [B0]. Here the methods for validating the hypothesis of the ions with multiple charges (IMC) are proposed. The presence of the IMC in plasma, according to the MA, is a strong evidence of both the EC and the relevance of the MA.

## 2.1 The discrete electric charge in Chemistry

Chemical particles possessing elementary electric charges are represented by ions and electrons. Terms "oxidation state" (an arbitrary electrostatic charge of the atom) and "effective charge" of the atom are also used.

Careful analysis of validity of using charge numbers and numbers of transmitted electrons in chemical equations and formulae shows that the discreteness of electric charges does not follow from electrochemical experiments and the laws of electrolysis [B0]. This conclusion is based on the following facts.

The oxidation state is a formal characteristic that refers to the reaction stoichiometry (its value can be non-integer) rather than to the charge numbers of ions or single-piece electrons taking part in the reaction.

Coefficients in chemical equations, electrochemistry (and in the Faraday's laws) which are assigned to the elementary electric charges, are defined by stoichiometry compositions of reagents and products.

Equivalents (including those in laws of electrolysis) are defined without taking into account the elementary electric charges from the stoichiometric numbers of reaction components basing on the law of multiple proportions. The chemical composition of a compound can be experimentally determined; it does not depend on the interpretation of a nature of chemical forces (unlike the number of transmitted electrons).

Effective atomic charges in molecules and crystals cannot be multiple by the EC and their values are rarely higher than two.

In the modern description of a chemical bond one uses not single-piece electrons but the probability of electrons to possess proper coordinates.

The equilibrium electrochemistry can do without consideration of charged particles, ions [9].

The laws of electrolysis do not prove the discreteness of electricity. Spontaneous chemical reactions taking place in a Galvanic elementproduce electric energy, whereas in a electrolyzer the "forced" processes can occur only when one uses the externalenergy sources.

It is postulated that during electrolysis electrodes are charging in the external circuit without electric current flowing through the electrolyte. The current intensity that flows from the electric source to the electrodes of the electrolyzer to make the voltage constant is determined by therate of the reaction on the electrodes: increasing the quantity of reagents leads to increasing capacity in the electrolyzer. The explicit relation between the potential difference $U$ and the rate of the electrode process in kinetics allow one to conclude that whenever the potential value differs from its equilibrium value, the electrode process proceeds. It is no matter what causes this process.

When the diffusion part of the electrochemical reaction starts, the further shift of the potential does not increase the reaction rate: limiting current is reached when diffusion does not have enough time to provide an electrode with a reagent. The rate of the electrode process is easily expressed through the current density because the latest can be experimentally measured. At any polarization the real diffusion rate is equal to the rate of the real electrode reaction; the current density in a diffusion region is defined by the quantity of reagents and products which are proceeded to the unit of electrode's surface per unit time.

Because the electrode process is a chemical reaction, one uses common equations of chemical kinetics to quantitatively characterize the

dependencies between the shifts of the potential from its equilibrium value and the rate of the reaction expressed through the current density. The reaction rate is expressed through the activity of the reacting ions, activation energy and temperature. The shift of the potential from its equilibrium value determines the reaction rate and effects on the activation energy value. This fact makes electrode reactions different from the common chemical processes [10].

Electric current flows as a result of chemical reactions. Consequently, electricity which is supplied to the electrodes of the electrolyzer to make voltage constant, is defined by a quantity of reagents which have reacted during electrolysis, not conversely.

## 2.2 About the discreteness of the ionic charges in electrolytes [B0]

An assumption that the Faraday's laws as well as the hypothesis about the existence of atoms lead to the conclusion that electricity should consist of discrete elementary electric charges. It was Stoney and Helmholtz who claimed it for the first time (in a speech devoted to Faraday, on 5th April, 1881). Let us analyze the proof of the existence of electric discreteness which was given by Helmholtz and others dividing this proof into theses [11, p. 11].

Thesis "A": "It follows from the laws of electrolysis that if the same quantity of electricity proceeds through the different electrolytes than the quantity of compounds which would be obtained in the solutions of monovalent ions will be proportional to the atomic masses of ions. If the quantity of electricity is equal to one that allows to obtain 1 gram-atom of ions than it will allow to obtain one gram-atom of ions in any electrolyte containing monovalent ions".

Thesis "B": "Electric current in electrolyte is caused by the ions' motion, so one gram-atom of monovalent ions containing the Avogadro number of particles: $N_{Av} = 6.02 \cdot 10^{23}$ always produces the quantity of electricity $F = 96485.31$ C. The whole electric charge should be uniformly distributed on all particles and the charge that is transferred by one ion will be $F/N_{Av} = e^-$, for divalent ion the charge will be $2e^- = 2F/N_{Av}$, *for z-valent ion it will be $z \cdot e^- = z \cdot F/N_{Av}$. I.e., different ions can possess charges which are divisible by $e^-$* ($1e^-$, $2e^-$, ..., $ze^-$)".

We begin the analysis of the thesis A citing the fact that "The quantity of compounds which is obtained in solutions of monovalent ions is proportional to atomic masses of these ions" when the same quantity $n$ of atoms or molecules acts in different chemical reactions because the mass of any product is *$m = n \cdot M$, where M is a molecular mass of*

*the obtained compound. The quantity of electricity which is equal to the Faraday's number strictly depends on $N_{Av}$ particles involved in a chemical reaction, so masses of obtained compounds are proportional to both the charge numbers of ions and quantity of electricity.*

*It should be also taken into account that the measured quantity of electricity is supplied to the electrodes from the external energy source rather than "passes" through the electrolyte. Notice that it is electric energy that is expended for the electrolysis, not the quantity of electricity. Electric energy $\Delta W = \Delta U \cdot I \cdot \Delta t$ is expended for the first acts of a chemical reaction. Without an external energy source the voltage on electrodes of the electrolyzer decreases up to $U_2$. The re-enabling of the source results in electric current due to the potential shift ($\Delta U = U_1 - U_2$) between the source and the electrodes. Electric current flows for a period of time $\Delta t$, while the voltage is recovered to $U_1$ (or to the value at which electrolysis can proceed). The quantity of electric current $\Delta q = I \cdot \Delta t$ which recover the voltage on electrodes is proportional to the quantity of a reagent involved into the reaction, because electric current is caused by the processes which occur during the period $\Delta t$. Because chemical reactions proceed according to the law of multiple proportions, the quantity of electricity is proportional to the equivalents of obtained compounds. The energy of electrochemical processes is supplied (or taken) by electric current which is measured* in the external circuit, rather than in the electrolyte.

Let us consider the generalized Faraday's law to solve the problem about the transfer of electric current by ions:

$$m = \frac{Mq}{zF}$$

(1)

where $M$ is molecular mass of the compound, involved to the electrolysis; $q = I \cdot t$ – is a quantity of electricity which is supplied to the electrodes during the electrolysis; $F$ – the Faraday's constant; $z$ – equivalent number (or the number of electrons).

Thesis "B" shows that the number of ions $n$ passing from the electrolyte to the electrode (or backwards) during the period of time $t$ and possessing the summarized electric charge $q = n \cdot z \cdot e^-$ is proportional to a quantity of particles $n$ reacting on electrode during this time. Current of ions $I = z \cdot e^- \cdot n / t$, *where $z$ is the charge number of ions proceeding to the electrode or backwards. If we assume that $z$ in the denominator of the Faraday's law (1) is the number of electrons taking part in the reaction, than $z$ in denomintor will be equal to $z$ in the numerator.*

*Substituting $q = n \cdot z \cdot e^-$ in eq. (1) and taking into account $F = N_{Av} \cdot e^-$ we* obtain the formula for Faraday's law without electric charges:

$$m = \frac{n}{N_{Av}} M$$

(2)

where $n/N_{Av}$ – *is the mole fraction of the obtained compound possessing molecular mass M; $N_{Av}$ is the Avogadro's constant. The mass m of the compound which has reacted on the electrodeis proportional to the multiplication of the mole fraction $n/N_{Av}$ and molecular weight of the compound M. Only the number of particles n taking part in the reaction remains in the formula (2) from the quantity of compound in eq. (1). According to (2), when the equal numbers of particlesn of different compounds are taking part in the reaction, we obtain the compounds with masses which are proportional to the molecular weights of these compounds. It was mentioned in consideration of the thesis "A" and it is postulated in the Faraday's laws.*

*The thesis "B" also claims that different ions can possess charges which are divisible by $e^-$ (1·$e^-$, 2·$e^-$, …, $z$·$e^-$).* It is believed, that current of electrons during the electrolysis flows from one terminal of the external energy source to the electrode and from the other electrode to the second terminal rather than it flows in electrolyte from one electrode to another. I.e. the measured quantity of electricity that is taken into account in the laws of electrolysis is supplied from the external energy source to the electrodes at which the chemical reaction occurs.

The motion of ions to the electrodes (or backwards) is a result of the diffusion of reagents and reaction products due to the concentration gradient between the bulk and the near-electrode region. The rate of diffusive ions' motion (other conditions being equal) is determined by the reaction rate which depends on the potential difference on electrodes.

The diffusion of electrochemical reactions products from the electrodes to bulk as well as the diffusion of reagents from electrolyte bulk (to electrodes) do not require electric forces. Ions diffuse taking the energy from the surrounding electrodes (their heat conductivity always differs from that of the electrolytes) and from the heat effect of the reaction. The supply (or taking) the energy for electrode reactions to electrodes (or backwards) by electrons and the motion of compounds performed by the ions is required only after the chemical reaction.

As we see, elementary electric charges are not required to introduce discreteness of the electricity.

The discreteness of electrons in an atom (or a molecule) which is essential for the MA is clearly expressed in the concept of ions with multiple charges as a particle with deficiency (or excess) of more than one electrons at the same time.

The presence of IMC in electrolytes is explained by an element valence, which is a possibility to interact with several atoms (or group of

atoms) "at the same time". It affects the lack of energy for the electrolysis, the rate of changing of concentrations near the electrodes and the diffusion rate of ions to electrodes (or backwards) and, consequently, the intensity of electric current that restores the voltage on the electrodes. For example, when one obtains pentavalent metal on the electrode from the electrolyte (or dissolves the electrode made of this metal) five anions are produced (or bound), whereas anion concentration increases only by one when monovalent element is obtained.

The lack of a reliable proof of IMC existence in chemistry as well as the fact that the main evidence of discreteness of electrons in atoms is the IMC in plasma lead to necessity of consideration the nature of these ions.

### 2.3. IMC in plasma [C0]

Only monovalent fragmentary ions from monoisotope clusters can appear as IMC in plasma[C0]. The hydrogen mass-spectrum is an illustrative example [13]. There are peaks with a half mass of a proton. They were assigned to fragmentary ions, according to the MA, rather than to double charged hydrogen ions.

IMC are commonly observed in plasma by mass-spectrometry as well as by X-ray or atomic optical spectroscopy [14]. The conducted analysis revealed [C0, D0] that obtaining of IMC and the subsequent formation of ionic beams [16] are accompanied with the cluster formation.

Cluster fragmentation after their interaction with electrons or high-energy photons is well-studied [17 – 20]. It becomes more complicated with increasing number of atoms in clusters and supplied energy. There are 966466 different combinations of fragment's masses when fullerene $C_{60}$ disintegrates in two fragments (neutral and singly charged ones) [21].

The daughter ions from monoisotope clusters are the most overlapping IMC peaks in mass-spectra [17]. If the lifetime of metastable ions is comparable with the time of their flight in a mass-spectrometer (~ $10^{-5}$ s), a part of parent ions $A_N^+$ consisting of $N$ atoms (or molecules) with the mass $A$ will reach a collector without disintegration, another part will disintegrate on the way from an ion source to the collector forming the daughter ions $A_X^+$ and neutral particles $A_{(N-X)}$, according to the scheme:

$$A_N^+ \rightarrow A_X^+ + A_{(N-X)} \tag{3}$$

Fragments $A_X^+$ causes the overlapping with peaks in mass-spectra with the apparent masses $M^*$ for monoisotope clusters,

$$M* = A \cdot \frac{X^2}{N}$$

(4)

where $X$ – is the number of atoms (or molecules) with the mass $A$ in a fragment $A_X{}^+$ which was decoupled from the cluster $A_N$. The overlapping between fragments $A_X{}^+$ from the clusters with different sizes $A_N{}^+$ and $q$-charged ions $A^{q+}$ occurs if

$$q = \frac{N}{X^2}$$

(5)

When the daughter ion with the mass $m$ is formed from the ion with the mass $M$ at fragmentation of a heteronuclear particle, its apparent mass $M*$ in a mass-spectrum can be determined using the formula:

$$M* = \frac{m^2}{M}$$

(6)

For any element monoisotope cluster can exist with the size leading to overlapping of the daughter ions' and IMC peaks in mass-spectra in proper conditions (eq. 3–6). For example, if a charged cluster possessing the mass $2A$ which is stretched and accelerated by the electric field from the ion source disintegrates to two particles, each having the mass $A$, until it reaches the magnetic analyzator, than this fragmentary singlecharged ion with the mass $A$ will deviate in the magnetic field as a doublecharged ion (eq. 4, 5). For other clusters possessing the masses $N \cdot A$ one obtains fragments in mass-spectra which are analogues to IMC with the mass $A$ and the charge $N$ (eq. 4, 5) when singlecharged ions with the mass $A$ detach themselves after the ion source and before the magnetic analyzator.

Basing on the above-stated and papers [B0, C0, D0, E0], one can assume that the IMC in mass-spectrometry is nothing but the fragment particles. This hypothesis can be experimentally verified, for example, using the isotope-resolved mass-spectrometry. (More elegant methods can be used depending on the instruments available). A mass-spectrometer with a magnet analyzator and pure isotopes $^{15}N$ and $^{14}N$ (or He, $O_2$, Ne and so on) and their mixtures are required for the experiment.

The work order is the following. One measures the mass-spectrum of one isotope $^{15}N$: peaks with apparent mass 7.5 for the ion $^{15}N^{2+}$ and for fragments $^{15}N^+$ are the same, according to eq. (3 – 6). The same

procedure should be done for $^{14}N$. One obtains the peak with the mass 7.0 for the fragmentary ion $^{14}N^+$ and the ion $^{14}N^{2+}$. Then one should measure the mass-spectrum of the mixture of these ions taking them in a ratio 1:1.

If there are doublet peaks in the mass-spectrum of polyisotope nitrogen with calculated masses of 6.76 and 7.76, fragmentary ions will also present in monoisotope nitrogen. In this case, the fragmentary peaks from the monoisotope nitrogen molecules $^{15}N$-$^{15}N$ and $^{14}N$-$^{14}N$ have masses of 7.5 and 7.0, respectively. Suppose that the equilibrium 1:1 mixture of isotopes consists of a one third of each of the molecules: $^{15}N$-$^{14}N$, $^{15}N$-$^{15}N$ and $^{14}N$-$^{14}N$. The composition of molecules can be preliminarily determined using mass-spectrometry in an individual experiment. Assuming that the intensities of the peaks (6.76 and 7.76) from the fragments of the molecules which consist of different isotopes $^{15}N$-$^{14}N$ are proportional to the intensities of the fragmentary ions from the monoisotope molecules (which are known from the preliminary experiments) and taking into account that under the same experimental conditions during the obtaining of mass-spectra from the molecules of individual isotopes, their concentration was three times higher than that in the mixture, we obtain their contributions to the IMC for monoisotope molecules. Since the one third of the polyisotope molecules of nitrogen from the 1:1 mixture decays either with the detectable ion of $^{15}N^+$ or $^{14}N^+$, the intensities of the peak signals with apparent masses of 6.76 and 7.76 will be six times less than the intensities in experiments with pure monoisotope nitrogen. In a mixture of isotopes, the intensity of the peaks of fragments from different monoisotope molecules will be equal to each other, twice as much as the intensities from polyisotope molecules, and each of them is equal to the sum of the peak intensities: 6.76 and 7.76. At constant intensity ratios $N^{2+}$ ions and, probably, other IMC do not exist.

In order to increase the accuracy of the experiment, it may be necessary to take into account contributions from molecular ions, fragments from the molecular clusters such as $(^{15}N$-$^{15}N)I$ and $(^{14}N$-$^{14}N)i$ to IMC peaks for monoisotope molecules, estimating the nature of the ions from fragmentary peaks$(^{15}N$-14N$)i$ and $(^{15}N_j$-14N$_k)i$. Where $i$ is the number of nitrogen molecules; $j$ and $k$ are the number of corresponding isotopes of nitrogen in molecules. The discrepancy in the dissociation energies of monoisotope molecules and molecules which contain different isotopes is still not taken into consideration. Changing the ratio of isotopes in the mixture being analyzed, one obtains different

proportions of the fragment ions, which allowsone to determine the existence of IMC more reliably.

The residual nitrogen from the air in the mass-spectrometer leads to the occurrence of a background. In order to reduce it, one should "flush" the instrument with argon or another gasand the spectrometer should be blown with argon during the experiment. A more suitable test gas can be chosen, or, for example, lithium or boron. For helium isotopes, the background of residual nitrogen also givesthe overlapping betweenimportant peaks in the mass-spectrum.

Among the many experiments, the elementary electric charge was directly measured only in Millikan's experiments with oil droplets [4] and in its modifications with droplets and particles formed by other substances, so let us consider the analysis of this method in detail.

### 2.4 The Millikan's experiment [4]

The EC in Millikan's experiments was calculated from the velocity of a drop moving in an electric field of known intensity. According to Millikan: "The very fact of the existence of a slightly different from each other velocities is a fine illustration of the atomic structure of electricity". However, "the fact of the existence of a slightly different from each other velocities" can be explained not only by the "atomic structure of electricity", but also by other unaccounted factors. Possible causes of changes in the droplet's velocity are further stated in the affirmative form, although some of them may be insignificant in their effect on the results of the experiments.

### 2.4.1 The role of dielectric permittivity of a medium in the Millikan's experiments

Millikan's formulae for the calculation of the EC include the electric field intensity, although, the dielectric permittivity (DP) of the oil-air gap between the condenser plates, and also the DP films on them are not taken into account.

The DP and the electric conductivity of the medium change "discretely" in a series of experiments: depending on the number and charge of droplets ("unwanted charged dust distorts the field of the capacitor" [22]); when the polarity of the electric field is switched; when oil droplets condense on the surface of condenser plates and on films existing on their surface; after the discharge of charged droplets from the electrodes.

If the charge is inside the droplet, for example: when irradiated with X-rays, UV-light, as a result of oil mixing, the oil DP will affect the

interaction between the ion or electron and the electric field of the capacitor.

Oil films and droplets can move along the surface of the plates in a region with differing electric field intensities, changing the DP at different points of the condenser.

In the Millikan's experiment, when the polarity of the field is switched, the DP changes in time.

The arc that illuminates the droplets is a source of strong UV-light, the effect of which leads to photoionization of the air-oil mixture, changes its DP and electric conductivity.

The polarization of the droplets and the electric charges induced on them depend on the DP and the electric conductivity of the medium (in addition to the voltage on the plates of the capacitor).

**2.4.2 The role of the electric field in the Millikan's experiments**

An electric charge density and, as a result, an additional electric field arise in the dielectric under the external electric field. To estimate the contribution to the uncertainty of the measurement of the EC dipole moments induced by the electric field on the droplets, we consider the experimental conditions from the ref. [23]. The total charge on the droplets is ~ $20e$; it is changed by photoemission; one commonly works with a positive electric charge; the magnitude of the electric field provides levitation of droplets with a charge of $+15e$; the typical droplet's density d is ~ 1 g/cm³; the droplet's radius is ~ $3.9d$; the air viscosity $\eta$ is ~ 182 µP; droplet's velocity is ~ 1.8 mm/s; mass of droplets is ~ $2.4 \cdot 10^{-10}$ g. The induced dipole charge can be of the order of $8000e$ [24] for the listed parameters and typical DPs of liquids which are close to one! The induced dipole moment of the droplet interacts with the gradient of the electric field, but even more strongly is the interaction between the polarized droplets.

Charging of any part of the droplet's surface (due to polarization, sorption, desorption, photoeffect) causes the motion of its surface and, consequently, the motion of the droplet in the air. For example, in polarography: "The electric field in the solution causes the potential difference, and, consequently, the difference in the surface tension between different points of the droplet's surface, which results in the tangential movement of the interface (the adsorbed layer), whose velocity is directly proportional to the tension gradient, and which causes the reactive repulsion of a mercury droplet from the surrounding solution. The tangential motion of the droplet's surface affects the rate of fall of the mercury droplet in the solution". An electrically charged layer is also

mobile on a dielectric, for example: an electric charge easily drains from a glass rod onto a conductor.

Switching on the field results in the movement of the droplet's surface which causes mixing inside leading to heating the droplet and changing its volume.

The shape (size) of droplets depends on the electric field (it is observed for droplets in a liquid). When the shape of the droplet changes, both Archimedes' force and air resistance change. The shape and size of the droplets vary in different ways in different media, after ionization of the air and without it, therefore, the droplet's velocity varies depending on the magnitude of the field.

The ions formed inside the droplet (under the X-ray and the illumination of droplets, as a result of the entering of electrons and ions into the droplet, during the motion of the surface layers) drift inside or on the surface of the droplet when the voltage is switched on, which leads to the dissipation of the energy of the ion or electron resulting in the motion of liquid and the heating of the droplet, and, consequently, the velocity of the droplet is not proportional to the charge of the electron or ion.

At a high field intensity, the surface of the liquid on the plates collapses, and points are formed on the liquid surface from which highly charged microdroplets are emitted.

The presence of a large electric resistance between the film, droplets and metal plates, as well as droplets or particles "dancing" on the electrodes, microdischarges between them and currents between the particles and electrode plates result in the heating of the plates and gas. Heated electrodes are not cooled instantly providing gas convection and changing the gas viscosity; their heat acts when the electric field is switched off during the free fall of the droplets.

Ions formed after the X-rays exposure penetrating the electrodes through the layer of oil and film charge the surface and the volume of the dielectric. The field is restored more slowly in places where oil or dielectric films coat the plates.

### 2.4.3 The role of X-rays in the Millikan's experiments

After the X-irradiation of the capacitor gap and the application of an electric field, most of oil and ion charged droplets settle on the plates.

X-rays, strong UV-light, ion bombardment lead to the formation of polymer films on the plates of the condenser.

A discharge occurs when X-irradiation of the gap of the capacitor takes place. After this, post-discharge emission is observed in the presence of dielectric and semiconductor films or inclusions. Thus (in a

vacuum) [25], "after excitation of the discharge, as a result of the emission of electrons from the cathode, under the influence of UV-light or ion bombardment, and also the deposition of ions, the surface films become charged, and local high-intensity electric fields that persist for a long time appear. Under the influence of these fields, the electrode can emit electrons even in the absence of an external field ... The current of post-discharge emission is very low, except the cases when films are applied using special technologies ... There is an emission of electrons through the thin films of dielectrics (0.01 - 0.1 µm) with high volumetric electric resistance".

The charge of droplets and charged films of electrodes affects the speed of the free fall of droplets when the electric field is switched off.

Both the Stokes'sand Archimedes' laws were unsatisfactory for small droplets.

Landing an ion on a droplet during its movement unpredictably affects the resultant velocity, because one measures only a time during which the droplet passes the known route.

To sum up the incomplete list of possible influences, one should note that the enormous number of effects is also found in the experiments of R. Millikan. In 1910-1913, Millikan, proving his point in a dispute with F. Ehrenhaft concerning the existence of a subelectronic charge, published an article with new accurate results. In the article it was reported that "it is not selective results for a separate group of droplets, but the results for all droplets measuredduring sixty days". However, the subsequent study of Millikan's laboratory journals [26, 27] revealed that each of the preliminary results was marked with special comments like "very low, something is wrong" or "fine, it should be published". As a result, only 58 of 140 results were published! It means that there were 2.4 times more rejected results than published ones due to some unaccounted factors. Unsorted data from Ehrenhaft had a much wider dispersion than selective Millikan's results. Although Millikan seems to be right in the dispute with Ehrenhaft about the subelectron, the question concerning the low reproducibility of his results remains open. F. A. Joffe [22] received fractional electric charges in his experiments on metal particles as it did Erenhaft.

Many of the influences on Millikan's experiments listed in the previous section were detected and taken into account in experiments on the search of a subelectron [23, 28 – 41].

### 3. Conclusions
### 3.1 Reflection concerning the nature of the EC.

### 3.1.1 The dependence between the EC, electric and mechanical forces.

### 3.2 Prerequisite of hypothesis about the EC nature

As it was shown in [B0] and discussed above, the laws of electrolysis are not the proof of the discreteness of electric charges in atoms and molecules, and in chemistry there are no reliable proofs for the existence of discrete electricity and IMC.

Scientists are not inclined to publish results which do not fit with official models and theories in scientific journals. A good example of it is the dispute between Millikan and Ehrenhaft (section 2.4), when Millikan did not dare to publish more than a half of his experimental data. What type of results and why did he remove? The dissatisfaction with the reliability of determining the EC by the Millikan method (section 2.4) leads to the necessity to check the existence of discrete electricity in the IMC.

It can be assumed that the experimentally established deviations of the IMC velocities from the calculated ones for the corresponding charges' multiplicities are not published.

The lack of significant success in achieving ultrahigh energy on accelerators when working with IMC can be associated not only with technical difficulties or relativistic effects but also with the absence of IMC in nature.

The author [C0] found a (qualitative) correlation between the width (and, consequently, the dispersion of ions' energies) of mass-spectral peaks of fragmentary ions and those with multiple charges. Therefore, the width of the IMC peak increases with increasing the ion charge. The width of the peak of the fragment ion also increases with the increasing of multiplicity of the charge of that ion, on the signal of which it is possible to overlap this fragment in the mass-spectrum. From this, and also from [B0, C0, D0, E0] it follows that in plasma single-charged fragmentary ions can be taken for IMC.

To intensify efforts of verifying the proposed hypothesis, it is important to realize that the experimental establishment of the nature of IMC is the identification of the "quantization" of the EC and the verification of the present atomic model.

### 3.3. IMC hypothesis and its experimental validation

The hypothesis concerning the existence of ions with multiple charges: "the charge of any atomic ion is equal to unity; i.e., there is no atomic ions with multiple charges because they are particles having a lack or excess of several electrons"

It follows from the hypothesis that the charge of α-particles is equal to unity, and their velocity should be 1.414 times smaller than it is assumed, for example, in alpha-spectroscopy.

To validate the hypothesis, it is proposed to conduct a range of experiments:
• mass-spectrometric verification of the nature of IMC (Section 2.3);
• determination of the velocity of α-particles before their entry into the alpha spectrometer;
• determination of IMC velocities before their entry into the mass-analyzer or (in the determination of ionization losses, particle path lengths) into the substance.

The preliminary conclusion (which may be final) about the "quantization" of the electric charge (see subsections 3.1 and 3.1.1) can be formulated as follows: the EC is a constant which is proportional to the minimum kinetic energy of the charged particle obtained after it passes through the potential difference of 1 V. This consideration can explain the nature of the EC if hypothesis that there is no atomic IMC in nature is right.

## References

4. R. Millikan Electrons (+ and –), protons, photons, neutrons and cosmic rays. M – L.: GONTI, 1939, (page 108); R. A. Millikan, Electrons (+ and – ), Protons, Photons, Neutrons, and Cosmic Rays, Cambridge, At the University Press, 1939

6. D. L. Anderson, The Discovery of the Electron, M.: Atomizdat, 1968; D. L. Anderson. The Discovery of the Electron. The Development of the Atomic Concept of Electricity. Princeton, New Jersey, Toronto – London – New York, 1964.

9. G. Hertz, Electrochemistry. New views, M.: Mir, 1983; H. G. Hertz. Lecture Notes in Chemistry. Electrochemistry. Reformulations of the Basic Principles. Springer-Verlag, Berlin – Heidelberg – New York, 1980.

10. V. V. Skorchelletty, Theoretical electrochemistry, L.: Himiya, 1970.

11. E. V. Shpolsky, Atomic physics, Volume 1, Introduction to atomic physics, M.: Nauka, 1974.

13. N. N. Tunitsky, R. M. Smirnova, M. V. Tikhomirov, About "fractional" peaks in a hydrogen mass spectrum, Reports of Academy of Sciences of the USSR, Volume 101,1083 – 1084. (1955).

25. I. N. Slivkov, Processes at high voltage in a vacuum, M.: Energoatomizdat, 1986, (p. 49).

43. G.A. Mesyats, Ektona in the vacuum discharge: breakdown, spark, arch, M.: Nauka, RAS, 2000.

# B: About the discreteness of electric charges in Chemistry

The concept of the discrete structure of electricity is initially based on electrochemical experiments and is directly related to the atomic model: according to this model, the ions are carriers of elementary electric charges.

The analysis of the validity of using ionic charge numbers and numbers of electrons in chemical equations and formulae shows that the discreteness of electric charges does not follow from electrochemical experiments and electrolysis laws, and it is possible not to involve elementary electric charges in chemistry.

"Since it is Chemistry that allows to know the structure of the bodies, it is extremely difficult to see the truly ground of electricity without it" M. Lomonosov

### 1. Introduction

In the laws of electrolysis and chemical equations, the coefficient "$z$" (sometimes $n$ or another symbol) is used as an indicator of the discrete structure of electricity: the number of electrons participating in the reaction or the charge numbers of ions. The charge number $z_i$ is the number of elementary electric charges $e$ ($e = 1.6 \cdot 10^{-19}C$) that make up the charge of the $i$th ion, taking into account the sign. (The term "charge number" should be distinguished from the term "ionic charge", which is defined as the product: $z_i \cdot e$).

Throughout the paper, the symbol "$z$" denotes the modulus of the charge number and the degree of oxidation or the number of electrons participating in the reaction (and also the valence and the difference in degrees of oxidation which are used, along with electrons, in calculating chemical equivalents).

This paper aims to evaluate whither the interpretation of the charge number "$z$" as an index of the discreteness of the electric charge of the ion or the number of electrons participating in the reaction is valid and to provide the evidence of the inadequacy of these representations. The determination of the nature of the charge number "$z$" will lead to understanding of the question: "Are the discrete electrons of atoms and molecules responsible for the chemical bond and chemical transformations."

We begin the list of the facts on the basis of which one can question the adequacy of the representation of "z" as the charge number of the ion or the number of electrons participating in the reaction with the work of H. Hertz [1]. It describes the field of knowledge that arose at the intersection of Electrophysics and Chemistry without invoking the concept of electric charge, since "there is no need for the concept of electric charge, and it is not introduced". Hertz derives the fundamental theses of equilibrium Electrochemistry without using the concept of "ion", consequently, the basic equations of equilibrium Electrochemistry are given without introducing the charge of particles making up solutions.

It is generally accepted that the oxidation state of the atoms that make up the reacting substances changes during the oxidation-reduction (redox) processes, and electrons move from one atom, molecule or ion to another. However, the oxidation state is a formal characteristic, and the statement that redox reactions occur with the addition or loss of electrons does not correspond to the real mechanisms of the reactions. This model of electron transfer is convenient for determining the change in the oxidation state, for finding stoichiometric coefficients, and for interpreting the nature of the redox reactions basing on the concept of redox potentials.

Experimental methods for determining the "charge" of ions in solutions of electrolytes reduce to the determination of stoichiometric coefficients of compounds. For example, to determine the "charges" of complex ions using molecular spectroscopy, one takes the values of the stoichiometric coefficients. The latest can be obtained by any method which allows to determine the composition of the complex, for example, one measures how an optical density changes with changing concentration of components. A similar method is applied in Electrochemistry: the composition of a complex ion is determined by measuring the potentials of an electrochemical cell after changing the concentrations of the components in the system. In these cases, we can talk about determining the composition of complexes, but not the "charges" of ions.

The experimental and theoretical studies of solids reveal that the transfer of electrons from one group of atoms to another does not occur. Therefore, the effective charges of ions are close to the nominal ones (which are equal to the oxidation states) only for halides; for oxides, the charge of oxygen ion is close to " –1," and for chalcogenides and other compounds it is significantly less than one [2]. X-ray spectroscopy for the oxygen atom, which is a part of a wide diversity of compounds, also gives

an effective ion charge about minus one. Levin, Syrkin and Diatkina, using the solution of the Schrödinger equation for electrons localized on oxygen ions in a crystal, estimated the depth of its potential well as a function of the ionic charge. It turned out that itsdepth decreases rather rapidly with the increase of the absolute value of the effective ion charge and when it is about "1.2" the potential well vanishes. Consequently, the authors of [2] came to the conclusion that there is no double-charged ions of non-metallic elements in nature, and the effective ion charges, determined both by exact X-ray diffraction and by semiempirical methods, can never bedivisible by the electron's charge and is rarely higher than ± 2.

From the papers of G.A. Mesyats [3] it follows that the emission of electrons from a substance can be explained without involving fundamental discrete particles, since in electric discharges electrons are emitted not by elementary particles, but by separate portions which are called ectons.

Almost all elementary particles possess electric charges $e^+$ or $e^-$ (or no charge). The nature of this "quantization" of electric charge is still unclear.

R. Millikan did not detect ions with a charge greater than one in his experiments on the measurement of elementary electric charge [4] (using oil and mercury droplets, charged in various gases and vapors). He concluded that "he and other researchers obtained direct and unmistakable evidence that ionization of gas molecules by X-, $\beta$- and $\gamma$- rays consists in the extraction of a single elementary electric charge under all experimental conditions". Millikan did a similar conclusion regarding the impossibility of obtaining IMC in gases also for fast α-particles. A "one-stage" double change in the charge of oil droplets was registered only during the irradiation of helium with α-particles.

The discovery of IMC in plasma still remains the most important (and nowadays, almost the only experimental) proof of the discreteness of electrons in atoms. IMC are investigated by mass-spectrometry, X-ray and atomic spectroscopy, etc. However, it cannot be unequivocally determined whether the ion is a multiple charged one or a fragmentary one from a monoisotopic cluster. This problem is caused by overlapping between the fragmentary ions from clusters, which are present in any ion source, and peaks of IMC. Abstracting from the present atomic model, the IMC peaks in mass-spectra can be unambiguously interpreted as fragments from monoisotopic clusters [C0].

X-ray and optical emission of clusters' fragments which scatterwith enormous velocities as a result of the Coulomb explosion can be taken

(due to the Doppler effect) to be the emission of IMC [G0]. There are a lot of clusters in any IMC source [C0], and also in practically allatomic spectra excitation sources [D0, E0].

## 2. About elementary electric charges in Chemistry
### 2.1 Redox processes without discrete electrical charges

Form the above mentioned it follows that when recording standard potentials of electrodes one can do without involving charge numbers of ions and "single-piece" electrons; because the charge number "$z$" is determined by the stoichiometry of the reactions in electrochemical processes (9b – 9m).

### 2.2 Galvanic element

The processes in the GE can be described without the concept of ions as electrically charged particles [1]. In accordance with the chemical theory of a Galvanic element, electrical energy is produced as a result of chemical reactions at the electrode-electrolyte interface. The current generated in the GE is determined by the rates of the reactions occurring in it: the more matter isconverted per unit time, the greater is the power of a chemical current source.

... It should be noted that the coefficient $1/z$ (the inverse value of the "charge number $z$") enters into equations (11$a$) and (11$b$) as an equivalence factor before the introducing of electrical characteristics in the formulae. This equivalence factor is determined using the stoichiometric numbers of the reaction components and, therefore, it refers to the quantity of matter, rather than to the number of elementary electrical charges. Later it enters into the equations of Electrochemistry having the same meaning.

As we see, the number $z$ in the equations for the galvanic element depends on the stoichiometry of the process rather than on elementary electric charges, entering the equations before the appearance of electrical characteristics.

### 2.3 Electrolysis
### 2.4 Chemical reactions under electrolysis – why does electric current flow

The discussion above shows that during electrolysis chemical transformations cause electric current as in the GE. The primacy of the chemical processes (rather than the electric current) that begin after imposing a sufficient potential difference on the electrodes proves that in Faraday's laws and other equations of electrochemistry the coefficient "$z$", which is considered "an indicator of the discreteness of electricity," refers not to electrical characteristics, but to quantity the reacted matter;

"$z$" refers to the stoichiometry of chemical reactions and to the compositions of reagents and products, rather than to the charge numbers of the reacting ions, or to the numbers of discrete electrons. The composition of reagents and products can be reliably determined, unlike the transfer of "single-piece" electrons, by methods of quantitative chemical analysis.

**2.5 Laws of electrolysis** reflect the general low of conservation of matter when electrochemical reactions proceed. The laws are used to derive equations which describe the electrochemical conversion of matter at the boundaries of conductors of the first and second kinds.

Since electric current flows as a result of chemical reactions, it is the quantity of electricity supplied to electrodes of an electrolyser to recover the voltage which is defined by the quantity of matter which reacted during the electrolysis, not conversely.

**3. About the discrete structure of ionic charges in electrolytes**.
**3.1 Electric current in electrolytes**
**4. Conclusions**

Being a "sovereign scientific field", Chemistry should have a reliable "immune system" which allows one to check physical models and theories for their suitability in this "sovereign" area of knowledge. Any theory of chemical bonding is based on the atomic model, and the latest, in turn, is based on the discreteness of electricity. Consequently, the clarification of the nature of ions and the verification of the atomic model will be responsibilities of Chemistry itself if it is a "sovereign scientific discipline."

The main part of the work is devoted to elucidating the nature of the coefficient "$z$" in the equations and formulae of Chemistry. Since the concept of discreteness of electricity was introduced to science basing on understanding the number "$z$" as the number elementary electric charges which are transferred in electrolytes by ions, electrical forces were chosen to explain chemical interactions and elementary electric charged particles were included into the atomic model. Moreover, each section of the article shows that the interpretation of the number "$z$" does not require the elementary electric charges.

**4.1** The value "$z$" in chemical equations, does not refer to the quantity of electricity, the number of electrons participating in the chemical reaction or to the ionic charge, but it refers to the quantity of matter and to the reaction stoichiometry.

The laws of electrolysis, which are attributed to have an important role in understanding the nature of the chemical bond and the development of the atomic-molecular theory, do not prove that chemical

forces have electrical nature and that electrical charges in atoms and molecules are discrete.

The lack of the reliable evidence of the existence of IMC in the Chemistry of electrolytes, and also the fact that the main evidence of the discreteness of electrons in atoms is the existence of IMC in the plasma, lead to the necessity to clarify the nature of ions in plasma.

IMC in plasma are investigated primarily by methods of mass-spectrometry, therefore, the verification of the atomic model can be carried out by mass-spectrometry [A0]. It is important to take into account that the peaks of mass-spectra of any IMC can be interpreted as fragmentary particles from clusters, without involving discrete electricity.

If ions with multiple charges that are not detected in electrolytes (solutions, melts, superionic conductors) and in crystals do not exist in gases and plasma, then there will be no reason to introduce discrete electric charges into the atomic model and to explain a chemical bond using the concept of electron.

Elucidation of the nature of IMC makes it possible to understand the mechanisms of electrochemical processes, as well as to determine the elementary nature of the electric charge.

### References

1. G. Hertz, Electrochemistry. New views, M.: Mir, 1983; H. G. Hertz. Lecture Notes in Chemistry. Electrochemistry. Reformulations of the Basic Principles. Springer-Verlag, Berlin – Heidelberg – New York, 1980.
3. G. A. Mesyats, Ektona in the vacuum discharge: breakdown, spark, arch, M.: Nauka, RAS, 2000.
4. R. Millikan, Electrons (+ and –), protons, photons, neutrons and cosmic rays. M – L.: GONTI, 1939, (p. 108); R. A. Millikan, Electrons (+ and – ), Protons, Photons, Neutrons, and Cosmic Rays, Cambridge, At the University Press, 1939.
15. V. V. Skorchelletty, Theoretical electrochemistry, L.: Himiya, 1970, (pp.: 252, 438).
16. E. V. Shpolsky, Atomic physics, Volume 1, Introduction to atomic physics, M.: Nauka, 1974, (p.11).

# C: The role of cluster fragmentation in mass-spectrometry of ions with multiple charges

Analysis of the experimental material proves the presence of clusters in all ion sources, which use the energy of the electron impact, laser,

spark, arc, inductively coupled plasma or glow discharge for the ionization of matter. The processes of cluster formation in sources of ions with multiple charges are considered: electron cyclotron resonance, with electron beam, trap with an electron beam, storage ring of heavy ions. Evidence of a change in the composition of ion beams during their formation, transportation, recharging and stripping on targets is presented.

Fragmentation of clusters in ion sources and beyond them contributes to ion signals, which seriously complicates the design of experiments on ions with multiple charges and the interpretation of results. A method of mass-spectrometric verification of the atomic model is proposed.

## 1. Introduction

Ions with multiple charges (IMC) are both an object and a research tool in Atomic Physics. Firstly, the main practical interest when obtaining and studying IMC was caused by the possibility of controlling the reactions of thermonuclear fusion and fission, as well as simplifying and reducing the cost of equipment for accelerating heavy ions to high energies [1].

The reliable IMC identification is complicated by cluster formation and fragmentation in ion sources (IS) and beyond them, in ion beams. The presence of cluster ions in the beams of IMC leads the fact that the beam drawn from the IS initially consists of a set of particles, and IMC are injected into accelerators together with cluster fragments, and numerous operations with ion beams (transportation, focusing, acceleration, bunching, cooling, recharging, stripping) lead to a further change in the composition of the beams.

The work aims to provide the evidence of the formation of clusters during the obtaining of IMC and operations with them, to consider the role of cluster fragmentation when working with ion beams. The work focuses on the necessity of taking into account the contribution from the fragmentary ions to the IMC signals in cases where it is not usually expected. For example, in ionization of gases, monoisotopic clusters which can overlap with signals from ions with high charge multiplicities are not usually expected to form and decompose. Also, the presence of such overlaps in linear time-of-flight mass-spectrometry may be unexpected.

In order to compare the conditions of plasma generation in IS with the conditions for formation and existence of clusters, the article briefly discusses the ways of producing ions and clusters. Also, methods for

distinguishing fragmentary ions and ones with multiple charged are considered, some difficulties of the mass-spectrometric experiment are discussed (besides the cluster formation and fragmentation).

Mass-spectrometry has successfully coped with the precise determination of the atomic mass, and with its help one can verify the atomic model. In the modern atomic model, the equality of the number of orbital electrons to a charge of an atomic nucleus is postulated. Confirmation of the discreteness of electrons in an atom is the existence of IMC in plasma. The concept of verification consists in the mass-spectrometric determination of the charges of bare nuclei (from the ratio of the mass of the ion to its charge), after the complete removal of all the electrons surrounding the nucleus and comparing them with the ordinal numbers of the corresponding elements; since there are devices, allowing to obtainbeams ofbare nuclei [1, 6, 7]. If the nuclear charges correspond to their charge numbers in a periodic system, the experiment will contribute to the confirmation of the consistency of the modern atomic model.

**2. Methods of producing ions with multiple charges (IMC)**

Particles (atoms, molecules, clusters, fullerenes) with the multiplicity of charge more than one are referred here to the ions with multiple charges. IMC can be produced using ion sources (IS) – ions are drawn from them and form beams. After the beam was formed in the IS and isolated in a certain charged condition by the deflecting magnet (or by another technique), it is delivered to an accelerator, ionic trap, a storage ring or to a detector. Consideration of the PSs – plasma sources – in the article is limited by those physical principles and phenomena underlying their action, which lead to the appearance of clusters simultaneously with the formation of IMC. The state of Physics and Technology of the main ion sources is described in detail in the collective monograph [6].

ISs using the energy of a laser, a spark, an arc, an inductively coupled plasma or a glow discharge [6, 8 – 11] are applied in mass-spectrometry. For the production of IMC beams in accelerators and experiments in Atomic Physics are widely used electron cyclotron resonance ISs, ECR [12-18], PIG-type ISs [19], electron beam EBIS [20], ion traps with electron beam, EBIT [ 1, 2, 7, 21 – 23], etc.

**2.1 Electron cyclotron resonance ion sources [12]. 2.1.1 Metal ions obtaining using ECR sources [14].**

**2.1.2 Metal ions obtaining from volatile compounds**

IMC beams of different elements were obtained using the method of gas-like production of metal ion beams, Metal Ions from Volatile Compounds, MIVOC [15 – 18]. Besides metals, carbon, hydrogen,

oxygen, halogens and other elements can form compounds which are used in this method. High vapor pressure of volatile compounds at a relatively low temperature allows them to be treated as gases.

**2.2 Ion source with electric beam**

**2.3 Ionic trap with electric beam, EBIT**

Ions with high charge multiplicities and bare nuclei are obtained in EBIT, using EBIS principles. The EBIT traps are divided into "cryogenic" [1, 7, 21, 22] and "warm" [23] as in EBIS. EBIT traps are used both to obtain ions with multiple charges [1, 2, 7, 21 – 23] (the NIST EBIT scheme is available on the site [22]) and to study atomic spectra (X-ray or optical) [2, 26, 27]. IMC can be extracted from EBIT, analyzed and/or delivered to special devices.

**2.4 Ionic PIG-source [19]**

**2.5 Laser ion source**

Laser plasma is an impulse emitter of atoms with single or multiple charges as well as of polyatomic and negatively charged ions, neutral atoms with low and high energies [9].

**2.6 Ion sources with vacuum arc or spark. 2.7 Ion source with a glow discharge. 2.8 Ionization by ions [38 – 43]. 2.9 Ionization of ions by electrons [44, 45]. 2.10 Ionization by stripping on targets [3, 46 – 50].**

**3. Methods of producing clusters [53]**

A weakly ionized plasma contains appreciable amounts of cluster ions. However, the plasma generation method is more suitable for clusters with high binding energies of atoms, since the high temperature of the plasma and the presence of vigorous atomic particles in it lead to the destruction of fragile formations.

**3.1.1. Sputtering of liquids to small droplets or aerosols in plasma [55]. 3.1.2 Arc discharge [56 – 57]. 3.1.3 Magnetron and glow discharges [55]. 3.2 Laser generation of clusters [9, 60 – 63]. 3.3 Ionic sputtering of solids [37, 64 – 68].**

**3.4 Cryogenic plasma – a source of cluster ions**

Along with molecular ion, formation of clusters is also typical for cryogenic plasma. Paper [53] shows that at room temperature there are predominant positive ions of nitrogen: $N^+$, $N_2^+$, $N_3^+$, $N_4^+$ and $N_5^+$. Cluster ions up to $N_9^+$ are present when one lowing the temperature [69].

I was established by the mass-spectrometric investigations of cryogenic helium plasma [70] that at T = 300 K and a pressure of $10^3$ Pa there are $He_2^+$ ions in plasma. Decreasing temperature leads to an increase in the $He_2^+$ content and to the formation of $He_3^+$ and $He_4^+$.

Their presence in small amounts is detected even at room temperature. $He_3^+$ dominates at a temperature of liquid nitrogen [71].

**3.5 Method of generation of cluster beams from vapor or gas [55]. 3.6 Aggregate cluster generator [55]. 4. Cluster transformations. 4.1 Bond energy in clusters [73 – 80, 100]. 4.2 Cluster fragmentation.**

**4.2.1 Translation energy of fragments**

It has been established that the broadening of peaks in mass-spectra is due to the conversion of the internal energy of the parent metastable ions to the superkinetic energy of daughter ions and neutral particles during the decay process [89]. If the ion decomposition reaction occurs sequentially, then the increase in the average kinetic energy of the ions is the result of the accumulation of the kinetic energy of the ions due to the contribution of each separate decay process [90].

In addition to the consistent evaporation of particles from the cluster, intense fragmentation can occur as a result of the Coulomb explosion – this is when the Coulomb repulsion potential between cluster atoms turns into a enormous kinetic energy of the fragments. However, it follows from the calculations that the explosion of a large cluster of xenon atoms is determined by the gas-dynamical force, rather than by the Coulomb repulsion of atomic IMC [92].

**5. Analysis of methods for experimental registration of fragmentary ions' contribution to mass-spectra of ICM**

The signal of the presence of fragment ions in IMC beams (if impurities and other influences on the measured signals are taken into account) is mass-spectral lines that do not correspond to the expected positions of ions $m/q$ ($m$ is the atomic mass and $q$ is the ion charge). This statement is also held true for transmission of bare nuclei through targets. Another signal is the change in the isotopic ratios for the element in the IMC mass-spectra when the transition from one multiplicity of the ionic charge to the other is taking place.

**5.1 Method for determination of charge of α-particles [101]**

**5.2 Isotope-resolved mass-spectrometry [89, 95]**

The method of isotope-resolved mass spectrometry is limited by the presence of impurities in the system. The intensities of isotopes given in [104] for different charge states vary significantly as a result of the presence of hydrogen, oxygen and carbon. Decoding of mass-spectrum of fullerene can significantly complicated by adding even a single hydrogen atom.

The presence of hydrogen ions is noted in many experiments. For example, in papers [14, 105, 106], observing bare nuclei of carbon, nitrogen and oxygen was difficult due to the presence of hydrogen.

Obtaining IMC by titanization of its volatile organic compound [15] is a more remarkable example. Isotopic ratios for titanium, calculated from its mass-spectrum, show a significant discrepancy in comparison with the known isotopic composition. For mass numbers: 46, 47, 48, 49 and 50 Da it were received, in %: 6.2 (8.0); 15 (7.3); 54.5 (73), 21 (5.5) and 4.7 (5.4). (Natural isotope content is given in brackets). The authors suggest a contribution to mass-spectra from TiH particles.

The use of low temperatures can contribute to the IMC mass-spectra from fragments of hydrogen clusters since at the temperature of liquid nitrogen there are ions $H_2^+$, $H_3^+$, $H_5^+$, and clusters $(H_2)_N$ are formed at a temperature of 20-30 K [107].

The effect of hydrogen is also confirmed by the sputtering of fullerenes [108, 110, 111].

The possibilities (not only) of isotope-resolved mass-spectrometrycan be also affected by the additional kinetic energy obtained by fragments during the fragmentation of molecules or clusters. For example, it was shown in [43] that the IMC of atoms obtained from molecules containing two atoms with comparable masses have peaks shifted to the higher $m/q$ ratios than monatomic targets. Moreover, these shifts increase with the increasing of charge multiplicity of the atomic ion due to their original kinetic energy, obtained as a result of the Coulomb explosion of molecular IMC. Energy shifts of IMC were observed for the following molecules: $N_2$, $CH_4$, $C_2H_2$, $NO$, $N_2O$, $NO_2$, $CO$, $CO_2$, $SF_6$ and $I_2$.

Problems noted above for isotope-resolved mass-spectrometry may lead to the fact that, the authors of refs. [102, 103] additionally use another method for determining the corresponding part of fullerene $C_{60}^{q+}$ ions and coinciding with them less charged fragmentary ions in mixed ionic beams. This method, in their opinion, is "significantly more accurate than high-resolution mass spectrometry".

**5.3 Kinetic electron emission from the pure metal surface**

The method of kinetic electron emission is based on the assumption that, at a certain collision rate, the kinetic electron emission from a pure metal surface bombarded by large molecules or clusters $(CN)^{q+}$ is proportional to the number of particles $N$ composing the molecule, while no dependence on the charge $q$ is observed [103].

Fragmentation of particles before the metal surface should be taken into account, since fragments (including neutral ones) with sufficient energy contribute to kinetic electron emission.

**5.4 Identification of fragmentary ions basing on the width of their peaks**

Assumption that ions formed through the non-dissociative ionization have small internal energies, and ions after dissociative ionization have excess energy distributed in the degrees of freedom of the products, allows one to verify the composition of the beams emerging from the IS [74].

To determine the energy of ions from the width of their peaks, the MIKES method [81, 94, 95], performed on a mass-spectrometer with an inverse geometry (the magnetic cascade precedes the electrostatic analyzer) is used.

**5.5 Method of differing negative ions with multiple charges and fragmentary ones**

**5.6 The role of cluster fragmentation in linear time-of-flight mass-spectrometry**

Linear time-of-flight mass spectrometry, TOFMS [122] can be successfully used to detect fragmentary ions in IMC beams. However, the presence of clusters in IS leads to experimental difficulties. To estimate the difficulty in decoding the time-of-flight mass-spectra (TOF spectra), we consider a number of examples [43, 95, 123 – 126].

If any delaying, deflecting or focusing fields are used before the detector, separation of the parent ions and fragments will occur, and, consequently, there will be signals of fragmentary ions and neutrals in the TOF-spectrum [104].

**5.7 Studying the cluster fragmentation using the coincidence method**

To study metastable decay and to determine uncharged fragments in ionic beams, the coincidence method is used [128 – 130].

**5.8 The difficulties of mass-spectrometric experiment**

**6. Analysis of possibility of cluster formation during IMC obtaining**

Comparison of the methods of IMC (Section 2) and cluster (Section 3) shows the obvious similarity between the conditions of obtaining both of them under the influence of powerful energy flows on the condensed phase. Intense evaporation and/or sputtering of the material under investigation take place in a buffer gas (or vacuum), leading to the formation of clusters when one uses spark, arc, laser, glow discharge or ion bombardment as a IS.

There are also conditions for cluster formation at a softer ionization of the condensed phase. For example, in liquid metal ion sources, LMIS, polymeric particles are formed during the emission of monomeric ions.The fraction and size of polymeric particles increase with increasing current.A significant part of mass loss at high currents is due to the charged microdroplets [141]. The mechanism of cluster formation is not entirely clear. In LMIS, working on metals of IVA and VA groups, a significant contribution of cluster ions is noticeable.This contribution is relatively small in the LMIS working on metals of IIIA group. The mechanism of cluster formation in IS of this type was proposed in [142].

In electrospray ionization, ESI [143], charged droplets are produced at atmospheric pressure, and gaseous IMC are formed from droplets in a heated capillary, which does not exclude the formation of clusters.

Matrix-activated laser desorption/ionization, MALDI, allows one to ionize non-volatile unstable substances. In this method, the laser energy is absorbed by the matrix, and the complex component does not have enough time to decompose. It is carried to the gas phase by an evaporating matrix and is rapidly cooled by adiabatic expansion of the cloud formed by the matrix molecules [144]. In this case, suitable conditions for the formation of clusters are created.

### 6.1 Input of metals into plasma

### 6.1.1 ECR-source for metal ICM formation

In the LBL-ECR ion source (see section 2.1.1.), the atoms of the vaporized metal exit the furnace located in the second stage of the source, enter the ECR-plasma and are ionized by electron impact. The plasma is maintained by introducing the reference gas ($N_2$ or $O_2$) at the first stage [12].

Similarly, the atomic steam produced in the furnace is further expanded along with the buffer gas through the nozzle into the vacuum during the production of clusters. For example (3.1.2), the flux of evaporated tungsten atoms, obtained from metallic tungsten at a temperature of about 4500 K, cools down when collide with argon atoms and eventually merges into clusters [57].

### 6.1.2 Electric discharges

In the MEVVA IS [30, 31] – a vacuum arc in metal vapor is a plasma discharge between two metal electrodes in vacuum.

In the production of clusters, the sputtering of heat-resistant metals can be carried out by means of a gas discharge if it provides high erosion of materials [55]. The magnetron discharge causes the cathode sputtering and it can be an effective generator of cluster beams. For the generation of clusters, the pressure of the argon buffer gas is 10 – 100 Pa. The

discharge with a hollow cathode (glow discharge) is characterized by a higher efficiency of sputtering the cathode under ion current and is also suitable for the formation of atomic vapor, which is further converted into clusters.

### 6.1.3 Input of metal-containing molecules into plasma

The introduction of volatile metal compounds into the buffer gas plasma is used (2.1.2) in the MIVOC ion source. Analogously (3.1.2), it is possible to form clusters in a high-pressure plasma from refractory metals halides [56, 64]. The review [64] notes that the input of molecules containing metal atoms into plasma is a method of generating intense atomic beams for cluster light sources.

### 6.1.4 Input of aerosols into plasma

Analytic mass spectrometry often resorts to the input of aerosols into plasma. In those IS (microwave discharge, arc discharge, high-frequency inductively coupled plasma [10, 145 – 147], etc.), where the substance under study is introduced as an aerosol, clusters are formed, similar to the method of their production by the introduction of aerosols into the plasma (3.1.1). After the desolvation of the aerosol, micro/nano particles (crystals of oxides, halides, etc.) are obtained. They are further evaporated and/or sputtering by ions and plasma electrons, giving atoms, ions and clusters. Small clusters form and grow from atomic vapor and ions in regions with a lower temperature.

### 6.1.5 Laser vaporization of matter

Laser plasma is a source of mono- and multiply ionized atoms (2.5), negatively charged ions, neutral atoms and clusters (with small and large energy) [9, 148].

### 6.2 Secondary ion emission

As a result of secondary ion emission, both clusters (3.3) and IMC are formed (2.1.1). The Minimafios source (2.1.1) uses ion sputtering (or vaporization) of a metal film condensed on the walls of the second stage of the IS.

In the PIG source (2.4), the IMC beam is formed better when one edge of the slit of the pulling electrode covers a part of the outgoing beam. One of the possible reasons is the sputtering (stalling) of deposits from the slit by ions and their fragmentation; the other one is surface-induced dissociation, SID, of particles emerging from the IS.

The formation of polyatomic ions: $AuX$, $AgX$, $NiX$, $CuX$, and $AlX$ (where $X$: Ar, O, N and H) from the material of the mass-spectrometer component (skimmer) was observed in the inductively coupled plasma IS [150].

### 6.3 Using of cryogenic temperatures when obtaining IMC

Achieving low temperatures is an important condition for the formation of gas clusters (section 3). Cryogenic temperatures are used to obtain a high vacuum and strong magnetic fields in the IS [118, 151, 152].

## 6.4 Cluster formation under gas ionization

Gas plasma seems to have low quantity of clusters; however, one should not ignore the possibility of cluster formation when interpreting the mass-spectra of IMC of gases.

The analysis of the possibility of cluster formation during the production of IMC is complicated by the incomplete knowledge of the physical phenomena underlying the functioning of IS. "The basic principles are a set of hypotheses which are generally accepted among researchers working with ion sources, rather than experimentally confirmed facts [12]". In addition, the methods of cluster formation are related to beams of large, stable particles that are produced in sufficient quantities, whereas for mass-spectrometry of IMC, the presence of an insignificant number of small metastable clusters may be critical, since the cross sections of the formation of ions possessing high charge multiplicity are very small. An increase in the yield of IMC is usually accompanied by an increase in cluster formation and fragmentation.

Generation of gas clusters usually requires one or more of the following conditions: low temperature, high pressure, presence of buffer gas, presence of ions, large number of collisions of ions with neutral particles. Any of the above conditions always occur in the production of IMC of gases.

The plasma characteristics (temperature, pressure, density) and its composition vary depending on the IS's section. The formation of clusters from vaporized vapor occurs in any gas system with variable temperature, and they appear not in hot plasma, but in afterglow plasma [153].

Gas IS are filled with a gas medium for ion-molecular reactions and cooling throughout the entire volume.

Mixtures of gases are usually used to produce gas IMC. The presence of a buffer gas is also necessary to form clusters effectively.

In a weakly ionized gas-discharge plasma of different types (at normal temperature and average pressures), cluster ions are present in appreciable amounts [53]. At low temperatures or at high pressures, cluster ions are the major component in a weakly ionized gas (3.4). At a temperature of liquid nitrogen, there are ions $H_2^+$, $H_3^+$, $H_5^+$, and clusters $(H_2)_N$ are formed at a temperature of 20-30 K [107].

Due to the fact that some properties of gases are well described, based on the presence of clusters [155, 156], their initial presence in gases can be assumed.

**6.5 Clusters in EBIT sources. 6.6 Ionization of ions with intersected electric beams. 7. Cluster formation in accelerators**

**7.1 Changing composition of ion beam during its formation, transfer, recharge**

The complex composition of monoenergetic ion beams can be demonstrated by the example of the production of hydrogen anions by a recharge [121]. In this experiment, a beam of hydrogen cations with energy of 9 keV is passed through a supersonic jet of sodium vapor. (In this case, the formation of sodium clusters is possible, and even the formation of hydrogen clusters is possible according to a scheme analogous to cluster production in an aggregate particle generator (Section 3.6)). The source of positive ions, whichgives the maximum current of negative hydrogen ions, $H^-$, forms a beam containing, after passing the target, about 48% of 9 keV $H^-$ ions formed from $H^+$ ions, 26% of $H^-$ ions with energy 4.5 keV formed as a result of $H_2^+$ decay, and 26% of 3 keV He ions formed as a result of the dissociation of $H_3^+$ ions. Therefore, 50 – 75% of the $H^-$ anions are produced from the molecular ions of the beam. The identical particles $H^-$ with discrete energies are separated by the analyzer, as different ions.

**7.2 Changing of the beam's composition during the stripping**

Stripping on gas targets or foils is widely used to obtain high multiplicities of ion charge in accelerators [46 – 50].

Stripping on gas targets is reminiscent of the dissociation method, activated by collisions (spectroscopy of the kinetic energies of fragmentary ions formed due to the collisions of ions with gas) [81].

From the previous point (7.1) it follows that the beams bombarding the target are not monoatomic.

The interaction of hydrogen clusters $H_N^+$ (N = 1 – 13) with a carbon foil was investigated in [163]. Surprisingly, $H_9$ clusters penetrate through a 300 nm thick foil.

**7.3 Cluster formation in a storage rings of heavy atoms**

The storage ring of heavy ions is an extremely long trap which represents itself an annular, evacuated vessel in which the beam rotates. It is used for capturing a part of the ion beam [2].

The formation of complex particles in ion beams introduced into accelerators is possible as a result of the processes considered above (7.1 and 7.2). Cooling of ion beams leads to additional changes in their composition and properties. In this context, the paper [164] should be

noted. The anomalous behavior of a small number of particles in IMC beams cooled by electrons was observed there. The cold ion beam makes more than $10^6$ circulations in the storage ring without significant temperature increase even without cooling. Cooling of ion beams to an extreme spatial phase density leads to the generation of an ordered structure, often called a crystal beam. The existence of such ordered structures was demonstrated in traps of charged particles at rest [157].

Depending on the linear density, the beam can be transformed into a one-dimensional string or, for a higher linear density, in a two- or three-dimensional crystal. However, for two- and three-dimensional structures it is not clear whether they can survive when subjected to strong destructive loads in rotary magnets or focusing fields of the quadrupole magnets of the storage ring.

## 8. Conclusions

Analysis of the experimental data shows that the IMC production and the subsequent formation of ion beams are accompanied by the formation and fragmentation of clusters, which seriously complicate the work with IMC and the correct interpretation of the results obtained. Monoisotopic clusters with fragments' dimensions that overlap with daughter peaks of IMC in mass-spectra can be formed by any elements.

It was experimentally shown [106] that the average kinetic (and maximum) energy of IMC grows practically linearly with a wide range of ion charge. The Coulomb explosion of clusters of the same size yields quantities with discrete energies [127], and identical particles A with different energies are obtained when the clusters of different sizes $A_N$ disintegrate monoatomically (compare with the discreteness of the energies of hydrogen ions obtained by a recharge (Section 7.1)). It corresponds the discreteness of the signals of the fragments in TOFMS (5.6) and the increase in the excess ion energy with increasing their charges (5.4).

(5.4) This is due to the fact that according to formula (5), the translational energy of the daughter ion $A_X{}^+$, which appeared as a result of reaction (1), (with other conditions being equal) increases with the increase in the number of particles $N$ of mass $A$ in the parent cluster $A_N{}^+$, which it leaves. Basing on the equations (2) and (3), during the evaporation of one particle $A_X{}^+$ (that is, at $X = 1$) from the cluster $A_N{}^+$ (in the space with no fields), there will be an overlapping in the mass-spectrum between this fragmentary ion and the ion $A^{q+}$ with charge multiplicity $q = N$.

It is difficult to choose the only one method above ones, listed in Section 5 for distinguishing between fragmentary and multiply charged

ions, which makes it possible to uniquely determine the type of particles arriving at the ion receiver.

The progress toward mass-spectrometry verification of the atomic model can be started with gas IMC, which seem to have a low content of clusters. A "pilot" experiment to test the MAT can be the study (by the isotope-resolvable mass spectrometry method (5.2)) of the presence of particles in gas IS, the fragments of which can be mistakenly identified as IMC. This requires a "simple" mass-spectrometer with good resolution and sensitivity, as well as light gas isotopes (He, $N_2$, $O_2$, Ne or others). If there are fragmentary peaks from the polyisotopic particles of the analyzed gas at the places of the mass-spectrum calculated for them according to formula (4) and not occupied by multiply charged ions, one should also expect the overlappingbetween fragments from monoisotopic clusters and IMC signals formed from the atoms of the element of this gas. In addition, the analysis methods (Section 5), the ionization energy, the conditions for input into the IS (gas or clusters), and/or the gas composition can be varied. To detect the presence of fragments in beams of "stripped" ions, it is necessary to pass beams of bare nuclei through targets.

**8.1** The IMC production is accompanied by the formation of clusters. It also happens for molecular clusters, for example, benzene [84, 168], methanol [84], water [80, 127], ammonia [80], carbon monoxide [74] and even fullerenes (which have associates) [133].

The composition of ion beams is determined by the initial presence of clusters in them, and their collimation, transfer, numerous focusing, deflection, acceleration, bunching, cooling and interaction with the target lead to further complication of the beams. It turns out that for optical and/or X-ray spectroscopy it is difficult to single out a pure monoatomic beam or a IMC beam with a certain charge multiplicity, without the presence of complex particles in it.

The IMC production by the stripping method (p.7.2) leaves many questions to the current explanation of this ionization method. Can the nature of the stripping be explained only by the ultrahigh energies of the particles being stripped, or is it caused by cluster formation and fragmentation?

The presented analysis of the extensive experimental data shows that one should take into account the formation and fragmentation of complex particles when interpreting the results of mass-spectrometric experiments with IMC.

## References

6. The Physics and Technology of Ion Sources, M.: Mir, 1998; The Physics and Technology of Ion Sources, edited by I. G. Brown, a Wiley-Interscience Publication, New York-Chichester-Brisane-Toronro-Singapore, 1989.
55. B. M. Smirnov, Generation of cluster bunches, UFN, 173, 609 – 648 (2003).
58. Yu. I. Petrov, Clusters and small particles, M.: Nauka, 1986.
70. E. I. Asinovsky, A.V. Kirillin, A.A. Ragovets, Cryogenic discharges, M.: Energoatomizdat, 1988.
90. P. Taubert, Kinetic energy of fragmental ions, in book: Advances in mass spectrometry, Volume 1, (edited by D. D. Waldron), M.: Inostr. Lit., pp. 482 – 495, (1963).
121. M. Messey, Negative Ions, M.: Mir, 1979; H. Massey, Negative Ions, Cambridge University Press, London-New York-Melbourne, 1976.

# D: Clusters in radiation sources. Part I. Traditional excitation sources of atomic optical spectra: flame, ark, spark, plasma, laser

The presence of clusters in all traditional excitation sources of atomic optical spectra (flame, arc, spark, laser, plasma) and in gas lasers is proved basing on the extensive analysis of experimental data.

Clusters can produce narrow photon emission lines, which should be taken into account when interpreting atomic spectra. The study is of an interest for the development of the theory of atomic spectra.

### 1. Introduction

Experimental facts show that clusters are present in a wide variety of radiation sources, atomic and ion beams and gas lasers. Clusters can produce narrow emission lines. Thus, in [1], the luminescence of Ar, Kr, and Xe clusters is considered, which arises when particles are removed from clusters, due to the necessity to dump excess energy, i.e. the contribution to radiation is provided by the fragmentation of clusters.

The input of molecules containing metallic atoms into plasma is used for cluster light sources [2]. The interaction of a cluster beam with a powerful femtosecond laser pulse is used to create efficient, compact X-ray sources [3]. It is noted in [4] that the appearance of soft X-ray radiation of neon under the influence of femtosecond laser pulses (after cooling the gas below 150 K) clearly indicates the formation of clusters formed by neon atoms. X-ray spectroscopy is a more sensitive indicator of the presence of small clusters than the Rayleigh scattering method.

The inevitability of the formation and fragmentation of clusters in excitation sources of radiation, prompts us to investigate the role of clusters in the emission and absorption of light in order to take this fact into account when interpreting atomic spectra. In this connection it is interesting to consider the work of N.G. Gerasimov [5], in which the optical spectra of binary mixtures of inert gases are investigated. It was shown that in the mixtures (when an admixture less than 0.1% of a heavier gas was used in the case of a small addition), the observed intense narrow-band VUV radiation is not due to atomic transitions but to spectroscopic transitions of the heteronuclear molecule.

Knowing the composition of plasma and the processes occurring in the excitation sources of spectra (ESS) is necessary to optimize the functioning of the existing ESS, to create new effective radiation systems, and to develop fundamental physical theories and models, such as the theory of atomic spectra and the atomic model.

**2. Atomizers and excitation sources of spectrum**

Atomic optical spectroscopy usually uses flame, furnace, electric discharge, laser and plasma as ESS.

**2.1 Flame. 2.2 Arc, arc plasmotron, arc discharge in high-pressure lamps. 2.3 Spark. 2.4 Plasma discharge. 2.4.1 Inductively-coupled plasma (ICP). 2.4.2 Microwave plasma discharges. 2.4.3 Electrodeless high-frequency lamp. 2.4.4 Ball bulb. 2.5 Glow discharge, Grimm discharge. 2.5.1 Hollow-cathode lamp (HCL). 2.5.2 Low-pressure lamp. 2.5 Laser ESS.**

**2.7 Gas lasers: gas-discharge, gas-dynamic, ionic, recombination, excimer**

**3. Methods of producing clusters**

A careful reader can find more information about the producing and properties of clusters elsewhere [2, 3, 22]. Cluster is a system of bound atoms or molecules and being a physical object it is an intermediate class between molecules and condensed matter. In the current work all particles containing more than one atom are referred to clusters.

Clusters of metals, carbon and other refractory elements are characterized by a strong bond (1 – 10 eV) due to the clusters with weak Van der Waals forces (~ 0.05 – 0.5 eV). They do not collapse at strong excitation when the energy for one atom in a cluster is higher than 1 eV (see, for example, [23]).

**3.1 Ionic sputtering of solids. 3.2 Laser generation of clusters. 3.3 Method of generation of cluster beams from gas or vapor. 3.4 Aggregate cluster generator. 3.5 Plasmic methods of clusters production. 3.5.1 Method of cluster generation based on high-**

**pressure afterglow plasma. 3.5.2 Cryogenic plasma. 3.5.3 Aerosol spraying in plasma. 3.5.4 Arc discharge. 3.5.5 Spark discharge. 3.6 Magnetron and glow discharge. 3.7 Microwave discharge**

### 4.4.1 Radiation source plasma – cluster plasma

Cluster plasma represents itself a low ionized gas, containing clusters. To substantiate the thesis that traditional sources of spectra excitation plasma is a cluster plasma lets juxtapose conditions in which clusters form and exist (section 3) with processes taking place in light sources (section 2). We will take into account that cluster producing methods are concerned with beams of large (N ~ 1000 – 100000) stable particles N, that are obtained in large quantities, whereas for spectroscopy presence of small metastable clusters (N ~ 2 – 1000) in ESS may be sufficient enough or more crucial.

In ESSs of spark, arc, laser, glow discharge type and light sources such as FCL, ball-point lamps, high and low-pressure lamps as well as in gas lasers sputtering and cooling of explored material in buffer gas and/or plasma takes place (section 2). These processes are followed by formation of different size particles consisting of many atoms (section 3). This is confirmed by the fact that cluster formation from the evaporated vapor takes place in any gas system with varying temperature [43]. In radiating media – in SES torch, in arc, in thin and long capillaries of gas lasers – concentration of atoms, ions, electrons as well as temperature differs in various regions of plasma.

In such ESSs in which the explored substance is injected in the shape of aerosol: flames, ICP, arc plasmatrons – clusters will form similar to their production method of aerosol injection into plasma (subsection 3.5.3 and 3.5.4). After desolvation of aerosol micro/nanoparticles are obtained (small crystals of oxides, chlorides, fluorides etc.), which then are being evaporated and/or sputtered by ions and electrons of plasma. In this case, small clusters can form and grow in regions with lower temperature. Metal-containing clusters can be injected directly on to SES plasma in the shape of suspensions and finely divided powders, which is practiced in analytical atomic spectroscopy. Clusters in this case form as a result of material sputtering by plasma ions (subsection 3.1).

Injection of metal-containing molecules into plasma is the method of generation of intensive atomic beams for cluster sources of light. The vapor pressure of volatile compounds at low temperatures allows treating those as gases.

In case of thermal atomization and spectra excitation material is evaporated in the inert gas medium (for example in atomic-absorption analysis evaporation of sample from the furnace occurs in the argon

flow). Similarly, in case of cluster obtaining the atomic vapor which is formed in the furnace is thereafter extended in vacuum through the nozzle. For example [44], the flow of tungsten evaporated atoms, obtained from metallic tungsten at the temperature of 4500 K, is cooled by a collision of tungsten atoms with argon atoms and eventually condenses into clusters. The buffer gas role is reduced to drawing aside of the redundant heat, which promotes cluster growth [3].

The obvious similarity to recombination lasers excitation conditions [21] (and the majority of other discharges) is retraced in the method of cluster generation based on afterglow plasma because in high-pressure discharge with small adding of metal to the buffer gas clusters are formed outside the discharge cord in the afterglow plasma.

Laser plasma is a source of single and multionized atoms (subsection 2.5), negatively charged ions, neutral particles (with low and high energy) and clusters [17].

### 4.2. About the possibility of gas clusters formation in ESS

Gas plasma seems to be the least burdened by the presence of clusters, that is why it is necessary to take a more detailed look at the analysis of gas excitation conditions.

In order to obtain narrower atomic spectral lines, they seek to lower the temperature of the radiating medium. At the same time reaching lower temperatures is an important condition of gas clusters formation (subsection 3.5.2).

In gas lasers (subsection 2.7) conditions corresponding to at least one way of cluster production (subsection 3.5.2) are reproduced during the radiation excitation.

In gas lasers in order to form the active medium electric discharges are used: glow, high frequency and arc discharges as well as in traditional SESs.

In gas dynamical lasers (in order to obtain the inversion) the process of gas dynamical "freezing" by gas extension and cooling is used. The subsidiary gas (argon or helium) only takes away the redundant heat energy from the radiating gas (just like in clusters production method). Serious demands are claimed to the depth of cooling of gas flow in case of ultrasound cooling. In carbon dioxide laser the gas flow cooling depth is 40 – 80 K [20]. Carbon monoxide laser possesses the high intensity only at low temperatures [18]: the tube with active medium was lowered into liquid nitrogen (77 K) in order to lower the temperature. These are conditions of cryogenic plasma existence [subsection 3.4].

Excimer lasers usually operate at high pressures and low temperatures, which corresponds to cluster formations of any gases.

**4.3** The carried out analysis of the experimental material shows that conditions of cluster formation and existence (section 3) are obviously similar and in many cases – identical to conditions of radiation excitation (section 2).

Theory of atomic spectra – is a descriptive theory (and a good mnemonic rule) and at the current stage, it does not pretend to an explanation of true nature of atomic spectra.

Proceeding from the ability of molecules and clusters to give narrow lines of photon emission and luminescence, the formation (or decaying) of polyatomic particles in the SES plasma should be taken into account.

It might be supposed that some forbidden lines appertain not to atomic spectral lines but to those of molecules or clusters.

Proceeding from the inevitable presence of clusters in traditional [1] and specific radiation sources (considered above), the formation of similar particles in solid-state lasers (including semiconductor lasers) might also be assumed. The citation form [36] may serve as a basing for that assumption: "metallic clusters occur on ionic crystals or photosensitive glasses during the irradiation by high energetic electrons, hard UV, and X-ray photons". These are themselves methods of laser pumping. The initial presence of complex particles in active media of solid-state lasers might be assumed: neodymium clusters in crystals and glasses (the neodymium lasers), chromium clusters in corundum (the ruby laser).

From the analysis of the experimental material comes impression that in SESs gas lasers the selection of atomic spectra excitation conditions is directed to the formation of clusters in the certain range of sizes and/or states (crystal or liquid).

## References

1. E.A. Bondarenko, E.T. Verkhovtseva, Yu.S. Doronin, A.M. Ratner, The influence of the cluster size on the energy relaxation manifested through the luminescence spectra of the Ar, Kr, and Xe clusters, Izvestiya. AN, Ser.: Fizika, Vol. 62, 1103 – 1106 (1998).
2. B. M. Smirnov, Cluster plasma, UFN, 170, 495 – 534 (2000).
3. B. M. Smirnov, Generation of cluster bunches, UFN, 173, 609-648 (2003).
5. G. N. Gerasimov, Optical spectra of binary mixes of inert gases, UFN, 174, 155 – 175 (2004).
22. Yu. I. Petrov, Clusters and small particles, M.: Nauka, 1986.

# E: Clusters in radiation sources. Part II. Atomic and ionic beams, ionic traps, beam-foil-spectroscopy

The carried out analysis of experiments with ionic and atomic beams, that are generated in order to obtain atomic spectra or radiation parameters, tell about the presence of clusters in beams and ionic traps. This should be considered while interpreting the belonging of spectral lines or determining of radiation parameters.

## 1. Introduction

Wide application of atomic, ionic and cluster beams in physics and technology presupposes the reliable knowledge of their composition and processes occurring in them.

In the current work, the formation of clusters in atomic, molecular, ionic beams and ionic traps is examined – these are specific light sources, that weren't included in the first part of the research [D0].

Using atomic beams, we can decrease the width of a spectral line without utilizing low temperatures [6]. To excite the beam radiation, the electron shock, light irradiation and target collision are used.

In all specific radiation sources (except atomic beams) considered in the current work, ions with multiple charge (IMC) are most commonly used. IMC spectroscopy has always been of interest for pure physics (in research of atom's structure the precise measurement of IMC energy levels ensures the validation of atom's structure theory) and applied science as well (plasma diagnostics and development of X-ray spectroscopy).

Having a number of limitations, beam-foil-spectroscopy is used to determine the lifetime of excited states of atoms and ions [7].

Characteristics of optical (and X-ray) radiation of ions such as a lifetime of excited states, oscillation force, ionization potential are also determined in ionic traps and guard rings of accelerators [8].

The aim of this work is to show the possibility of formation and fragmentation of clusters in specific excitation sources of atomic spectra (ionic and atomic beams, ionic traps and beam-foil spectroscopy), basing on the analysis of the experimental material.

## 2. Atomic beams in spectroscopy

Until the middle of the last century, atomic beams were widely applied for the determination of optical radiation characteristics [6]. The advantage of atomic beams consists in the practical elimination of Doppler's line broadening. This is achieved by the observation in the

direction perpendicular to the atom motion. Despite the sufficient advantages of atomic beam sources compare to other sources in obtaining narrow spectral lines, they had found a wide application in spectroscopy method because of construction difficulties and low precision of measurements.

### 3. Spectroscopy of ions

Lately, much effort has been directed to studying of plasma radiation in regions of UV spectrum: vacuum ultraviolet (VUV) and extreme ultraviolet (EUV) [8 – 14].

Since the main object of the current research is ions, let us take a look at some devices that are used to generate IMC. To get closely acquainted with physics and technology of IS you can go to collective monographies [15] and [C0].

**3.1 Production of ions. 3.2 Ionic traps. 3.2.1 Ionic traps with electron beam EBIT[29 – 31, 32]. 3.3 Experiments on the guard ring for heavy ions**

**3.4 Ion beam interaction with a target. Beam-foil-spectroscopy**

The difference of obtaining IMC by the stripping method from electron shock ionization consists in the following: in the first case, fast ions and cold electrons-targets are utilized, in the second – on the contrary: cold ions and fast electrons.

For a long time, the beam-foil spectroscopy had been the only technique capable of measuring lifetimes of ions of any element in any charge state. In this method, the beam of fast ions is sent through the thin foil, where it collides electrons of targets material [7].

In order to precisely determine optical properties of which particles are being measured it is necessary to clearly know the reliability of extraction and identification of ions of the given charge multiplicity. In order to be sure in the pureness of atomic and ionic beams, used in the determination of optical characteristics, we shall examine the possibility of cluster formation in beams and traps.

**4. Clusters in atomic and ionic beams and ionic traps**

You can get the full information about producing and properties of clusters in [34 – 37].

**4.1 Cluster formation during obtaining of the atomic beams**

Usually, atomic beams are obtained from substances which exist in condensed state at normal conditions [6]. It is considered that all materials evaporate mostly as atoms and in less degree as dimers and

trimers; major components of the saturated vapor of a metal consist mostly of clusters: from dimers to decamers [37].

In order to achieve the maximum sensitivity of spectral measurements on atomic beams, they increase their intensity by increasing the vapor pressure with the increased temperature in the cell. This may bring the effusion regime of the atomic beam outflow closer to the gas dynamic regime. In the first case the saturated vapor in the effusion camera serves as a source of the atomic (molecular) beam, in the second case – the molecular beam is formed at the end of the gas dynamic jet and consist, besides everything else, of clusters, that were formed during the process of condensation of adiabatically extending gas.

The overgrowth of the outlet of the effusion cell due to vapor condensation will lead to a change of its shape: lengthening (and formation of something like nozzle which is used in cluster production). Utilization of capillaries instead of outlets in thin lids promotes the cluster formation in the atomic beam. Also, a partial reflection of the beam from outlet edges or narrow collimating slit leads to additional alterations in the beam. In this case, the substance of the beam that is deposited at the edges may be resputtered by atoms of the beam in the shape of small clusters.

High pumping rates used in order to obtain the high vacuum in the device lead to beam enrichment by clusters since lighter atoms are scattered and pumped in the first place.

**4.2 Cluster formation during the spectra excitation in atomic beams**

In order to obtain atomic spectra and radiation parameters, they use the excitation, ionization of atoms (or ions) by the electron beam or laser beam. The occurrence of clusters (or their fragments) in beams may be caused by the fact that the beam irradiation by powerful streams of electrons (or laser photons) leads to the formation of cations and/or anions and also to altering of trajectories of some part of atoms or ions due to electron pressure (similarly to the electron wind in plasma accelerators) or light pressure (similarly to radiation accelerators). This causes ion-ionic and ion-molecular reactions in presence of neutralizing electrons (primary or secondary). Usually, cluster ions are formations of greater stabilitythen neutral complexes.

**4.3 Clusters on ionic beams**

**4.3.1 Beam compound's measurements during its formation, transportation, and recharging**

Canal rays may serve as an example of alterations occurring with the beam during motion [65]. If there is a narrow aperture in the cathode,

positively charged ions, moving in the dark cathode space, go through it and form canal rays in the after cathode space. Gas on the way of such beam glows. Due to recharging (and/or stripping) the beam also consists of fast neutral molecules and atoms that are partially excited, and negatively charged ions. Under the influence of the magnetic field the canal ray splits into three beams: positively charged, negatively charged and neutral. During the secondary passing through the magnetic field, each of these beams gets split into three again. This tells us that beams of ions and neutral particles undergo changes constantly.

It is also stressed in [66] that real ionic beams are rarely laminar and that in every place there are trajectories that are inclined to the main axis which leads to the non-laminar stream and thus to interaction inside the beam.

At fast pumping rates (that are used to obtain the maximum vacuum) enrichment of the ionic beam emerging from the IS is possible. It is similar to the example that was quoted many times by now [34], when the afterglow plasma moves after the nozzle, atomic particles are scattered and pumped out of plasma, whereas the collision of cluster with atoms doesn't lead to noticeable scattering due to its large mass, and over time plasma stream transforms into a cluster stream.

It is stated in [67], that reactions between ions and neutral molecules may take place during the beam's motion from the source to a detector in mass-spectrometer, which leads to complication of mass-spectra, observed at a high sensitivity that is needed to analyze IMC.

Processes occurring while the beam is in a mass spectrometer or an accelerator taking place under influence of deviation in magnetic and electric fields, multiple focusing, defocusing, cooling, bunching, rebunching etc. alter its compound and properties [68].

### 4.3.2 Alteration of beams compound during stripping

The stripping of gas targets or foils is widely used in accelerators in order to obtain IMC of high charge multiplicity [69 – 73].

### 4.4 Clusters in beam-foil spectroscopy

As it was shown in subsection 4.3.1 the beam, coming upon the target (to detect spectroscopic data after passing it), has a complex composition. Developing the theme of complication of beams that passed through the target, let us take a look at factors that might lead to the formation of complex metastable particles, which fragments may be further concerned as IMC and their spectroscopic lines emitted be very fast fragments or clusters may be assigned to atomic particles, during the process of stripping.

During the ion bombardment of thin targets besides the regular sputtering, the forward sputtering of the material also takes place, which is confirmed by the presence of spectral lines of targets atoms in emission spectra.

In case of using thin targets (5 – 300 nm), the emission of such particles is observed from both sides of the foil during its bombardment by ions, molecules or clusters. The interaction of hydrogen clusters $H_N^+$ ($N = 1 – 13$) with carbon foil was investigated in [77]. The yield of electrons, formed in the energy range 40 – 120 keV/proton, as a function of cluster size and foil thickness was measured in the direction of bombardment and in the opposite direction. It was quite a surprise that $H_9$ clusters were penetrating the 300 nm thick foil.

Many experiments in beam-foil spectroscopy are carried out with carbon target [7], and due to experimental and theoretical investigations, small clusters $C_N^+$ are very active, which increases the possibility of mixed carbon clusters formation.

**4.5 Cluster formation in accelerators**

**5. Conclusions**

It is stated in [49] and a number of other sources that cluster emission during the interaction of high energy particles with solids is one of the least understood section of physics and that's why close attention is paid to this question [49 – 53].

Ion production is accompanied by cluster formation [C0] since the major IS (arc, spark, laser, plasma etc.) as excitation sources are in the same time sources of cluster plasma [D0]. In certain conditions for any element, there may exist multinuclear clustersof such size that during their decay the overlapping of fragment ions and IMC peaks in mass-spectra occur. For spectroscopic measurements, it is hard to extract a single-atomic beam or an IMC beam with a certain charge multiplicity, without the presence of complex particles in them.

The peculiarity of IMC spectra is that they are significantly wider than those of regular atoms, which typically possess very sharp and well-defined lines of spectral emission [29, 84]. The significant wideness of IMC spectra may be explained, among other factors, by the emission of clusters, possessing narrow emission lines, and/or fragmentation of multiatomic formations. It is known, that generation of fast ions leads to the deformation of spectral line profiles due to Doppler's effect [86]. The Coulomb's explosion of clusters of the same size gives particles with discreet energy [87] as an outcome, and during the multiatomic destruction of different sized clusters $A_N$, identical particles $A$ with different ("quantized") energies, different ("quantized") Doppler's shift is

formed (you can compare with discreetness of hydrogen ions energy, obtained by recharging (subsection 4.3.1)).

The excitation of ionic and atomic beams causes emission of visible, VUV, EUV and X-ray spectra. Clusters also effectively emit in these spectrum regions.

**5.1** Comparison of excitation methods of atomic spectra with cluster production methods [1] and ion production methods (sections 3, 4 and [C0]) shows the similarity of obtaining all three.

Beam compound is determined by the initial presence of clusters in them and their collimation, transportation, deviation, acceleration, bunching, cooling and interaction with target lead to farther complication of beams.

From the current article and [C0, D0] the necessity of taking into account of the contribution of complex particles during the interpretation of atomic spectra and obtaining of most important atomic characteristics, that serve as a base for fundamental physical theories, becomes obvious.

## References

84. E. B. Aglitsky, V. V. Vikhrov, A.V. Gulov, etc., Spectroscopy of multicharged ions in hot plasma, M.: Nauka, 1991.

# F: Atomic spectroscopy of plasma which is in a magnetic field. Causal relationship between Doppler's and Zeeman's effects

The understanding and consideration of macroscopic processes, occurring in the magnetized plasma, are important for atomic spectra systematization and direct influence on radiation sources during the optimization of their operation.

In the current research, the analysis of properties transformation of radiating plasma after the application of magnetic field is presented. Attention is accented on sharp alteration of plasma parameters during reaching of critical magnetic fields.

The special role of Doppler's effect, contributing into Zeeman's effect during macroscopic movement of emitting (absorbing) particles, such as anomalous diffusion across the magnetic field, rotating and wave motion, is noted.

The theory of macroscopic nature of Zeeman's effect is suggested and the model clarifying it is considered. The schemes of experimental verification of the hypothesis are offered.

The work is of interest to atomic spectra theory and thus to the theory of atomic structure.

## 1. Introduction

Line splitting in atomic and molecular spectra under the influence of magnetic field (here and after MF) is called Zeeman's effect (here and after ZE).

Explanation of ZE's from the strictly inner atomic point of view absolutely doesn't consider many macroscopic phenomena and processes, occurring in radiating plasma under the influence of the external MF. In this case, alterations occur in magnetized plasma, which not only or rather not so much affects the inner state of emitting particles but the whole macroscopic system or its parts.

Objectives of current work include the analysis of macroscopic factor's role in the light emitting by magnetized plasma and their contribution into broadening of spectral lines (here and after SL). It is important to distinguish alterations in spectra, which are caused by changes in a macroscopic system, from quantum effects, determined by electronic structure of radiating (absorbing) atoms.

One of the main roles in explanation of ZE nature is assigned to Doppler's effect since in multiple experiments with magnetized plasma different forms of directed movement of radiating (absorbing) atoms and ions, such as anomalous diffusion, rotation, and waves, are found.

The possibility of estimation of electrons specific charge, based on macroscopic knowledge of ZE, is shown, Model and hypothesis that show the macroscopic nature of ZE are suggested, schemes of experimental validation are discussed.

## 2.1 Macroscopic properties of magnetized plasma. Critical magnetic field

Since the discovery of ZE, properties of magnetized were comprehensively investigated. Motion of radiating (absorbing) atoms and ions, considered in this paper as macroscopic, are: the anomalous diffusion across the MF, rotational and wavelike motion, each of these may affect the ZE through the Doppler's effect. Rotation of electrons in atoms is related to quantum and not considered here.

Significant splitting of SL may occur at critical MFs where plasmas properties change dramatically. In this case transitions from anomalous ZE to normal or quadratic Zeeman's effects may be observed, there also may occur (disappear) "forbidden" lines and other SL.

## 2.1.1 Anomalous diffusion of magnetized plasma

Investigations of plasma diffusion in the magnetic field have clearly shown that the anomalous transportation of charged particles across the MF is a quiet typical phenomenon for magnetized plasma [6].

**2.1.2 Spiral instability of electric charges in the magnetic field.**

**2.2 Peculiarities of spectroscopy on the magnetized plasma [27 – 39]**

The spectra picture depends on the radiation parameters: size, slope, the position of the plasma cord, concentration of radiation centers in it, speed and radius of its rotation etc.

Light source position, its size and form (cylinder, cord, hollow cylinder, ring, spiral etc.), in their own, depend upon conditions of charge burning, charge current, pressure, type of gas and its flow rate, size of the charge tube, form, type and size of electrodes etc., besides the source type and magnitude of the MF.

The shape of SL depends upon the width of slits, the way that is used for their illumination, the direction of observation and a number of other experimental peculiarities, and the compensation of the spectral equipment.

Discharge, during its rotation in the MF, deviating from the electrode axis, occupies only a certain part of interelectrode space. Not only the plasma cord emits the radiation but also does the region that it has just left.

Significant differences occur in the case of axial (lengthwise) and perpendicular (transversal) observation of plasma: the sensitivity of measurements during the axial observations is almost ten times higher than during transversal observations.

As an obvious example of spectra alteration in the MF may be taken the work [29], in which the part of the charge tube between poles of the magnet had turned intensively blue in the electrodeless argon plasma, while the other part had emitted the red light, that allowed to visually distinguish arc and spark spectra of argon.

**2.3 The causal relationship between Doppler's and Zeeman's effects**

The directed movement of atoms, ions in magnetized plasma in the case of anomalous diffusion, rotation, and wavelike motion will lead to shift (and/or broadening) of SL due to Doppler's effect.

The degree of SL splitting depends on characteristics of spectral equipment: slit widths, type of condenser system, diffraction lattice, interferometer etc. Since the optic system of the device significantly cuts of light beams from radiating plasma particles, approaching the detector,

as well as particles, moving in the opposite direction, the Doppler's shift will be observed on both sides of primary SLs.

$$\Delta\nu = \nu_0 \, (V/c) \cos\theta \tag{1}$$

where $\nu_0$ – wave frequency of the observed line, $V$ – velocity of the radiating object, $\theta$ – angle between velocity $V$ and direction of observation, $c$ – the speed of light.

The estimation of normal ZE [1, page 321] gives $\Delta\lambda = \pm 4.67\lambda^2 B$ (l – wavelength in cm); $\Delta\nu = \pm 4.67 \cdot 10^{-5} B$ (in cm-1), B – induction of the MF in Gs. At a rather high field of B=20 kGs, for $\lambda$=500 nm, the splitting $\Delta\lambda = \pm 0.023$ nm is comparable with Doppler's broadening of components, so not single components but the summary broadened outline, which width depends on the magnitude of the magnetic field, is observed.

### 2.3.1 The role of radiating plasma rotation in Zeeman's effect

In the external magnetic field, several types of rotational motion of radiating plasma particles are possible: wobbling of the plasma cord around the axis of the MF, cord's rotation around its own axis, rotation of the media carried along by the radiating cord and rotation of atoms around their axis. It is necessary to consider that radiuses of various rotations are different. This may lead, along with everything else, to different illumination of the spectral apparatus's slit (condenser lens) and to different observation angles from various rotational motions. Consequently, this factor will influence the outcome of summation of wobbling speed with velocities of other rotations of the radiating charge.

ZE is quiet multiform [28, 40], which might be explained by Doppler's effect, caused by the motion of radiating centers. Various splittings of SLs and their broadening occur due to summation and subtraction of velocities of corresponding rotational motions: wobbling and self-rotation of the plasma cord. And if the anomalous diffusion and/or various wave-like motions will contribute, spectra of ZE will be much more complicated.

Interaction of self MF with the eternal MF in certain conditions changes the scenario of radiation centers macroscopic motion.

At critical MFs "degeneracy" of any forms of motion is possible, which leads to alterations of ZE, for example to quadratic or anomalous ZE. Changes in spectra are possible when conditions of the electron or ionic cyclotron resonance in the radiation plasma are reached.

It also should be considered, that along the plasma column rotation velocities of radiating particles are different: they decrease near the wall and the surrounding cold gas [41]. This will lead to various Doppler's shifts of SLs in different points in plasma.

### 2.3.2 Rotation of radiating plasma in the magnetic field

The rotation of plasma in MF was investigated intently for a long time [42 – 45]. Some peculiarities of magnetized plasma rotation are given in [34, 35].

### 2.3.4 What rotates in magnetized plasma and in which conditions?

The short overview of the majority of works, discussed above, concerning the magnetomechanic effect [46 – 50, 53, 55] is given in [57].

### 2.3.4 Speed of the magnetized plasma rotation

In the research [46] with the help of spectroscopic method, that was used earlier in researches on the determination of the directed motion of ions in plasma [59], the rotation of the neutral gas was discovered in the positive charge columns, placed in the magnetic field.

The speed of plasma rotation in the MF was determined in [60], using the Doppler's effect, when the homopolar apparatus with rotating plasma was used for investigation of the interaction between magnetized plasma and neutral gas. The experimental setup included the system of coaxial electrodes and was placed in the axial MF, generated by iron poles of the magnet, $H_2$ and $N_2$ gases at pressures $5 \cdot 10^{-3} – 2 \cdot 10^{-2}$ mm Hg, MF $B_0$ in the center from 2 to 10 Gs, discharge current – several kA. Doppler's shift was measured on spectrograph along the chord in the equatorial plane of the charge, at the distance of 14 cm from the center. When the direction of plasma motion was changing due to alteration of the MF, C III (229,7 nm), Si III (254,2 nm) lines have been displacing on 0.058 and 0.062 nm correspondingly, which corresponded to the mean speed along the radiation direction of $3.7 \cdot 10^4$ m/s. Intensive Ballmer's were observed, but they hadn't shown Doppler's shift. The Doppler's shift was distorted during the photographing due to different velocities when plasma was accelerated and when it was permanently burning and rotating. It might be concluded from measurements that presence of the neutral gas limits the speed of plasma rotation. The absence of Doppler's shift of Ballmer's lines shows that the neutral gas doesn't move.

In experiments, carried out on the Ixion III plant in Los Alamos [61], the drift speed of deuterium was determined $V_{dr} \sim 8 \cdot 10^4$ m/s (circular motion with the frequency of $\sim 4 \cdot 10^7$ s$^{-1}$). In the next experiment [62] speed of $V_{dr} \sim 1.3 \cdot 10^5$ m/s was determined.

In the research work [41] it is also said of the dependence of plasma rotation speed in the MF upon the ionization potential of the gas. The speed was determined from the Doppler's shift as a projection along the chord of the rotational axis of atoms and ions on the radius of 22 cm and greater. The alteration of MF doubled the Doppler's shift of lines. The

maximum determined speed was no less than $1.3 \cdot 10^5$ m/s. It occurred that hotter regions of plasma rotate with higher speed than surrounding cooler regions (and speed must decrease almost to zero on the outer side of plasma border). Neutral atoms of carbon and silicon move with speeds less than $5 \cdot 10^3$ m/s. In case of hydrogen, only the upper limit of speed was observed.

The aim of the research work [64] was to investigate the speed distribution of the rotating plasma in detail, to partially extend the investigation of critical speed phenomenon (the determined one $\sim 5 \cdot 10^4$ m/s). The maximum plasma speed magnitude in the middle part of the apparatus agrees well with their earlier researches of Doppler's shift [41].

The fact, that plasma as an absolutely conducting liquid must rotate with constant angular velocity around MF's lines, that will become equipotential, was confirmed by the series of early experiments [44, 65].

An unusually high Doppler's shift was observed in ORNL on the magnetic separator of isotopes [68]. It was shown that in the low-pressure high-current arc, placed in the MF, "the skew" of ionic lines is observed, that is caused by plasma ions rotation. In the geometry, possessing the cylindrical symmetry of crossing electric and MF, charged particles may be drawn into rotation around the symmetry center. The speed of deuteron motion $\sim 3 \cdot 10^5$ m/s. In [68] the experiment in homopolar apparatus, in which plasma rotation was observed, along with everything else, by Doppler's shift of the radiation, emitted by the device, is described. Through the tangent port, the light entered the spectrometer. When the MF's direction was altered – the rotation in the opposite direction. The rotation speed, calculated by the Doppler's shift, occurred to be in agreement with calculations from another method (the current row bar).

In the research work [68] the Axion apparatus is considered, which distinguishes from the plane geometry of the homopolar setup by the prolonged form (0.86 m) and operation regimes. Deuterium with a pressure of 0.001 mm Hg. Plasma rotation was illustrated by the Doppler's effect, which was observed on carbon's line profile after the direction of the MF was reversed and by another method. The drift speed of $4 \cdot 10^4$ m/s, determined from the SL, occurred to be in agreement with the calculation of speed, carried out from applied electric and MF.

**2.3.5 Role of wavelike motion in Zeeman's effect**

Plasma, placed into an MF, is anisotropic. So waves in magnetized plasma show a significant diversity. The propagation speed and dispersion character depend on the motion direction of the wave with respect to the direction of the MF, on mutual orientation of the plane of

the wave electric field vector's oscillation and a magnitude of the MF, in which plasma is placed.

If in plasma without the MF spectra of possible waves is mainly restricted by lengthwise Langmuir and ion-sound waves and a transversal plasma wave, in magnetoactive plasma besides these waves there are many new ones. These are transversal Alfven waves, magnetosonic waves (or a magnetic sound) and their varieties, also there are such types as fast, slow, "oblique" magnetosonic waves; cyclotron resonances and cyclotron waves, including electron-cyclotron waves, low-hybrid waves and high-hybrid waves, helicons (spiral waves) and others [69 – 73].

Oscillatory movements of radiating (absorbing) particles in the wave directed to the detector and from it, depending on the observation angle, will give the SL shift and/or their broadening due to Doppler's effect. In case of additional directed motion of radiation centers (diffusion or rotation), oscillating particles will give a set of SL shifts.

Presence of oscillation modes in the magnetized plasma (subsection 2.1.1, subsection 2.1.2) may lead to series of SL shifts, peculiar to their own mode.

### 2.3.6 Doppler's effect contribution to Zeeman's effect during light reflection

In the research work [74] it is reported of SL broadening of light, scattered on Hg atoms, which corresponds to Doppler's effect. At low pressures of the radiating gas (fractions of mm Hg), the Doppler-Fizeau phenomenon is the main cause of broadening. Nevertheless, when the density of reflecting Hg vapor reaches values, corresponding to the mirror reflection, the light, reflected from such a dense hot vapor, is characterized by the width of the incident light. Likewise, there is no line broadening in case of light reflection from the aluminum mirror as well, though thermal speeds of light Al atoms are significantly higher than those of Hg atoms, and the expected SL broadening should be at least three times greater than in case of scattering on the Hg vapor. For the regular (mirror) reflection Doppler's effect is absent.

At certain critical MFs magnetized plasma (or its certain parts) may acquire properties of molecular movement or, contrarily, mirror properties. Certain regions of the magnetized plasma may possess different properties, concerning the Doppler's effect.

In addition to this, in the scattered light in directions, other than the direction of the regular reflection, change of wavelength should be observed, which is caused by Doppler's effect, nevertheless determined

not by the movement speed of single atoms, forming the mirror, but the speed of surface waves.

If we pretend that magnetized plasma (or its particular regions) is elastic fluid, then all stated above will be applicable to plasma in the MF. Numerous waves in magnetized plasma will lead to light scattering with Doppler's shifts of SL.

In plasma diagnostics [1 p.353, 75, 76] during laser irradiation, the outline of the reflected SL may split into components, which are shifted from the frequency of incident radiation. This splitting is caused by the presence of self-Langmuir (or other) oscillations. The full spectra may consist of the central narrow structure with ion-sonic component and electron satellites with shifts. In certain sense, the collective scattering of acoustic waves or plasma oscillations (plasmons) may be likened to phonon scattering in solid or on molecular oscillations. Because of that sometimes it is also called combinational [1, p. 353].

Since the Doppler's effect in affected by the observation angle, different SLs reflected on (or emitted from) the wave of the magnetized plasma, can be registered under certain angles, depending on plasma characteristics.

Light reflection in magnetized plasma may occur on rotating plasma cord when the light is emitted from all other parts of plasma. In case of screw shape of the plasma cord light will enter the spectral device after reflection from different parts of the screw, besides everything else. This may lead to Doppler's shift of SL and change of light polarization.

Besides the periodic and quasiperiodic oscillations and waves moving or quasistationary surfaces occur in plasma, in the vicinity of which the dramatic almost abrupt changes in plasma parameters take place: thermal, radiation, shock waves, and double electric layers. Light reflection (or emitting) from such surfaces will lead to alteration of radiation polarization and to shift and broadening of SL. In the research work [77] the analytical equation for the field, reflected from the heterogeneity of the moving medium, is obtained. Peculiarities of the reflected radiation, depending on the speed and size of the heterogeneity region and incidence angle with respect to the motion direction, are studied. In [78] it is shown that Doppler's shifts of frequencies may be uniquely determined when complex frequencies are taken into account and initial conditions for radiation and medium are given. In the article [79] the complex Doppler's effect is demonstrated when two complex values of frequency of the reflected light correspond to a single (material) frequency of the incident radiation.

**2.3.7 About possible macroscopic contributions in Zeeman's effect**

**2.4 Experimental investigation of Zeeman's effect**

We are compelled to quote old sources [27, 29, 31 – 33, 84 – 99] since systematization of SL and theory of atomic spectra, alongside with explanation of ZE, are based on experiments, carried out in conditions and with the use of equipment, that correspond to the technology level of that time.

**2.5 Some apparatus effects in spectroscopy of plasma in a magnetic field**

**3. Reflections, hypotheses, and fantasies about Zeeman's effect macroscopic nature**

**3.1 Similarity of macroscopic movement in the plasma in a magnetic field to intra-atomic rotation of electrons**
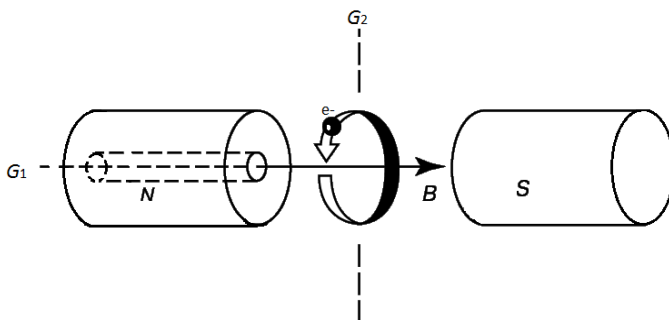


Figure 1. The scheme of Zeeman's effect observation.

Zeeman's effect can be investigated with help of spectral apparatus, installed on $G_1$ or $G_2$ position if the discharge radiates, moving in a circle between poles of the magnet (figure 1).

Suppose that the radiation receiver is situated in point G1 (figure 1). Orbits with a clockwise and counterclockwise rotation of electrons are corresponded by highly polarized light with frequencies $v_{clk}$ and $v_{aclk}$. If the orbit's plane coincides with the direction of the field, then the light's frequency $v_0$ remains constant. Thus three SL will be observed.

If we drill the aperture in the pole tip of the magnet (or take the solenoid coil instead of the magnet), then it is possible to observe two σ-components in $G_2$ direction, that are circularly polarized clockwise and counterclockwise.

If plasma as an absolutely conducting liquid should rotate with constant angular velocity around MF lines, that will become equipotential, which was confirmed by the series of earlier experiments

[44, 65]. If rotation of magnetized plasma electrons is transferred to a rotation of the plasma cord around its axis (or to a cord's wobbling around the MF axis), then SL splitting in the MF will be proportional to the angular velocity: $\omega_B = V/r$.

In the magnetized plasma, speeds of radiating particles, when observed along the direction of the MF ($G_2$ position, figure 1), directed to the detector or from it, will give splitting (broadening) of SL. The motion of radiation centers, perpendicular to the optical axis of the device(along with the receiver), will not lead to Doppler's shift of SL. Factor, affecting the splitting (broadening) of SL (when observing from the $G_2$ point), may also be the radiators rotation. In this case, radiation enters the capacitor and then goes through the entering slit, if the emitter possesses speed components, corresponding to atom, approaching the receiver, as well as atom retrograding it.

When observing plasma rotation across the MF ($G_1$ point, figure 1) multidirectional Doppler's shifts are obtained from radiating particles, approaching the detector with speed of +V and retrograding it with the speed of –V. When the emitter moves perpendicularly to the optic axis of the spectral device, the speed component directed to the receiver equals zero, and there is no SL shift. (In the last case as is it is in case of observing from the $G_2$ point, contribution of speed components, directed to the receiver and from it, during movement along the long axis of the entering slit, is possible though).

SL frequencies $\nu_{\pm}$ according to the Doppler's effect (1) increases while radiation center's approaching to the observer and decreases while retrograding:

$$\nu_{\pm} = \nu_0(1 \pm V/c \cdot \cos\theta) \tag{7}$$

Since the rotating plasma is not a point source, spectra view will depend on the radius if the plasma cord and radius of its wobbling around the axis of the MF.

In terms of Doppler's effect, this manifest itself in the dependence of the observation angle $\theta$ upon the radius of radiating plasma rotation $r$. In this case, taking (6) and (7) into consideration we will express Doppler's through the angular velocity of radiation center rotation:

$$\Delta\nu_{\pm} = \nu_{\pm} - \nu_0 = \nu_0(\omega/c) \cdot r \cos\theta \tag{8}$$

**3.2 Estimation of the specific charge e/m, based on the macroscopic nature of Zeeman's effect**

In addition to the possibility of an explanation of ZE by SL splitting and determination (rough estimation) or *e/m* from the macroscopic movement of emitters, the difference of properties of radiating

magnetized plasma from properties of plasma without the MF is convincingly shown in the research work. All this gives grounds for consideration of the hypothesis that Zeeman's effect has anon-quantum nature.

### 3.3 Hypothesis about the macroscopic nature of Zeeman's effect

Splitting of spectral lines in Zeeman's effect is caused by Doppler's effect from directed movement of radiating (absorbing) atoms in the external MF.

Quantum model of electron motion in an atom may be likened to experimentally observed macroscopic movements of radiating particles in the magnetized plasma.

### 3.4 Macroscopic model of Zeeman's effect

Let us consider the model, that clarifies the nature of ZE from macroscopic positions instead of the quantum point of view basing on real processes, occurring in the magnetized plasma.

In the rotating MF the arc discharge column wobbles [23, p. 185, figure 5.15]. Let's designate the speed of discharge column rotation with respect to MF rotation axis as $\omega_2$ and the wobbling radius as $r$, the angular velocity of arc column rotation as $\omega_1$. The increase of $\omega_1$ may be achieved by increasing of $\omega_0$ speed of rotation of the MF (and a decrease of sliding). The wobbling of the arc column leads to the motion of the surrounding medium, to medium increase the most common element of which is its rotation around the axis of the MF with the speed $\omega_3$.

Rotation of the plasma column around the MF axis with the speed $\omega_2$ – wobbling – may be likened to the orbital motion of an electron in an atom. Alongside with that the movement of the surrounding medium with the angular velocity $\omega_3$, caused by the arc's wobbling, is also similar to the orbital rotation of electron, but this motion does not belong to atoms of the plasma cord, but to radiating particles, located in the dragged medium.

Arc column rotation around its own axis with angular velocity $\omega_1$ may be likened to the spin of an electron.

To get the full picture, besides the possibility of the simultaneous existence of several plasma vortices in the MF, the rotation of atoms around their own axis may be added.

The splitting of SL in the macroscopic model of ZE is explained by changes of directed movement of radiating particles in the MF. When observing spectra across the MF multidirectional Doppler's shifts are obtained from particles approaching the receiver and retrograding from

it. Unshifted lines emerge due to the motion of radiating particles across the optic axis of the spectral device.

Basing on the suggested hypothesis multiple types of SL splitting in MF are explained by summation of speeds or different rotational (and other) movements of radiating particles. It coincides with the quantum description, when the summation of the orbital moment and spin lead to complex types of SL splitting, emerging on different images of ZE. That is quantum spin-orbital interaction is similar to summation-subtraction of wobbling (orbital) and self ("spin") rotations of the plasma column. Superposition of movements with summary speeds ($\pm \omega_2 \pm \omega_1$) may be compared with L – S-links in the quantum spectra theory.

Alterations in spectra when critical MF is reached is caused by abrupt changes in plasma properties. For example, degeneracy of some forms of motion is possible: coincidence of cyclotron frequencies of electrons or ions with rotation frequencies of the plasma cord and its wobbling; ceasing of plasma cord rotation around its axis, coincidence of its wobbling radius around the MF axis with the radius of its rotation around its own axis, ceasing of cord wobbling etc. Separation of plasma cord into several vortices is possible. These alterations in plasma may manifest themselves either in spectra simplification due to transition from the anomalous ZE to the normal ZE or in the appearance of the quadratic ZE or other transformations in spectra.

**3.5 Experimental validation of macroscopic factors role in Zeeman's effect**

It is logical to suppose that, if during plasma magnetization form, size, bending, sloping, position of the emitter with respect to the optical axis of the spectral device are altered, and new forms of motions of radiating particles emerge in plasma, then these alterations (some of them) must manifest themselves in spectra.

To confirm the hypothesis about the macroscopic nature of ZE it is important to do the following: to reveal factors leading to alterations in the MF. To seek out links between critical MF, plasma parameters, and its radiating ability. To find correlations between changes of macroscopic properties of the magnetized plasma and alterations in spectra. To determine the contribution of geometrical parameters of the magnetized emitter in spectra (spatial positioning, form, size, sloping etc.)

**3.5.1 Experiments with the rotating magnetic field. 3.5.2 Experiments with atomic absorption**

**3.5.3 Variants of experiments with the mechanical model of plasma**

The mechanical model of plasma can be constructed – "the construction", combining emitter's (absorber's) wobbling and its rotation around its own axis (see [80] for examples). Foreseeing of rotation of speeds and radii of wobbling and self-rotation of the emitter as well. The contribution of angular velocities of the emitter (absorber) in ZE may be estimated. It is possible that summation-subtraction of speeds of various motion of emitters (absorbers) will be observed. The presence of surveyed emitters (absorbers) of different size and form will allow verifying the role of these factors in spectroscopy. "The construction" will also allow checking the contribution of emitter's displacement from the optic axis of the apparatus.

Studying of alterations of reflected spectra occurring due to independent rotations (wobbling, rotation of "the column") and their different combinations are possible by irradiation of "the construction" with light from different angles and observing of changes in reflected spectra. Doppler's laser anemometry should be used [54].

**3.5.4 Verification of position and charge change of the emitter contribution in spectra. Verification of rotation's role of the radiating plasma in Zeeman's effect. 3.5.5 Verification of the wavelike motion in Zeeman's effect. 3.5.6 Light reflection from plasma. 3.5.7 Some considerations, concerning the experimental verification of Zeeman's effect (Temperature shift. Plasma interaction with radio waves). 3.6 Observations, considerations, and fantasies, concerning the nature of Zeeman's effect and theory of atomic spectra.**

**3.6.1 About light's interaction with the magnetized plasma (The role of plasma crystals. Diffraction of light in plasma waves. Light's absorption in plasma. Light's polarization)**

As an example, confirming the possibility of the polarization plane rotation in the rotating plasma, the double magnetic refraction in gases and vapors, which as predicted by Fokht basing on his theory of magneto-optical phenomena may be quoted. Eventually, he had managed to observe this phenomenon in Na vapors in the vicinity of D-lines. Following this work, Zeeman and others had shown, that Fokht's theory quantitatively proves to be correct by the nearness of absorption lines, when the anomalous dispersion is observed. Now it is commonly considered that double magnetic refraction near the absorption line is directly linked to ZE.

About the role of "non-quantum" properties of light in the context of quantum interpretation of atom's model success

The model of an atom is based on the experimental spectroscopy, which is linked to light's transformations (dispersions, diffraction, refraction, polarization, interference) after its interaction with parts of the spectral device.

Each of discrete atomic states, transition between which is accompanied by emission light's quantum, is characterized by four quantum numbers. Permissible variations of these numbers are determined by selection rules. For example, selection rules for the magnetic quantum number $m$ ($\Delta m = 0, \pm 1$) are the basis for the quantum theory of radiation polarization. When $\Delta m = 0$ the linearly polarized light is radiated (absorbed). When $\Delta m = +1$ – the light with right-handed circular polarization, when $\Delta m = -1$ – the light with left-handed circular polarization [103].

One of the possible reasons of using small whole (and divisible ½) numbers and simple operations with them in selection rules and other cases of atom's "quantization" is instrumental. The apparatus mainly selects the light of two directed movements of radiating particles approaching the receiver and retrograding it. Example of "instrumental selection rule" in ZE: the SL shift $\Delta v$, occurring due to emitters movement towards the detector: "$+\Delta v$" – is "+ 1"; from the detector: "–$\Delta v$" – is "–1"; perpendicularly to the optical axis "$\Delta v$" – is "0".

Other possible reason for operating simple numbers when "quantizing" atom is instrumental-wave.

In spectra decomposition picturethere is a reiteration of spectral series in different regions of wavelengths. The spectra order $m$ is a number 0, 1, 2 etc.

Maximums and minimums on interference pictures emerge due to the superposition of coherent waves with the same polarization and phase shift being equal to whole or half of the number of wavelengths. From this multiplication of wavelengths with numbers $\pm½, 0, \pm 1, \pm 2, \dots \pm m$ occur, which are also operated in the quantum interpretation of phenomena.

In Zeeman's effect split SL possess different polarization. In case of polarized light that again numbers are operated which present in formulas with the factor $\pi$.

Linearly polarized light is a certain case of elliptically polarized light, occurring when phase difference is 0 or $\pi$, polarization ellipse degenerates into a straight line.

Circularly polarized light emerges due to the superposition of mutually perpendicular waves of the same amplitude when the phase difference is $\pm\frac{1}{2}\pi$.

Transition to wave mechanics in the theory of atomic structure had made the description of intra-atomic processes closer to the description of interference, diffraction pictures in optics and atomic spectroscopy, which itself is a source of experimental data for atomic theory.

## 4. Conclusions

### 4.1 Applicational meaning of research

If rotations in plasma and/or wavelike motions cause alterations in spectra and ZE, then it is possible to control the radiation reconstruction in lasers and spectral analysis by generating these processes with determined parameters. For example, if the sound (or radio weave) of certain frequency, power, direction changes frequencies of emitted (absorbed, reflected, refracted) light, then this might be used in analytical spectroscopy (for unselective absorption/radiation correction), lasers, plasma diagnostics.

### 4.2 Scientific meaning of research

The research work has shown that in theory of atomic spectra and in ZE theory it is impossible to persist in "abstracting" from macroscopic phenomena, occurring in the magnetized plasma. Especially since the theory of atomic spectra may be considered now only as a convenient method of systematization and description of the colossal experimental material. To prove the adequacy of the theory of atomic spectra it is necessary to prove the adequacy of the theory of atomic structure, whereas the theory of atomic structure itself is based on the atomic spectroscopy.

Even in the case of the falsity of the hypothesis about the macroscopic nature of ZE, the research work will be valuable for quantum description of spectra and ZE, since taking into account contributions of macroscopic phenomena in ZE will allow us to reduce the number of SL splitting types in the MF and improve systematization of SLs.

The irrefutable advantage of macroscopic ZE model is its obviousness and its realism: occurrence of motions in plasma cause Doppler's effect. The opportunity of direct experimental validation is attractive.

The meaning of experimental verifying of the hypothesis about the macroscopic nature of ZE is determined by the fact that ZE is one of the most important experimental proofs of the justifiability of quantum mechanics bases.

Since various wavelike (or other) motions are present in the radiating plasma without external MF, and also due to presence of self MF of the discharge, it is necessary to consider their possible contributions into spectra formation, taking into account the numerous reradiations, reflections of light, generated by plasma, as well as radiation of the surrounding medium.

The conclusion that operating with small whole (or divisible ½) numbers (quantum numbers, selection rules etc.) in the atomic theory is linked with the basing of this theory on the experimental atomic spectroscopy as well as properties of light waves and their transformations when interacting to each other is worth considering.

### References

1. B. H. Ochkin, Spectroscopy of low-temperature plasma, M.: Fizmatlit, 2006.
6. A. A. Gurin, L. L. Pasechnik, A. S. Popovich, Diffusion of plasma in magnetic field, Kiev: Naukova Dumka, 1979.
23. P. A. Kulakov, O. Ya. Novikov, A. N. Timoshevsky, Stability of burning of an electric arch. Low-temperature plasma. Volume 5, Novosibirsk: Nauka, 1992.
34. N.V. Buyanov, V.P. Zamarayev, A.K. Tumanov, Increase in accuracy of the spectral analysis magnetic stabilization, M.: Metallurgy, 1971.
35. D. G. Muhambetov, Spectroscopic investigation of the effect of an external magnetic field on the distribution of matter particles in a low-temperature arc plasma. The abstract (01.04.05 – Optics), Alma-Ata, Kaz.GU, 1975.
37. A glow discharge of a direct current. Under the editorship of V. Fortov, Encyclopedia of low-temperature plasma. Introductory volume, M.: Nauka, 2000.
42. Rotation of plasma by electromagnetic fields. Bibliographic Index, Novosibirsk: AS USSR, Institute of thermophysics, 1978.
54. B. S. Rinkevichus, Laser diagnostics of streams, M.: MEI, 1990,.
71. A. B. Timofeev, Resonance phenomena in plasma oscillations, M.: Fizmatlit, 2000.
72. T. Stiks, Theory of plasma waves, M.: Atomizdat, 1965.
73. B. Ellis, S. Buksbaum, A. Bers, Waves in anisotropic plasma, M.: Atomizdat, 1966.
75. Methods of plasma research, M.: Mir, 1971.
76. Diagnosis of plasma by scattered radiation. Under the editorship of V. Fortov, Encyclopedia of low-temperature plasma, Volume II, M.: Nauka, 2000, pp. 569 – 572.

80. U. I. Frankfurt, A. M. Frenk, Optics of moving bodies, M.: Nauka, 1972.

101. V. A. Bazylev, N. K. Zhevago, Radiation of fast particles in matter and in external fields, M.: Nauka, 1987.

# G: Interpretation of Moseley's law and atom's model. "Cluster quantization" in atomic spectroscopy

In the research work, the analysis of the interpretation of Moseley's experiments is given. The invalidity of interpretation of X-ray spectra link with the charge of element's nuclei is shown. The different interpretation of Moseley's law is suggested. The number of "claims" to the Rutherford-Bohr atom's model is noted. The possibility of using "cluster quantization" idea to explain nature of atomic spectra is considered.

### 1. Introduction

In 1913 British physicist Moseley had established the law, connection frequencies of X-ray spectra lines with the charge number of an element [3]. Moseley's law (ML) shows that square roots from X-ray terms depend upon charge numbers almost linearly. It is considered that knowing wavelengths of characteristic X-ray radiation lines it is possible to establish the number of protons in atomic nuclei.

The importance of Moseley's experiments analysis is determined by the link of ZE with such fundamental questions as nature of radiation generation and atomic spectra, adequacyof nucleus model and model of the atom (MAT), nature of ions with multiple charge (IMC). This law is of greatest importance for chemistry since ZE is linked with the periodical system and any theory of chemical bond is based on MAT.

To understand the reason of such interpretation of experiments, it should be considered that Moseley had carried out the research of X-spectra (Roenrgen spectra = X-ray spectra) in times of Rutherford-Bohr MAT, being a research worker in Rutherford's scientific center.

Working in Rutherford-Bohr team Moseley was an ardent supporter of the quantum atomic point of view. This reviles Moseley's motivation to interpret results of his experiments as a confirmation Rutherford-Bohr MAT. So the setting up of Moseley's experiments was grounding on the idea that "correct successive positioning of elements should occur according to their charge number".

The success in the advancement of "charge number" idea was given to Van-der-Bruk [2], who had introduced index numbers of elements in

his extended periodical system of elements (the year 1913) as a result of his multiple endeavors to improve Mendeleev's table.

In 20-s Moseley's law had helped to discover several new elements, which were unknown earlier, but predicted by Mendeleev. This had increased the number of ML supporters, and since the planetary MAT was linked to it – this increased the trust to this model. As a result, ML was used as one of the main confirmations of Rutherford-Bohr MAT and as a confirmation of main predictions of quantum theory.

History shows that interpretation of Moseley's experimental data was predetermined: the radiation frequency (to be more precise: square root of the frequency divided by Rydberg's constant) was linked namely to charge number, though in a pure state, without the screening constant, charge number is not present in ML. Moreover, ML has an approximate character. On Moseley's graphics even for K-spectra fracturing is present [6, 7]. Moreover, the linearity of the graphical dependence of square roots from X-spectra frequencies upon the atomic mass is hardly worse than for charge numbers. But there are ejections for three pairs of elements. There are also ejections on isobars. The atomic mass hadn't been considered as a base of ML, since the explanation of spectra nature from point of view of mass's responsibility, hadn't been introduced. To justify the link of atomic spectra with atomic mass the idea of "cluster quantizing" may be considered.

Though ML was first discovered in the region of X-ray terms, it is clear that Moseley operated formulas that were obtained earlier (in 1885 Balmer had suggested them, and Rydberg had improved them later) in optic spectroscopy.

The similarity of ML with the expression of isoelectric series and spectral formulas of Hydrogen atom allows interpreting Moseley's law without bonding to the charge number.

**2.** The varied out transformation leads equation (2) to the form:
$$E = h\nu = Ry \cdot (Z - \alpha)^2 \cdot (1/n_1^2 - 1/n_2^2), \tag{3}$$
which in form
$$(E/Ry)^{1/2} = (Z - \alpha) \cdot (1/n_1^2 - 1/n_2^2)^{1/2} \tag{4}$$
or
$$(k/R)^{1/2} = (Z - \alpha) \cdot (1/n_1^2 - 1/n_2^2)^{1/2} \tag{5}$$
is known as Moseley's law. From expression (4) it is obvious that energy level also obeys to Moseley's law. In Moseley's law (5) $k$ – is a wave number, $k = 1/\lambda\,\mathrm{cm}^{-1}$, Rydberg's for stationary nucleus $R\infty = 109737.3157\ \mathrm{cm}^{-1}$.

ML expression (5) doesn't differ from Rydberg's formula (6) for spectral series of Hydrogen, alkali metals and isoelectric series.

$$k = 1/\lambda = R(Z - \alpha)^2(1/n_1^2 - 1/n_2^2) \tag{6}$$

Moreover, for the majority of spectral transitions in atoms with multiple electrons, the formula (6) gives correct results.

Assumptions and inaccuracies made for ML derivation show that ML for atomic levels is only an approximate law. Deviations of Moseley's graphics from linearity are observed with the increase of Z and X-radiation wavelength. Since ML is based on levels, the first if these laws are also inaccurate as well as the second one.

Deviations, that are quite significant for K- and L-terms, become more noticeable during the transition to outer shells M, N, Q. Lines that express the dependence from Z on Moseley's graphics have characteristic fracturing in certain places (figure 1).
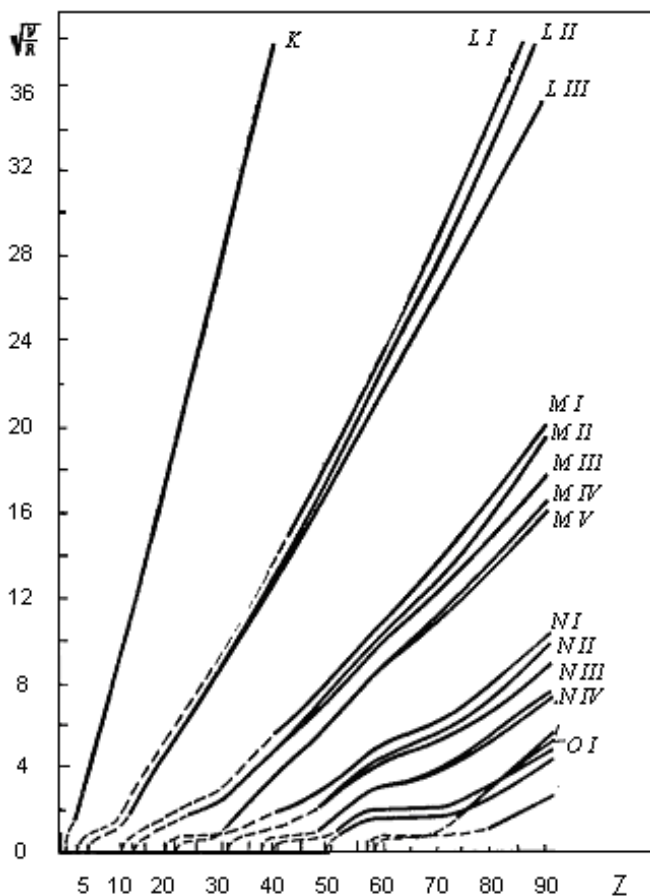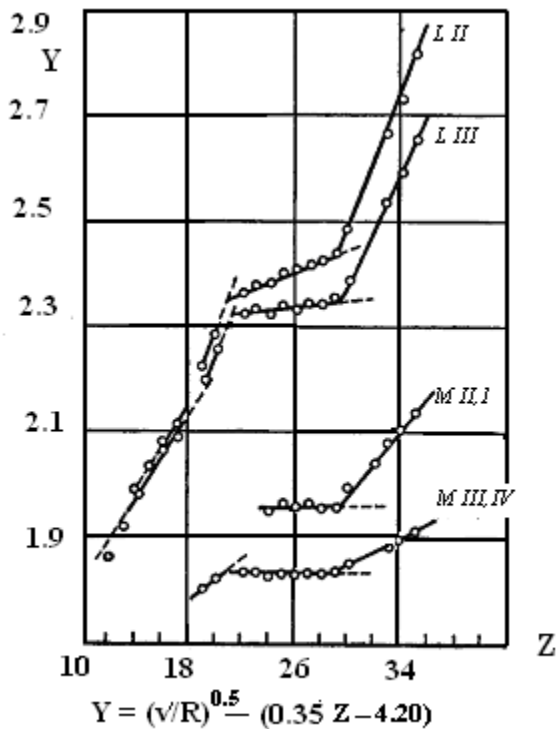


Рис. 1

$$Y = (v/R)^{0.5} - (0.35\,Z - 4.20)$$
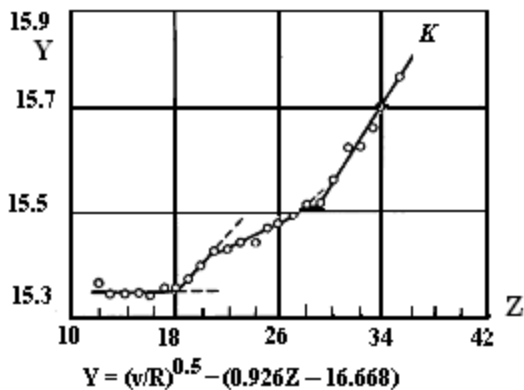
Рис. 2



$$Y = (v/R)^{0.5} - (0.926Z - 16.668)$$

Рис. 3

They are more sharply expressed graphically if the difference between $(v/R)^{1/2}$ and an image of correspondingly selected linear dependence upon Z, having the shape: AZ-B is plotted along the Y-axis instead of $(v/R)^{1/2}$. If X-ray terms had strictly followed Moseley's law, this

difference would have a shape of a line, but it can be seen from figure 2, that for L-levels is gives sharp fractures for Z=19 (K), Z=21 (Sc) and Z=29 (Cu). Sharp fractures for Z=29 also occur for M-levels. K-levels (figure 3) [7] give though less sharp but still rather clearly noticeable fractures for Z=19, 21, and 29.

## 2.1 Isoelectron series.

The common character of optic and X-ray spectra is well seen from (5) and (6) formulas, that also describe isoelectric series. Examples of ML applicability for isoelectron series are taken from [7].

Frequencies of hydrogen-like ions series: He II, LiIII, BeIV, B V, C VI may be expressed in the shape of ML: $(v/R)^{1/2} = Z \cdot (3/4)^{1/2}$. Rydberg's constants in series differ insignificantly. Moseley's graphic for them is present in figure 4.

Spectra of the series Be II, B III, C IV, … are shifted to the ultraviolet region in comparison with Li I spectra thanks to large nuclei charge. For three groups of most deep terms dependencies upon Z are expressed as
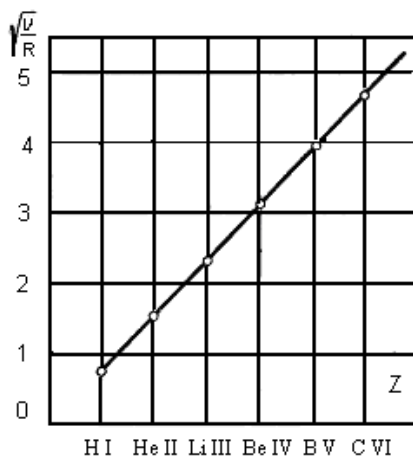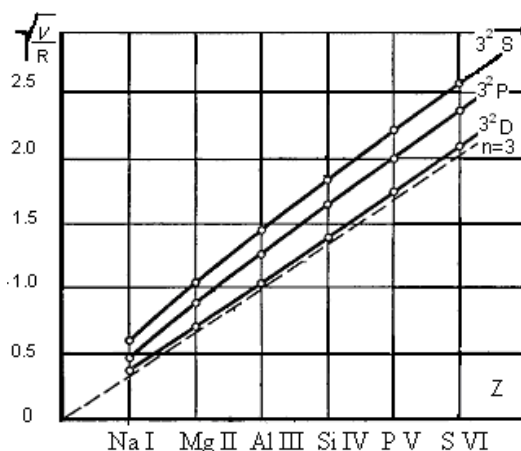


Рис. 4

Рис. 5

straight lines. Straight lines concerning to terms $2^2S$ and $2^2P$ go parallel to the straight line: $(\nu/R)^{1/2}$upon $Z/2$, the straight line corresponding to terms $3^2D$– is parallel to the straight line: $(\nu/R)^{1/2}$upon $Z/3$.

Moseley's formula (5) is well satisfied for most deep terms $2S$, $2P$, $2D$ of isoelectronic series Na I, Mg II, Al III, ... (figure 5).

Isoelectronic series for inert gases and ions similar to them are well described by Moseley's law.

The similarity rule for isoelectronic series spectra says: the spectrum of ion, corresponding to $k$ degree of ionization ($k$ electrons are absent), is similar to the spectrum of a neutral atom, which is positioned $k$ places earlier in Mendeleev's table. For example, Cl II spectrum is similar to S I spectrum, spectrum Cl III – with P I spectrum etc. up to the case of Cl VII spectrum, which is similar to Na I spectrum. The rule stays valid in the case when the transition to the preceding element is linked with the transition from one Mendeleev's table row to another.

Ionization potentials for isoelectronic series obey to the same Moseley's law as well as terms and are determined by meanings of deepest of them.

$$U_i^{1/2} = (R/e)^{1/2}\cdot 1/n\cdot(Z - \alpha).\tag{7}$$

From this expression follows that ionization potential to naked nuclei is increased along with the increase of the index number, and square roots of ionization potentials of isoelectronic series increase proportionally to the charge number $Z$. the linear dependence upon $Z$ persists during the transition through meanings of $Z$, corresponding to inert gases.

Graphic of ionization potential dependence upon the charge number (figure 29 [7]) doesn't differ in any manner from Moseley's graphics in terms of isoelectronic series of different elements. And it shouldn't be different since meanings of terms and ionization potentials of IMC are obtained from spectral data by the convergence lines to series limits.

### 3. Discussion

### 3.1 Moseley's law interpretation

In Moseley's law the $"(\nu/R)^{1/2}"$ varies not absolutely linearly in relation to the parameter $(Z - \alpha)$. From the "unclear" fundamental conclusions about the nucleus composition and atom's structure are made.

ML is expressed by the formula (5) which is analogues to Rydberg's formula (6). Spectra of hydrogen and isoelectronic series are described by it. Even linear dependencies for isoelectronic series (figure 4, 5) are called Moseley's graphics. With all this interpretation of X-spectra radiation nature differs from the interpretation of optic spectra emerging. In ML for X-spectra only singly charged ions are considered, in isoelectronic series spectra of neutral's as well as IMC are operated. In isoelectronic series, not only X-ray but also optic spectra appear.

The common character of X-spectra in ML is related to change of electron energy bond along with element's charge increase in case of singly charged ions, while in isoelectronic series spectra of ions with a sequential increase of charge multiplicity occurs to be similar.

Hydrogen spectra in MAT definition may be interpreted only as spectra of neutral or single ionized atom. Still terms of hydrogen atom series obey to ML (5) and are described by formula (6), which is similar for IMC of isoelectronic series and ionization potentials of IMC (7). What is the reason causing such similarity of formulas? What does the charge number $Z$ in spectral formulas show?

### 3.1.1 Atom's model and Moseley's law

Rutherford-Bohr model of atom almost absolutely lacks experimental confirmation. Moseley's experiments were used for confirmation of this MAT: during the ML derivation, the whole number Z was derived purposely and interpreted as the charge number, equal to the index number of an element. But number Z in ML is never whole. In order to achieve approximate linearity Moseley's graphic, Z is corrected by the introduction of the screening constant $\alpha$. In ML formula (5) there are other whole numbers: $n_1$ and $n_2$, squares of which may be incorporated with $Z^2$.

If constant a is interpreted as a constant of screening of electrons by electrons, then why should nuclei charges be whole and equal to charge numbers of elements? What is a dielectric permeability of a neutron? Why is the screening of nucleons by nucleons in nuclei not allowed? In case of different composition and stricture of nuclei of different elements, charge screening (and effective charges) should be different.

Fantasizing further, we will conclude that the decrease of nuclei effective charges lead to the decrease of nuclei possibility to retain electron, not by tens but, for example, no more than 10 – 20. And if there is a desire to appoint electrons responsible for the chemical bond, then, possibly, we will get to the nature of chemical individuality and periodicity of properties of elements, taking into account the fact that the number of electrons in atom leads to the chemical similarity of elements. Though truly speaking, the question of electron discreetness in atoms, molecules, condensed state of matter arises [A0, B0].

If the screening constant in (5), (6) and (7) is not a whole number, then the charge of an atomic shell after electron removal can't be whole. But then ion charges also must not be whole.

Since terms are, as rule, ionization potentials of atoms, and Rydberg's constant, derived from Hydrogen ionization potential, is present in ML, then spectral lines are considered in relation to Hydrogen ionization potential, transformed into Rydberg's constant.

In the planetary MAT, Bohr had expressed levels of energy of an atom through electron speeds and frequencies of their rotation on "quantized" orbits around the nucleus. But the speed of electrons in relation to the external source, exciting atomic spectra is the primary one.

**3.1.2 Link of the speed of electrons, exciting spectra, with charge numbers of elements**

How can we explain the fact that in ML namely the squared root of the radiation frequency divided by Rydberg's constant "$(\nu/R)^{1/2}$" is linked to the charge number of element Z, to be more precise to $(Z - \alpha)$? What should be changed along with Z increase for excitation of spectral lines with electron shock or hard radiation, which generates photoelectrons?

One of the obvious coincidences of spectral lines frequency dependence upon the square of index number $(Z^2)$ is their dependence upon the square of electron speed $(V^2)$, exciting spectra. That is speeds of electrons $V$, exciting spectral lines are changed sympathetically to charge numbers Z, which are interpreted as charges of an atomic nucleus.

In Moseley's during the transition from one element to another the energy (speed) of electrons, exciting characteristic X-spectra, changes

sequentially. The dependence of radiation frequency upon the energy of electrons is derived from (3).

It follows from the expression (7) that square roots from ionization potentials of isoelectronic series varies linearly along with the change of charge number Z. it occurs as in previous cases that there is a link of Z with the speed of ionizing electrons.

It might be said that in serial formulas (6) and in ML (5) there is a juxtaposition with electron energy (speed), that is needed for line excitation, to which Liman's series is converged, e.g. with energy (speed) of electrons, ionizing the hydrogen atom. The factor $1/n^2$ in formulas (5) and (6) gives information that electron speed is n times less than in case hydrogen ionization; Z is Z times higher than that speed, or speaking in different words: $1/n^2$ is a coefficient that lowers and $Z^2$ – increases the Rydberg's constant to the next limit if the spectral series.

If we do not bond ourselves to Rutherford-Bohr MAT, then in ML we can do it without Z, for example, making exchange of $((Z-\alpha)/n)^2$ to $(1/G)^2$, where $G=n/(Z-\alpha)$ shows how many times the energy (speed) of electrons, that is being supplied to the system, differs from the energy of electrons ionizing the hydrogen atom.

### 3.1.3 Possible role of electron speed in atomic spectroscopy
### 3.2 Atomic mass and Moseley's law

The necessity of experimental verification of electric nature of forces in planetary Rutherford-Bohr MAT had predetermined the interpretation of Moseley's experiments. The atomic mass was impossible to be used for explanation of spectra nature and interpretation of ML.

We can write down the formula similar to ML (but also being not so precise) in which the square root of frequencies of X-ray lines depends upon the mass of an atom. Sharp fractures on Moseley's curves (figure 2, 3), showing the dependence between charge number Z and difference of $(v/R)^{1/2}$ with the function of a shape $AZ + B$, overlap with ejections from the smooth change of mass of elements in Mendeleev's system. Fractures are seen at charge number 19 (the atomic mass of K is less the Ar), charge number 21 (Sc). After that fracture starts on Cu, charge number 29, right after the pair Co-Ni (mass of Co is higher than that of Ni). In the region of Te – I pair (charge numbers 52 and 53), there is no abrupt fracture on the graphics. It is possible that it is smoothed by the significant bending, starting at lanthanides (Ce, charge number 58).

If in X-spectra radiation in ML the mass is "involved", then what might be its link with atomic spectra? The mass might be called to account for light radiation in cases if spectra are not caused by intra-

atomic processes and/or spectra are linked to formation and fragmentation of clusters. "Quantization by mass" manifests itself well in multinuclear clusters.

### 3.3 "Cluster quantization" in atomic spectroscopy

Clusters are formed in conditions of spectra excitation [D0, E0]. The link between clusters and light radiation is well known [25]. Clusters may give narrow lines if photon emission.

The interaction of cluster beam with powerful femtosecond laser impulse is used for generation of effective compact sources of X-ray radiation. So in the research work [26], it is noted that (after cooling of gas to 150 K) the occurrence of soft X-ray radiation of Neon under the influence of femtosecond laser impulses obviously points to the formation of clusters from Neon atoms.

Among the generators of X-ray spectra, the source based on the stream of the liquid metal is known [27]. It is a cluster source of X-ray radiation: the liquid metal is sputtered under the high pressure through the small aperture and radiated my electrons.

**Excitation of X-ray radiation**

X-radiation may be linked with Doppler's shift, occurring due to fragmentation with huge speeds during Coulomb's breaking of a cluster (or due to the gas-dynamic force [29]). This is some analogy of energetics of spiral series.

When clusters explode under the influence of an ultra-powerful laser impulse ions with energies depending on sizes of preceding clusters are formed. For example, Coulomb's explosion of Xenon clusters leads to energy reaching of electron 3 keV and ions reaching 1 MeV [31]. It is possible that such high-energetic electrons will also give contributions in spectra.

Atomic fragments, evaporating from the surface of clusters of different sizes, possess sets of speeds. Here it should be considered that clusters have not only different number of atoms but different structure, states (crystal, liquid) as well; this will affect spectral characteristics of atoms estranged from a cluster, since evaporation of atoms from clusters and fragmentation depend on the bond energy of particles in a cluster.

Clusters may indirectly participate in the generation of X-spectra: they are powerful sources of continuous spectra in the optic region [25]. This radiation may interact with atoms, cluster fragments and electrons (primary and secondary, reflected and photoelectrons (in X-ray fluorescence)), generating characteristic spectra.

It may be assumed that interference pictures, refraction or scattering of Bremsstrahlung's X-radiation (or electrons) occur on clusters of different sizes.

In "cluster quantizing" light absorption may be explained by photon energy waste on desorption of atoms from clusters, electron emission. The radiation energy is *expended* on the breaking of chemical bond in a cluster, knocking out an electron, particle heating etc.

Light emission according to "cluster quantizing" scenario (besides Doppler's shift) occurs due to oscillation of atoms and/or electrons after transferring energy to a cluster during adsorption of an atom (a group of atoms), electrons on it. During interaction of an atom (group of atoms) with a big cluster, the main part of energy, that depends upon the energy of atom, adsorbed on the cluster and the chemical bond that it had formed with the cluster, will be *expended* on change of temperature of the new complex, the other part will be transformed into radiation.

Oscillation of atoms (groups of atoms) on clusters cause oscillations of electron density on them, which leads to light radiation (if it is who electrons are responsible for light radiation). Of course it may be assumed that oscillations of discrete electrons will generate light. It only is necessary to know that there is "an elementary electric charge". Do they exist discretely in clusters, in the condensed state?

The estimation of the role of "cluster quantizing" in atomic spectroscopy: the possibility of clusters being responsible for spectra that are related to intra-atomic processes, may be started, for example, from the research work [32], in which particle oscillations in small clusters are investigated.

## 4. Conclusions

Moseley's law is not precise. Interpretation of the index number of an element Z in Moseley's law (6) and in isoelectronic series (6) as an atomic nucleus charge (number of protons in the nucleus) is not sufficiently justified and motivated by the necessity of advancing the Rutherford-Bohr MAT (since there are no convincing proofs of this model and never were any).

The number of different interpretations of the charge number $Z$ in Moseley's law (5) and Rydberg's formula (6) may be suggested, for example, $Z/n$ is a coefficient, taking into account how many times the energy, that is supplied for the excitation of a spectral line, differs from the ionization potential of Hydrogen, transformed into Rydberg's constant or, speaking in different words, how many times energy (speed) of electrons, exciting spectra or ionizing an atom, differs from the energy (speed) of electrons, ionizing the Hydrogen atom.

Correlation of abrupt fractures on Moseley's graphics (figure 1, 2, 3) with ejections of three pairs of elements (Ar – K, Co – Ni, Te – I) in sequence of mass increase in Mendeleev's law allows to go back to verification of atomic mass's role in X-ray and optic spectroscopy. "Cluster quantizing" is one of many possible ways of using the atomic mass to explain the nature of atomic spectra and taking into account the role of intra-atomic factors.

Compounds of investigated systems [D0, E0], processes, occurring in them [C0, F0] show the necessity of revision of quantum views on the subject of macroscopic phenomena and non-intra-atomic processes contributions into the micro world, that are described by quantum mechanics. The speed of electrons, exciting spectra is also the eternal factor.

X-spectra are related to a singly charged ions, spectra of isoelectronic series in more significant degree – to IMC, and spectra of the Hydrogen atom – to neutrals. The common character of optic spectra and X-spectra, proceeding from formulas (5) and (6) is obvious. Possibly the natures of both should be similar.

The conception of IMC had been attracted to atomic spectroscopy for spectra systematization. Still, IMCs are not present in condensed phase [9] and, possibly, are not present in nature [A0, B0, C0].

In order to revise the MAT, the mass spectroscopy verification of IMC nature experiment setting up actualized [A0, C0].

Proceeding from the stated above, from the proximity of Moseley's law, follows the fact that such fundamental interpretation of X-ray spectral data is insufficiently justified: M: doesn't determine the composition of the atomic nucleus. If we reject the interpretation of ML as a law, establishing the number of protons in the atomic nucleus, then we will be able to obtain the more successful MAT and a nucleus model (which are currently presented by more than ten different models, describing characteristics of different nuclei).

As a component of the research of adequacy of the current MAT [A0, B0, C0, D0, E0, F0] this research work strengthens positions of supporters of revision of the model of an atom.

## References

7. C. E. Frisch, Optical spectra of atoms, M. – L.: Fizmatgiz, 1963.
14. D. Shintoism, T. Oikava, The Analytical translucent electronic microscopy, M.: Technosphera, 2006.
16. N.F. Losev, Bases of the X-ray spectral fluorescent analysis, M.: Himiya, 1982.

17. K. Zigban, K. Nordling, A. Falman, etc., Electronic spectroscopy, M.: Mir, 1971.
18. G. V. Pavlinsky, Fundamentals of physics of X-ray radiation, M.: Fizmatlit, 2007.
20. A.S. Lobko, Experimental studies of parametric X-ray radiation, Minsk: BGU, 2006.
32. N G. Guseyn-zade, A.M. Ignatov, Spectroscopy of Thompson's atom, Plasma Physics, V. 32, № 10, p. 907-920 (2006).

\*\*\*

The full version of the Shatov's digest (in English) is published on the website: shatov.org.

# Series: **PHYSICS and ASTRONOMY**

Etkin Valery A.

# Mechanics as a Consequence of Energodynamics

## Annotation

It is offered to consider classical mechanics as an equal branch of the uniform theory of transfer and transformation of any forms of energy (energodynamics) based on the principle of discernability of processes. It is shown that such approach demands correction of a number of her basic concepts and the principles. Along with it a synthesis of all three laws of Newton is undertaken: the principle of inertia - on rotary motion; the principle of force – on forces of any nature; the principle of counteraction – on the energy transformation phenomena. The unity of the nature of all forces is opened and the uniform way of their stay is offered. A theoretical conclusion of the world law of gravitation, proceeding from the heterogeneity of distribution of matter in space is given. The conclusion is drawn on a possibility of further synthesis of theoretical fundamentals of modern natural sciences.

## Contents

### 1. Introduction.

Mechanics was the first of natural sciences that reached maturity and became a theoretical basis of the technical civilization. Its object of investigation, viz. the motion of macroscopic bodies has long since been

most demonstrative for investigators. This put mechanics in a special position among other natural sciences with its notional and conceptual system having up to date served as a basis for the majority of the natural science disciplines.

These merits of mechanics at the same time engendered some mechanicalism, viz. the intention to "bring all natural phenomena to attractive and repulsive forces, which value depends on their distance" [1]. However, it appeared impossible to create an exclusively mechanical vision of the world. On this understanding, it is worth considering mechanics as an "equal partner" among other scientific disciplines dealing with non-mechanical forms of motion. In this connection, the main attention will be focused on obtaining by deductive way fundamental principles of mechanics as a particular case of the unified theory of real processes named herein, for short, energodynamics.

Presentation of mechanics usually starts off with kinematics that deals with the motion of bodies in space and time irrespective of physical nature of this motion. The notions of trajectory, the coordinate of a point lying on it, velocity and acceleration of this point are herein accepted "a priori" – before the background of motion and formulate the laws of motion have been clarified. Only then dynamics starts – with introducing the notion of material point, its mass, and momentum. At the first glance, such a structure of mechanics (from simple to the difficult) seems quite natural. However, as De Broglie rightly noted, such an approach is rested upon an assumption that the results of abstract kinematical consideration may be applied, without an additional analysis, to the real motion of more complicated physical objects [2].

**2. Correction of initial concepts of mechanics.**
The corrections made from energodynamics [3] when considering mechanics as its deduction start off with the object of investigation. In kinematics, an abstract point is such an object, which has neither mass nor the most important property of any material object – the extension. As a result, the state of this object, its displacement, acceleration, etc. are characterized by the various-order derivative of the only coordinate – radius-vector **r** of the point. In energodynamics, the object of investigation is the entire set of the interacting material points comprising a system. To define the state of such an object from the positions of kinematics requires the definition of a great (in case of continuum – infinite) number of coordinates of state and their derivatives. Such a description, while being generally received, contradicts, however, the distinguishability process principle . According to this principle, the

number of variables conditioning the state of a system equals to that of independent processes running in the system. In case of a solid body, such processes are the translation motion of the center of mass and the rotation of a body about the instantaneous center of inertia, as well as its acceleration. Besides, the variables pretending to be the coordinate of state of a system must be extensive values just like the energy of the system they describe. For the *quiescent* state (rest) such a variable is the moment of system mass distribution $\mathbf{Z}_m = M\mathbf{R}$, which derivatives with respect to time $t$ define the motion of the system. According to the process distinguishability principle [4], this motion is characterised by a system impulse

$$\mathbf{P} \equiv d\mathbf{Z}_m/dt = M\mathbf{v}. \tag{1}$$

In turn, speed $\mathbf{v}$ of the systems asa  whole can be spread out on two components: forward speed $\mathbf{v}_0$ the centre of mass $M$ and speed of the systems, as whole rotation $\boldsymbol{\omega} \times \mathbf{r}_\omega$, where $\mathbf{r}_\omega$ - instant radius of rotation [4].

According to it and systems impulse $\mathbf{P}$, it is possible to spread out on an impulse of forwarding movement of a body

$$\mathbf{v} = Md\mathbf{r}_0/dt, \tag{2}$$

and on an impulse of rotary movement:

$$\mathbf{P}_\omega \equiv \boldsymbol{\omega} \times M\,\mathbf{r}_\omega, \tag{3}$$

where $d\mathbf{r}_0 = \mathbf{e}dr_0/dt$ - a displacement vector; $\mathbf{e}$ - an unity vector in a direction of speed $\mathbf{v}_0$; $r = |\mathbf{r}|$.

Instead of the last expression is usually used as coordinate of rotary movement the moment of an impulse of system $\mathbf{L} = I\,\boldsymbol{\omega}$, in which $I$ - the moment of body inertia). The variables $\mathbf{P}_0$ and $\mathbf{L}$ characterize now the *motion* state. They are associated with the two independent terms in fundamental equation of energodynamics [3] and the two independent components of the kinetic energy of the system corresponding to, respectively, its translation – $E^k = Mv^2/2$ and rotation – $E^\omega = I\omega^2/2$. The time variations $d\mathbf{P}_0/dt$ and $d\mathbf{P}_\omega/dt$ of the coordinates $\mathbf{P}_0$ and $\mathbf{P}_\omega$ characterize two other independent processes (translation and rotation accelerations, respectively), i.e. the variation of the motion state, viz. its acceleration.

Although such a description of a set of the material points comprising a moving continuum looks like, from positions of continuum mechanics, approximate (lacking information on the motion of each of the volume elements), within the framework of energodynamics this sufficiently characterizes the energy state of the system in whole. Transition to the more detailed description of a moving continuum (material or spatial) is beyond of energodynamics. Such over-

determination is fraught with the loss of some properties of the system as a whole. The over-determination is demonstrably instantiated with the concept of an "oriented point" introduced by Elie Cartan in the early 20th century, where the oriented point is endued with the capability to rotate while moving along some trajectory. As a result, the state of the point needs to be defined by as many as six independent coordinates (three translation and three rotation ones), whereas a moving material point with no extension possesses only the translation kinetic energy so that its rotation coordinates do not characterize any real process. Naturally, the Cartan-Einstein gravitation theory based on the above will endue the space with properties really absent. G. Shipov [5] goes still further in this direction enduing a material point with three more rotation coordinates in space/time domain . As a result, the space of variables becomes neither more, nor less than 10-dimensional (including the time coordinate), and the theory of physical vacuum based on this foundation leads to a series of paralogisms (from God as entity up to perpetual motion as a real possibility).

Together with the above, the "under-determination" of mechanical systems may be also instantiated. This happens, e.g., when a material body is described without due consideration given to its density distribution over space it occupies. Then the bodies with the different orientation of mass distribution moment $\mathbf{Z}_m$ become indistinguishable, which excludes from consideration a whole series of the real processes of *reorientation* possible in heterogeneous systems. They take into consideration that the bodies differently space-oriented are not equivalent mechanically [6].

The adequacy principle modifies also such fundamental notions of mechanics as mass, velocity, and acceleration. Let us consider first the notion of mass $M$ as the measure of body inertial properties. Such an interpretation of $M$ was chronologically substantiated by the Newton-adopted method of introducing the notion of force $\mathbf{F} = M\mathbf{a}$ as a value directly proportional to the body acceleartion a, where the mass value M figured as a proportionality factor. Hence it followed that with the same force $\mathbf{F}$ acting on a body the greater the body mass $M$, the lower its acceleration should be. The mass $M$ thereby stood immediately for a measure of the body inertiality. With the special relativity theory and general relativity theory appeared such an interpretation of mass has been common in the notions of "inertial", "gravitational", "electromagnetic" mass, "rest mass", etc. [7].

A different situation arises with energodynamics where the notion of mass should be introduced long before the acceleration process has

been considered, i.e. regardless of inertia. The mass here stands for a measure of extensive properties of any energy carriers $\Theta_i$ and the system energy $U$ as their function, i.e. a quantity measure of matter contained in the system. Then such an interpretation is further supported by introducing the state parameter varying in the processes of matter exchange with the environment, i.e. the mass exchange coordinate.

The final difference of mass from the measure of system inertial properties is set with the transfer laws formulated. With a single force $\mathbf{F}_i$ applied to a system these laws become:

$$\mathbf{F}_i = \Sigma_i \bar{R}_i \mathbf{J}_j , \tag{4}$$

where the $\bar{R}_i$ factor characterizes the resistance of the system to its state variation, i.e. its "inertiality" relative to the $i$th forces $\mathbf{F}_i$. As applied to the acceleration process its generalized rate $\mathbf{J}_i$ is expressed by the time derivative of the system momentum $d\mathbf{P}/dt = M\mathbf{a}$. Substituting this expression to equation (3.14) gives:

$$\mathbf{F}_i = \bar{R}_i \, d\mathbf{P}/dt \quad (i,j = 1,2,\ldots,n), \tag{5}$$

The factor $\bar{R}_i$ is seen to appear as a function of the acceleration process, which characterizes the measure of the system inertial properties and has nothing to do with the mass $M$ of the system as the function of its state and the quantity measure of matter therein. This becomes especially evident when comparing (5) with the Ohm law in electrical engineering, where $\mathbf{F}_i$ – electromotive force; $\mathbf{J}_i$ – current strength, and the to-current resistance factor $\bar{R}_i$ does not depend on conductor mass at all. By the way, in Newton's second law of motion, with the $\bar{R}_i$ factor adopted as unity, it does not depend on mass either. This means that the notions of mass as the measure of inertia and the quantity measure of matter are obviously distinguishable and their identification is inadmissible. Based on this, we will call $\bar{R}_i$ as the "*inertia factor*" or *inertiality* for short.

Let's pass now to the concept of acceleration. In kinematics, velocity is construed as the total derivative of radius-vector of the point $\mathbf{r}$ (or its component) with respect to time $t$, i.e. $\mathbf{v} \equiv d\mathbf{r}/dt$, while acceleration is construed as the derivative of velocity with respect to time, i.e. $\mathbf{a} \equiv d\mathbf{v}/dt$. This derivative comprises both the variation of the particle velocity $\mathbf{v} = \mathbf{v}(\mathbf{r},t)$ without variation of its direction $\mathbf{a} \equiv \mathbf{e}(dv/dt)$ and the variation of the particle velocity direction $vd\mathbf{e}/dt$ without variation of the velocity value. As a result, *any rotation of a point appears to be the motion with acceleration,* whereas these processes cause motion state variations distinctive in kind and, from positions of energodynamics, must be

considered as *independent*. This means that the process of translation acceleration of a material point or a body with the coordinate $a \equiv \mathbf{e}(dv/dt)$ should be distinguished from the process of *reorientation* of the body or the particle trajectory expressed, in particular, in a rotation of the body or the particle. The velocity of this process is expressed as $vd\mathbf{e}/dt$, while the coordinate of the process is construed as the angular velocity vector $\boldsymbol{\omega} = d\boldsymbol{\varphi}/dt$. The fact should be taken here in consideration that a particle can not be accelerated unless its spatial position (i.e. the $\mathbf{r}$ coordinate) is changed. Therefore, the acceleration may be expressed in the developed form [7]:

$$a \equiv d\mathbf{v}/dt = \mathbf{e}\,(\partial v/\partial t)_{\mathbf{r}} + \mathbf{e}\,(\partial v/\partial \mathbf{r})d\mathbf{r}/dt = v\nabla v. \qquad (6)$$

since the notion of the acceleration local component $\mathbf{e}(\partial v/\partial t)_{\mathbf{r}}$ for the particle (with its position unvaried) does not make physical sense. This detail is a matter of no small consequence stressing the point that the acceleration process is inseparably associated with the locally heterogeneous velocity profile featuring the gradient $\nabla v \equiv (\partial v/\partial \mathbf{r})$ and generated in space. The generation of any heterogeneity demands time and energy consumption. This is the time delay that makes physical sense of the inertia conception.

The similar comments may be made on also the rotation acceleration $d\boldsymbol{\omega}/dt$. From a standpoint of energodynamics, a uniform rotation of bodies with their kinetic energy $E^{\omega} = I\omega^2/2$ remaining unvaried can not be classified as accelerated. This statement is even more right, because, the energy is constant, the rotation acceleration process does not demand work consumption as for the translation acceleration. Being considered from these positions, the uniform electron-around-nuclear rotation is non-accelerated, while the notion "centripetal acceleration" intrinsically inadequate. The correction of all these concepts will further impact many of the applications of mechanics [8].

### 3. Law of Inertia (Newton's First Law of Motion) and Its Generalization to Rotational Motion

Newton's first law [9] is a statement of the law of inertia discovered by Galileo and reading that *"a body at rest remains at rest, and a body in motion continues to move in a straight line with a constant speed unless and until an external unbalanced force acts upon it".*

For the mathematical substantiation of this law let us apply the fundamental identity of energodynamics

$$dU \equiv \Sigma_i \Psi_i\, d\Theta_i - \Sigma_i \mathbf{F}_i \cdot \mathbf{e}_i dr_i - \Sigma_i \mathbf{M}_i \cdot d\boldsymbol{\varphi}_i. \qquad (7)$$

to an arbitrary closed mechanical system (with no external forces $\mathbf{F}_i$ or their moments $\mathbf{M}_i$ exerted on). Thereby the system energy remains unvaried ($dU = 0$) and expression (7) will become:

$$\Sigma_i \Psi_i \, d\Theta_i = 0. \tag{8}$$

For a mechanical system not involved in rotational motion, the momentum $\mathbf{P}$ of the system as a whole associated with the velocity $\Psi_i \equiv \mathbf{v}$ is the only parameter $\Theta_i$ characterizing the state of motion of the system. From here the law of conservation of momentum directly ensues:

$$\mathbf{P} = M\mathbf{v} = \text{const}. \tag{9}$$

It becomes clear at the same time that the Galileo's principle of relativity stating that uniform and rectilinear motion of a closed system does not impact the processes running in the system is just a particular case of the "equilibrium self-non-disturbance principle" (the general law of thermodynamics). In fact, from positions of thermodynamics (and energodynamics too) the state of a mechanical system moving in a straight line is characterized by the only coordinate, viz. the momentum of the system. Therefore the only process is possible in it, viz. the acceleration of the system as a whole. The uniform motion means, in this case, the absence of such a process, i.e. partial equilibrium of the system. It is natural that only an external action can disturb such a state. However, the system is closed, neither of the processes is possible in it.

Let us consider now the additional consequences ensuing from treating mechanics as a particular case of energodynamics. This is first of all the law of conservation of momentum (Euler's law), which was absent in Newton's mechanics:

$$\mathbf{M} = I\boldsymbol{\omega} = \text{const}. \tag{10}$$

Both of these laws – (9) and (10) – may be unified in one statement reading that "any material body remains at rest or in motion unless and until some forces applied to make it change this state". It is easy to see that this statement generalizes Newton's first law extending it to rotating systems and demanding the legitimation of the notion of "coasting rotation". It is significant that with such an approach the Galileo's law of inertia appears to be valid irrespective of whatever theory of physical vacuum or assumption on homogeneity and isotropy of space and time [10].

Thus Newton's (9) and Euler's (10) laws pertaining to, respectively, translation and rotation of bodies ensue from energodynamics as particular cases. One can not now assert that "free" motion of a closed system, i.e. "coasting", is always rectilinear – it may also be rotational. It becomes clear at the same time that the Galileo's principle of relativity stating that uniform and rectilinear motion of a closed system does not

impact the processes running in the system is just a particular case of the "equilibrium self-non-disturbance principle" (the general law of thermodynamics). In fact, from positions of thermodynamics (and energodynamics too) the state of a mechanical system moving in a straight line is characterized by the only coordinate, viz. the momentum of the system. Therefore the only process is possible in it, viz. the acceleration of the system as a whole. The uniform motion means, in this case, the absence of such a process, i.e. equilibrium of the system. It is natural that only an external action can disturb such a state. However, the system is closed, neither of the processes is possible in it. This may be referred with the same degree of generality to also uniformly rotating bodies being in internal equilibrium [10].

Let us consider therefore a more general case of a mechanical system not being in internal equilibrium. In such a system, due to interaction (relative motion) of its macroscopic parts (subsystems), spontaneous redistribution processes ($d\mathbf{r}_i/dt \neq 0$) arise causing the variation of its ordered energy ($dE/dt \neq 0$). It becomes especially evident if to imagine the translation kinetic energy of such subsystems $E^k$ as a sum of the kinetic energy of entire-system-center-of-mass motion $\frac{1}{2}\Sigma_k M_k\mathbf{v}^2$ and the kinetic energy of system-parts-relative motion $\frac{1}{2}\Sigma_k M_k\mathbf{w}_k^2$ (where $\mathbf{v}$, $\mathbf{w}_k = \mathbf{v}_k - |\mathbf{v}|$ − velocity of the center of mass of the system and relative displacement velocity of its parts in the center-of-mass system). This kinetic energy of the system-parts-relative displacement can both decrease (due to the viscous force action) and increase (due to the work was done by forces of other nature when converting energy in a system with other degrees of freedom). The work of such kind is done, e.g., in oscillatory motions when converting kinetic energy into potential one and vice versa. Let us name this work as useful internal since the forces to be overcome in this process are internal with respect to the system as a whole. However, the internal work may also be dissipative if the oscillatory process is accompanied by damping of the relative motion among various parts (components) of the system.

The rotation kinetic energy of system parts $E^\omega = \frac{1}{2}\Sigma_k I_k\omega_k^2$ behaves the same. It may also be represented as a sum of the kinetic energy of entire-system-rotation $\frac{1}{2}\Sigma_k I_k\omega^2$ and the kinetic energy of system-parts-relative rotation $\frac{1}{2}\Sigma_k I_k(\omega_k - \omega)^2$. The latter can also both decrease due to the rotational viscous force action and increase due to the other-nature-force action. Therefore when constructing a math model of such systems it is necessary to allow for the variation of not only the momentums $\mathbf{P}_k = M_k\mathbf{v}_k$ of the $k^{th}$ components (parts) of the

system, but also of their angular momentums $\mathbf{L}_k = I_k\boldsymbol{\omega}_k$ (where $I_k$ – moments of their inertia). In this case expression (5) becomes for them:

$$\Sigma_k\,\mathbf{P}_k{\cdot}\,d\mathbf{v}_k/dt + \Sigma_k\,\mathbf{M}_k\cdot d\boldsymbol{\omega}_k/dt = \Sigma_k\mathbf{F}_k{\cdot}\mathbf{v}_k + \Sigma_k\mathbf{M}_k{\cdot}\boldsymbol{\omega}_k. \quad (11)$$

It follows that in case an isolated system contains the internal $k^{\text{th}}$ forces $\mathbf{F}_k = -\,(\partial U/\partial\mathbf{P}_k) \neq 0$ and their moments $\mathbf{M}_k = -\,(\partial U/\partial\mathbf{L}_k) \neq 0$), it is only the sum of the translation and rotation of kinetic energies of the $k^{\text{th}}$ subsystem that remains unvaried even when the laws of conservation of momentum and angular momentum

$$\mathbf{F}_k = d\mathbf{P}_k/dt\,; \quad \mathbf{M}_k = d\mathbf{L}_k/dt \qquad (12)$$

are valid separately for each of the $k^{\text{th}}$ parts of the system under consideration, i.e. the cross-impact of forces and moments is absent among various subsystems. However, since it is not so in general, the momentum of the system as a whole $\mathbf{P} = \Sigma_k M_k\mathbf{v}_k$ and its angular momentum $\mathbf{L} = \Sigma_k I_k\boldsymbol{\omega}_k$ are not bound to remain constant with a variation of the system-parts-momentums $\mathbf{P}_k = M_k\mathbf{v}_k$ and their angular momentums $\mathbf{L}_k = I_k\boldsymbol{\omega}_k$. In fact, when the right side of equation (7) is equal to zero, only the sum of the translation and rotation energies is retained, but not each of them separately. Hence it is quite legitimate to assume the variation of not only the internal state of the system motion but also its external state due to the reciprocal conversion of the translation and rotation energies. This does not violate energy conservation since the energy of the system as a whole does not vary in this case.

Thus a fundamental deduction follows from energodynamics: what is valid for any homogeneous system (lacking redistribution processes) is not always valid for a heterogeneous system. This statement is supported by results of the experiments conducted by N.V. Filatov (1969) followed by A.P. Gladchenko (1983) with inertioids [11]. N.V. Filatov investigated collision of two massive bodies installed on carts. One of the bodies comprised gyros fixed on the gimbal suspensions and have rotated in the opposite directions with the same angular velocity for mutual compensation of their moments. During the experiments, the gyros collided with a usual mass installed on another cart. That process was recorded on a film with a speed of 2000 frames per second followed by a treatment to define center-of-mass velocity of the system pro- and post-collision. As a result of a great number of experiments, it was discovered that in case the gyros precession started post-collision, the center of mass of the system varied its velocity. Thus the possibility of reciprocal conversion of the translation energy into the kinetic energy of gyros precession was revealed.

The similar experiments were conducted by A.P. Gladchenko in 1983 with the B.N. Tolchin's inertioids – a gyro additionally equipped with a motor-brake to govern its center-of-mass velocity [12]. Displacement of the cart with the gyro and the motor-brake was recorded on a film. Those experiments also revealed the possibility of displacing bodies due to partial conversion of the kinetic energy of system-parts-relative rotation into the system center-of-mass translation energy.

To more clearly explain the displacement of inertioid center of gravity against variation of kinetic energy pertaining to relative rotation of its parts, let us denote the inertia moments of two opposite-rotating parts and their angular velocities as $I_1$, $I_2$, and $\boldsymbol{\omega}_1$, $\boldsymbol{\omega}_2$, respectively, while the raduis vectors of their centers as $\mathbf{R}_1$ and $\mathbf{R}_2$, respectively. Then, according to the general definition (7), the *rotational angular momentum distribution* in such a system is expressed as:

$$\mathbf{Z}_\omega = I_1\boldsymbol{\omega}_1\mathbf{R}_1 + I_2\boldsymbol{\omega}_2\mathbf{R}_2. \tag{13}$$

Since $\boldsymbol{\omega}_2 = -\boldsymbol{\omega}_1$ and $I_1 = I_2$, the above expression becomes:

$$\mathbf{Z}_\omega = I_2\boldsymbol{\omega}_2\Delta\mathbf{R}_\omega, \tag{14}$$

where $\Delta\mathbf{R}_\omega = \mathbf{R}_2 - \mathbf{R}_1$ – displacement of inertia center for a system containing rotating weights due to the opposite directions of the angular velocities $\boldsymbol{\omega}_1$ и $\boldsymbol{\omega}_2$. Since the forces causing this displacement are internal, the variations of the *rotational angular momentum distribution* $\mathbf{Z}_\omega$ they cause should be referred to internal wells or sinks $d_s\mathbf{Z}_\omega$ of this value. According to the wells–sinks balance equation the corresponding wells or sinks $d_s\mathbf{Z}_w = Mvd\mathbf{R}_w$ should appear as pertaining to the *translational angular momentum distribution* $\mathbf{Z}_w$ (because the inertioid does not have other degrees of freedom). This means that in the system of inertioid–environment their relative movement should appear and continue till the energy $E^k_\omega$ of relative rotation for inertioid parts is completely converted into the energy $E^k_w$ of their translational motion. As an example of the rotational-to/from-translational angular momentum interconversion may serve the conversion of laminar (translational) motion of liquid particles into their turbulent (vortical) motion and vortical motion into laminar one with obstacles appearing and disappearing in the flow.

It is significant that to obtain such conclusions, we did not have to resort to whatever models of physical vacuum of ether. That is why energodynamics is a theoretical base to explain the UFO flights and to create "free-of-any-support" vehicles.

## 4. Law of Force (Newton's Second Law of Motion)

Newton's second law introduces the force concept and usually has the form:

$$\mathbf{F} = M\mathbf{a}, \tag{15}$$

where $\mathbf{F}$ – resultant mass force.

It is worth noting, however, that Newton's acceleration coordinate is not the velocity $\mathbf{v}$, but the momentum (quantity of force) in the form (this form better complies with the requirement of energodynamics for the extensive character of generalized coordinates and will further take on fundamental significance in the context of the relativistic mass conversion):

$$\mathbf{F} = d\mathbf{P}/dt . \tag{16}$$

I. Newton stated that law as follows: *"The rate of change of momentum of a body is directly proportional to the impressed force and takes place in the direction in which the force acts".*

Force enters in expressions (15) and (16) as a reason of the acceleration process generation. However, physics and natural sciences have generally to deal with forces causing also other processes (displacement, expansion, electrization, chemical, and nuclear conversions, heat and mass transfer, etc.). Therefore (15) and (16) need to be considered as a particular case of force rather than its definition. Energodynamics gives a more general force definition by expression (1), wherefrom, in the absence of the reorientation processes, it follows:

$$\mathbf{F}_i \equiv - (\partial E/\partial \mathbf{r}_i) . \tag{17}$$

This expression reflects the unity of various-nature forces in their definition as itself. In particular, if $\mathbf{r}_i$ is a vector characterising the heterogeneity of mass distribution in space, force $\mathbf{F}_i$ defines a gravitation field. If vector $\mathbf{r}_i$ characterize displacement of free charges, force $\mathbf{F}_i$ defines an electrostatic field, etc. Hence, *the force fields are generated not by masses, charges or currents, but rather by their heterogeneous distribution in space.* This statement is reasonable to be called for easy reference as a *field-forming Principle* [3].

It is easy to show that the expression for the acceleration force $\mathbf{F}$ ensues from the above one as a particular case. Taking into consideration that this force causes deviation from equilibrium (so that its sign is opposite to that of the force $\mathbf{F}_i$) and based on (17) one can get:

$$\mathbf{F} \equiv (\partial E/\partial \mathbf{r}_m) = \partial(Mv^2/2)/\partial \mathbf{r}_m = Mv\nabla v = M\mathbf{a}, \tag{18}$$

where $v$, $\mathbf{r}_m$ – the magnitude of velocity and radius-vector of the center of mass of the system, respectively.

It is significant that the representation of acceleration in the form $\boldsymbol{a}$ = v∇v is exactly what allows representing the acceleration work $dW_{v}^{e}$ in the same form as for other kinds of work:

$$dW_{v}^{e} = \mathbf{F} \cdot d\mathbf{r} = M\mathbf{v}^2/2. \qquad (19)$$

It is easy to show that definition (19) is applicable to also the centrifugal force concept:

$$\mathbf{F}_{v} \equiv (\partial E/\partial \mathbf{r}_{\text{II}}) = \partial(M\mathbf{v}^2/2)/\partial \mathbf{r}_{\text{II}} = M\omega^2 \mathbf{r}_{\text{II}}, \qquad (20)$$

On this basis, these are relationships (15) and (17) that ought to be considered the analytical expression of Newton's second law rather than the relation $\mathbf{F} = M\boldsymbol{a}$ referring only to acceleration process.

Let's discuss now specificity of "forces of inertia». Till now disputes have not ceased concerning the fact whether these forces are real or not, active or passive, external or internal, inherent in all processes or only acceleration, etc [5].

The answer to this question is facilitated if the entire set of interacting bodies is considered as a single whole. In that case, all forces become internal. As shown above, such forces arise only in pairs and simultaneously. Therefore the question which of them is primary disappears by itself. Both of them are real and a result of the action of a force couple featuring another nature, which has caused process of energy conversion. In this sense both of them are reactions. At the same time they, like any forces, either cause or a stressed state of the system or generate a process. In the first case, they become nonequilibrium state functions (like the reaction of support), in the second case – process functions. Forces of inertia relate to the latter. They exist only when a process is really running and disappear when the process has ceased. ($\mathbf{J}_{i} \neq$ 0). It necessarily follows from Newton's law, according to which forces of inertia F are absent in the absence of acceleration (at $\boldsymbol{a} = 0$). Such are Coriolis forces and the magnetic component of Lorentz's forces. Hence, the force of inertia does not exist as a state function. Summarising the aforesaid, forces of inertia may be defined as a variety of reactions which are process functions. Therefore any statements about specific "fields" of these forces existing in nature [5] are grounless.

This fact reveals a fallacy of the opinion that the concept of inertia cannot be generalized to nonmechanical processes. Such a narrowing of the concept of inertia contradicts the Le Chatelier–Braun principle according to which any external influence on a system causes changes in its state tending to weaken the result of this influence.

**Extended Interpretation of Newton's Third Law of Motion (Principle of Action and Reaction)**

I. Newton formulated his third law as the following statement: *"For every action force there is an equal, but opposite, reaction force"*.

This statement is most commonly written as:

$$\mathbf{F}^a = - \mathbf{F}^p , \qquad (21)$$

where $\mathbf{F}^a$, $\mathbf{F}^p$ – respectively, action forces and reaction forces. Thus it is meant, that active forces are enclosed to a body from the outside and have the same nature, as forces of the reaction of a body.

However, I. Newton himself repeatedly emphasized, that besides the enclosed forces it is necessary to distinguish operating forces, and action of force should be estimated as product of enclosed force size $\mathbf{F}_i$ for speed $\mathbf{v}$ of the moving of object [13]. In this connection Newton referred to Archimedes' law of leverage formulated as *"what we lose in velocity, we win in force"*. It is necessary therefore to clarify the statement of Newton's third law from the positions of energodynamics. For this purpose let us apply the energodynamics to an arbitrary heterogeneous system doing mechanical work, the said Archimedes' lever being the simple example of it. The lever arms displace in the opposite directions with velocities $\mathbf{v}_i$ and $\mathbf{v}_j$ by the action of the forces $\mathbf{F}_i$ и $\mathbf{F}_j$. Since all parameters $\Theta_i$ remains unvaried for such a system, equation (21) becomes:

$$\mathbf{F}_1 \cdot \mathbf{v}_1 + \mathbf{F}_2 \cdot \mathbf{v}_2 = 0 . \qquad (22)$$

This expression is nothing else but the law of conservation of energy (of power – to be more exact) in the context of mechanical phenomena. Just in a particular case, when $\mathbf{v}_1 = \mathbf{v}_2$ (e.g., when doing work is accompanied by displacement of the interface between two bodies, or the action is provided without whatever intermediate of the lever type), expression (22) goes over into (21). It is the relationship (22) that should be construed as a mathematical form of Newton's third law rather than its particular case (21).

It also worth noting that the statement of Newton's third law as per (22) does not demand the action force $\mathbf{F}_i$ and the reaction force $\mathbf{F}_j$ to be directed in the same straight line. This demand was quite evident for Newton's mechanics that "unfiled" rotational motion of bodies. However, from the positions of energodynamics, allowing for torques caused just by offsetting the lines, in which counter-forces are acting, this demand is superfluous. Withdrawing this demand enables eliminating the contradiction with Newton's third law in case of the interaction of, e.g., current-carrying conductors, when action and reaction forces appear to be directed not in the same line.

Further, as energodynamics operates not only external but also internal forces, it is extremely important to show, that such forces arise and disappear only in steams. Internal forces any $i^{th}$ nature have, as is known, no resultant $\mathbf{F}_j$. If $\mathbf{f}_j$ (H/м²) - the specific force enclosed to a unit of a surface $f$ (м²) of any closed system in a direction of a normal $\mathbf{n}$ for it, this resultant $\mathbf{F}_j = \int\mathbf{f}_j\cdot\mathbf{n}df$ is always equal to zero. Applying to this expression Gauss theorem, we have:

$$\mathbf{F}_j = \int\mathbf{f}_j\cdot\mathbf{n}df = \int\mathrm{div}\mathbf{f}_j\, dV = 0. \qquad (23)$$

It means, that if in any element $dV$ volume of such system $\mathrm{div}\mathbf{f}_j \neq 0$ (i.e. in it there is some volume force $(\partial\mathbf{F}_j/\partial V)$ in another element of volume it should have an opposite sign (opposite direction). In other words, any internal force has to counteract, as followed prove. This statement is reasonable to be called for easy reference as the "**force couple principle**": *internal forces in heterogeneous systems appear and disapper pairwise only.* Such forces often not without justification are called *as internal strain.* They also generate in spatially non-uniform systems internal processes of the energy transformation, studying being a subject of energodynamics. In the systems possessing several degrees of freedom, these strains have a different nature. It also causes the energy transformation which character depends by nature overcome forces. In particular, if internal force has disorder character, there is a process of "energy dispersion», i.e. transformation of a part of the ordered internal energy into chaotic (thermal). Such phenomena will be considered later in the section devoted to the thermodynamics of irreversible processes.

## 6. Theoretical Derivation of Law of Universal Gravitation

Based on Kepler's laws, I. Newton, from data available at that time on the masses of celestial bodies and the distances between them, calculated that the force of attraction of two point masses $m$ and $M$ was directly proportional to their product and inversely proportional to the squared distance $r$ between them. Later Cavendish experimentally proved that the inverse-square law was valid for also terrestrial bodies while having calculated the mass of the Earth and the gravitational constant $G_g$. So the law of gravitation has come into being:

$$\mathbf{F}_g = G_g mM/r^2, \qquad (24)$$

which impact on the science history can not be overestimated.

It is a matter of interest to derive this law from the first principles of energodynamics. One of such principal statements is a declaration that the force fields are generated by neither masses nor charges[1], but their non-uniform distribution in space. The gravitational field is known to be absent in the center of a massive homogeneous sphere. Thus the

gravitational forces appear only where the attraction of the "test" body is unequal on different sides, i.e. the masses are distributed non-uniformly. In this case the heterogeneity is characterized by the distribution moment $\mathbf{Z}_{\mathrm{m}} = M\mathbf{r}_{\mathrm{m}}$, which is the product of the body mass $M$ and the displacement of the radius-vector $\mathbf{r}_{\mathrm{m}}$ of the body center from its position at the homogeneous distribution. From the distribution moment definition it follows that $d\mathbf{Z}_{\mathrm{m}} = Md\mathbf{r}_{\mathrm{m}}$, then the mass of any set of material points or bodies heterogeneously distributed is defined by the expression:

$$M = \partial \mathbf{Z}_{\mathrm{m}}/\partial \mathbf{r}_{\mathrm{m}} = \int \nabla \cdot \mathbf{Z}_{mV}\, dV, \qquad (25)$$

where $\mathbf{Z}_{mV} = \varrho\Delta\mathbf{r}_m = \partial \mathbf{Z}_m/\partial V$ – distribution moment density.

Changing over from the integral over volume into that over the closed surface $f$ as based on the Gauss theorem the expression (25) becomes:

$$M = \int \mathbf{Z}_{mV} \cdot \mathbf{n}\, df. \qquad (26)$$

This expression is valid for a body of any shape. Therefore let us take, for convenience, a spherical surface $f = 4\pi r_c^2$ (where $r_c$ – radius of a sphere, filled with a mass $M$). Then instead of (26):

$$M = 4\pi \int \mathbf{Z}_{mV} \cdot \mathbf{n} dr_c^2. \qquad (27)$$

The heterogeneity of mass distribution per unit volume of the system described by the vector $\mathbf{Z}_{mV}$ generates the thermodynamic force $\mathbf{x}_{\mathrm{g}}$, which in our case is expressed by the negative gradient $-\nabla\psi_{\mathrm{g}}$ of the gravitational potential $\psi_{\mathrm{g}}$. This force is connected with the $\mathbf{Z}_{mV}$ parameter through the general equation of state $\mathbf{Z}_{mV} = \mathbf{Z}_{mV}(\mathbf{x}_{\mathrm{g}})$. Assuming this relation proportional to the ground that both values ($\mathbf{Z}_{mV}$ and $\mathbf{x}_{\mathrm{g}}$) disappear simultaneously and denoting the proportionality factor as $\varepsilon_{\mathrm{g}}$ gives instead of (27):

$$M = 8\pi\varepsilon_{\mathrm{g}}\int r_c \mathbf{x}_{\mathrm{g}} \cdot \mathbf{n}\, dr_c. \qquad (28)$$

The $\mathbf{x}_{\mathrm{g}} \cdot \mathbf{n}$ product characterizes the absolute magnitude $x_{\mathrm{g}} = |\mathbf{x}_{\mathrm{g}}|$ of the specific force $\mathbf{x}_{\mathrm{g}}$ acting along the normal to the spherical surface. The field of this force is known to be heterogeneous. If the mass distribution in volume $V$ is homogeneous, the force $\mathbf{x}_{\mathrm{g}}$ inside the body is equal to zero and discontinues on the body surface. However, the Gauss formula is known to remain valid also in this case – it is just enough to change from $-\nabla\psi_{\mathrm{g}}$ to the so-called surface divergence $\mathbf{x}_{\mathrm{g}\,+}(r_c) - \mathbf{x}_{\mathrm{g}\,-}(r_c)$, i.e. to the difference of forces on both sides of the sphere surface. In the case of the homogeneous mass distribution $\mathbf{x}_{\mathrm{g}\,-}(r_c) = 0$, and instead of (28):

$$x_{\mathrm{g}} = G_{\mathrm{g}}M/r_c^2, \qquad (29)$$

where $G_g = 1/4\pi\varepsilon_g$ – proportionality factor empirically defined and usually called the gravitational constant.

Since in the stationary field $\nabla\psi_g = d\psi_g/d\mathbf{r}$, it is easy to find the gravitational potential $\psi_g = -\int x_g dr$ in any point $r \geq r_c$. Integrating (29) within $r_c$ to $r$ gives:

$$\psi_g = G_g M (1/r_c - 1/r). \quad (r \geq r_c). \qquad (30)$$

The gravitational potential $\psi_g$ is known to be the force of gravity per unit mass $m$ of a test body. Therefore the force $\mathbf{F}_g = m\psi_g$ found from this expression exactly complies with the gravity law (24). However, now this law of force was found theoretically from the condition of heterogeneous mass distribution. According to (30) the potential energy of gravitating masses becomes zero not at their being infinitely apart from each other (as follows from (24)), but, on the contrary, when they occupy the same space (like components of a mixture), which complies with empirical facts. As a particular case, the fact follows from (30) that at homogeneous mass distribution (also inside a body with homogeneous density) the gravity force is equal to zero (constant potential $\psi_g$). Hence Newton's law of gravitation (24) does not work, i.e. the range of its validity is restricted to a provisional (equivalent) radius of the sphere confining the "field-forming" body $M$ (area $r \geq r_c$). Unlike (24), the potential $\psi_g$ and the gravity force $\mathbf{F}_g$ in (30) do not become infinity at $r \rightarrow 0$. This eliminates the problem of "divergences" which, as appears now, is caused by the arbitrary extrapolation of the results obtained from observations on celestial bodies to dimensionless "point" objects. Taking into account the minimum distance $r_c$ the test mass $m$ can approach the mass $M$ solves the problem. Indeed, whatever the value $r_c$ could be, the potential $\psi_g = 0$ at $r = r_c$. Hence, the intensity of gravitational interaction is defined not by the interaction constant, but rather by the force magnitude at the closest approach of the interacting objects. It is not less significant that despite the well-established conceptions the potential energy of gravitating masses can not be negative, which corresponds to the general definition of energy as the capability of a system comprising material bodies to do work (positivity of energy in any form follows from the energy definition itself as a capability for doing work – which is either available or unavailable).

One more correction to the law of gravitation will be needed if one desires to allow for the impact made on the gravitation from the relative orientation of celestial bodies with shape anisotropy. Different positions of bodies in space and their different orientation in the same are known to be not equivalent mechanically [6]. It is this fact that may explain the dependence recently discovered by astronomers of the gravitational

constant $G_g$ from the relative position of some celestial bodies. As a matter of fact, for a body of non-spherical form the value $R_s$ varies, generally speaking, as a function of the angle φ, at which the other body is observed, i.e. $r_s = r_s(φ)$. In particular, for the Earth as a field-generating body, the distance from its surface to the center of its mass is unequal at different latitudes and longitudes. This is allowed for by the gravitational potential written in the form

$$\psi_g(R) = (G_g M_1/4\pi)[1/r_s(φ) -1/r], \ (r \geq r_s). \tag{31}$$

where the energy of interaction appears to be a function of the relative position of non-spherical bodies, e.g. the spiral galaxies. Such an approach is preferable to the assumption the gravitational constant is changeable. It better corresponds to the methodology of energodynamics demanding the orientation processes with the coordinate $φ_i$ to be specifically classified.

Thus, mechanics consideration as one of the branches of energodynamics allows not only to receive its main principles, laws and the equations as its consequence but also to generalise the majority of them.

## References

1. Helmholtz, H. On the Conservation of Force. HathiTrust., 1847.
2. Де Бройль Луи. Революция в физике. (Новая физика и кванты). М.: Атомиздат, 1965.
3. Etkin V. Energodynamics (Thermodynamic Fundamentals of Synergetics).- N.Y., 2011.- 480 p.
4. Эткин В.А. Принцип различимости процессов. http://sciteclibrary.ru/rus/catalog/pages/_12499.html. 15.01.2013. (In Russian)
5. Шипов Г.И. Теория физического вакуума. – М. , Наука, 1997. 450 с. (In Russian).
6. Ландау Л.Д., Лифшиц Е.М. Теоретическая физика. Т.1. – М.: Наука, 1973. (In Russian)
7. Эткин В.А. О силах инерции. http://sciteclibrary.ru/rus/catalog/pages /9836.html.20.08.2009
8. Эткин В.А. Коррекция механики с позиций энергодинамики. (http://samlib.ru/e/etkin_w_a/ korrecziyamehanikispoziziyenergodinamiki.shtml, 27.09.2009
9. Ньютон И. Математические начала натуральной философии.– Петроград, 1916 г.
10. Эткин В.А. Обобщение принципов механики. // Доклады независимых авторов, 2014. – Вып. 27. С.178…202. (In Russian)

11. Filatov N.V. Investigation of bodies impact with large kinetic momentums: Letter of Filatov N.V. to Chicherin V.G. 08.07.1969. .(In Russian)
12. Толчин В.Н. Инерцоид, силы инерции как источник движения. Пермь, 1977
13. Smirnov A.P. Understanding of knowledge is relevation of the XXIII century. //Reports of Int. Sc. Club. St-Petersburg. Russia, 2002
14. Эткин В.А. Теоретический вывод закона всемирного тяготения. / Вестник Дома Ученых Хайфы, 2007.-Т.12, с.28-32.

Series: **PHYSICS and ASTRONOMY**

**Solomon I. Khmelnik**

# Hexagonal storm on Saturn

## Content

## Abstract

At the north pole of Saturn has more than 30 years there is a giant storm in the shape of a hexagon, each side of which is greater than the diameter of Earth. This hexagon does not move on the planet, rotates and maintains its shape. This phenomenon still has no explanation. The following is a mathematical model of such a storm similar to the mathematical model of an ocean whirlpool (proposed earlier by the author). Also in the article shows that the energy source, that allows the storm to spin for a long time, is the gravitational field of Saturn.

## 1. Introduction

For more than 30 years at the north pole of Saturn, there has been a huge storm of hexagon shape, which side exceeds the Earth's diameter [1, 2]. This hexagon does not travel around the planet, but rotates keeping its shape. Existing for more than 30 years, the storm demonstrates an amazing stability. Many works is dedicated to building mathematical models of this storm, but there has not been a generally recognized model yet [3].

The external similarity between this storm and the oceanic whirlpool is clearly noticeable — see Fig.1 and Fig.2. The main difference consists in the shapes of surfaces. We can say, emphasizing this similarity,

that on Saturn a <u>hexagonal</u> "gas vortex" exists unlike <u>round</u> water vortexes in oceans of the Earth.

Let's also notice that hexagonal gas vortexes can be observed on the Earth as well: analysis of the photos made by space satellites showed the presence of hexagonal clouds over the anomalous zone in the Atlantic Ocean known as the Bermuda Triangle - see Fig. 3 [4].
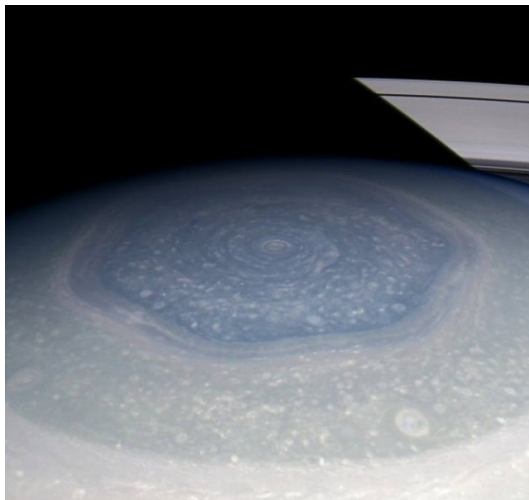

Fig. 1.


Fig. 2.

Fig. 3.

Further on, we're going to build a mathematical model of elliptic vortex first. It can be built in the same way as the round vortex model [5] based on the solution of Maxwell's equations for gravitomagnetism [6].

Then, we will show that hexagonal gas vortex is a sum of elliptic gas vortexes. Each gas vortex is determined by its own initial conditions in Maxwell's equations. In case of several sets of independent initial conditions, several solutions, or elliptic vortexes, occur. As the system of Maxwell's equations is linear, then actual solution is a sum of these solutions. The sum has a form of a hexagonal vortex.

## 2. Summary of mathematical model of water vortex on the Earth

In the mathematical model of water vortex [5] a system of quasi-Maxwell's gravitation equations is used [6]. The model is based on the following assumptions: Water flows can be described as <u>mass currents</u>. Mass currents in the gravitational field are described by Maxwell's equations for gravitomagnetism — quasi-Maxwell's gravitation equations [6] (hereinafter - QMG-equations). Interaction between moving masses is described by gravitational Lorentz forces (hereinafter — GL-forces), which are similar to Lorentz forces between moving electric charges in classical electrodynamics.

Mass currents in the vortex circulate within horizontal sections of the vortex, as well as vertically. Kinetic energy is spent on losses due to viscous friction. These energy comes from a gravitating body — the Earth. Potential energy of the vortex does not change, and therefore is

not spent, i.e. in this case, there is no conversion of kinetic energy into potential energy and vice versa. However, <u>the gravitating body expends its energy</u> on creating and maintaining massive currents, i.e. <u>preserving the vortex.</u>

The water vortex, being a type of water flow also satisfies Navier–Stokes equation for viscous incompressible liquid. In [5] it's shown that water pressure in the vortex can be calculated according to Navier–Stokes equation depending on mass currents. In this case, the locus, where vertical pressure component is constant on free surface, occurs to be a circle of given radius. Pressure at the free surface reflects the shape of the vortex surface. Therefore, the vortex surface shall contain concentric projections and deeps corresponding to wavelike dependency of pressure on radius. Based on this in work [5] an image of the vortex surface is reproduced – see Fig. 4.

The similar approach is used below. We only need to prove the existence of a solution of Maxwell's equations for elliptic vortex, and then, for hexagonal vortex.
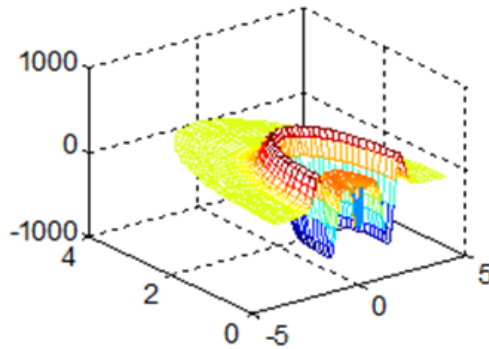


Fig. 4.

# 3. Mathematical model of elliptic vortex

Maxwell's equations for stationary gravitomagnetic field will be as follows:

$$\operatorname{div}(H) = 0, \tag{1}$$
$$\operatorname{div}(J) = 0, \tag{2}$$
$$\operatorname{rot}(H) = J, \tag{3}$$

where $H$ - <u>gravitomagnetic intensities</u>, $J$ - <u>densities of mass currents.</u>

Let's consider these equations in elliptic coordinate system $\xi$, $\varphi$, $z$ [7, p. 161] - see also Fig. 5:

$$\operatorname{div}(H)=\begin{pmatrix} \dfrac{1}{a\Delta^3}\big(\operatorname{sh}(\xi)\operatorname{ch}(\xi)H_\xi+\sin(\varphi)\cos(\varphi)H_\varphi\big)+ \\[2mm] \dfrac{1}{a\Delta}\left(\dfrac{\partial H_\xi}{\partial\xi}+\dfrac{\partial H_\varphi}{\partial\varphi}\right)+\dfrac{\partial H_z}{\partial z} \end{pmatrix}=0, \qquad (4)$$

$$\operatorname{rot}_\xi(H)=\left(\dfrac{1}{a\Delta}\dfrac{\partial H_z}{\partial\varphi}-\dfrac{\partial H_\varphi}{\partial z}\right)=J_\xi, \qquad (5)$$

$$\operatorname{rot}_\varphi(H)=\left(\dfrac{\partial H_\xi}{\partial z}-\dfrac{1}{a\Delta}\dfrac{\partial H_z}{\partial\xi}\right)=J_\varphi, \qquad (6)$$

$$\operatorname{rot}_z(H)=\begin{pmatrix} \dfrac{1}{a\Delta^3}\big(\operatorname{ch}(\xi)\operatorname{sh}(\xi)H_\varphi-\cos(\varphi)\sin(\varphi)H_\xi\big)+ \\[2mm] \dfrac{1}{a\Delta}\left(\dfrac{\partial H_\varphi}{\partial\xi}-\dfrac{\partial H_\xi}{\partial\varphi}\right) \end{pmatrix}=J_z, \qquad (7)$$

$$\operatorname{div}(J)=\begin{pmatrix} \dfrac{1}{a\Delta^3}\big(\operatorname{sh}(\xi)\operatorname{ch}(\xi)J_\xi+\sin(\varphi)\cos(\varphi)J_\varphi\big)+ \\[2mm] \dfrac{1}{a\Delta}\left(\dfrac{\partial J_\xi}{\partial\xi}+\dfrac{\partial J_\varphi}{\partial\varphi}\right)+\dfrac{\partial J_z}{\partial z} \end{pmatrix}=0, \qquad (7a)$$

where

$$\Delta=\sqrt{\big(\operatorname{ch}^2(\xi)-\cos^2(\varphi)\big)}, \qquad (7b)$$
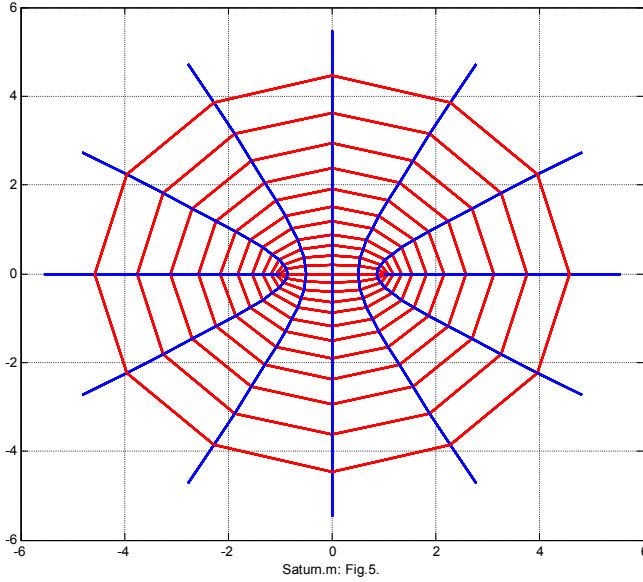
$a$ - half-focal distance,

coordinates $\xi,\ \varphi,\ z$ correlate with orthogonal coordinates $x,\ y,\ z$ through the following formulas

$$x=a\operatorname{ch}(\xi)\cos(\varphi),\ \ y=a\operatorname{sh}(\xi)\sin(\varphi),\ \ z=z. \qquad (7c)$$

With fixed $\xi,\ z$ the point draws an ellipse in horizontal plane. With fixed $\varphi,\ z$ the point draws a hyperbola in horizontal plane. Particularly, Fig. 5 shows ellipses and hyperbolas drawn in accordance with (7c) under $a=1$ in relation to $0\le\xi<1.2,\ 0\le\varphi<2\pi$. Fig. 6a demonstrates the same diagrams in logarithmic scale.

One of possible solutions of equations (4-7a) have the following form (as shown in Appendix 1):

Satum.m: Fig.5.

$$H_{\xi}. = h_{\xi}\Delta^{-2}\sin(\varphi)\cos(\varphi), \qquad (8)$$

$$H_{\varphi}. = h_{\varphi}\Delta^{-2}\mathrm{sh}(\xi)\mathrm{ch}(\xi), \qquad (9)$$

$$H_{z} = \Delta^{-2}, \qquad (10)$$

$$J_{\xi} = \frac{2}{a\Delta^{5}}\sin(\varphi)\cos(\varphi), \qquad (11)$$

$$J_{\varphi} = -\frac{2}{a\Delta^{5}}\mathrm{sh}(\xi)\mathrm{ch}(\xi), \qquad (12)$$

$$J_{z} = \frac{3}{a\Delta^{5}}\left(h_{\varphi}\mathrm{sh}^{2}(\xi)\mathrm{ch}^{2}(\xi) - h_{\xi}\sin^{2}(\varphi)\cos^{2}(\varphi)\right), \qquad (13)$$

where constants $h_{\xi}$, $h_{\varphi}$ correlate through the following relation

$$h_{\xi} + h_{\varphi} = 0. \qquad (14)$$

Diagrams of functions (8-13) under $a = 1$, $h_{\xi} = 1$, $h_{\varphi} = -1$ are shown in Fig. 6 on planes $(x, y)$, where $(x, y)$ are defined according to. Diagrams of functions (8-13) under $a = 1$, $h_{\xi} = 1$, $h_{\varphi} = -1$ are shown on Fig. 6 on planes $(x, y)$, where $(x, y)$ are defined according to function (7c) in relation to $0 \le \xi < \xi_{\max}$, $0 \le \varphi < 2\pi$.

The left column in Fig. 7 states functions $H_{\xi}(\xi)$, $H_{\varphi}(\xi)$, $H_{z}(\xi)$ under the stated value of $\varphi$. Furthermore, a solid line, dots and a dashed
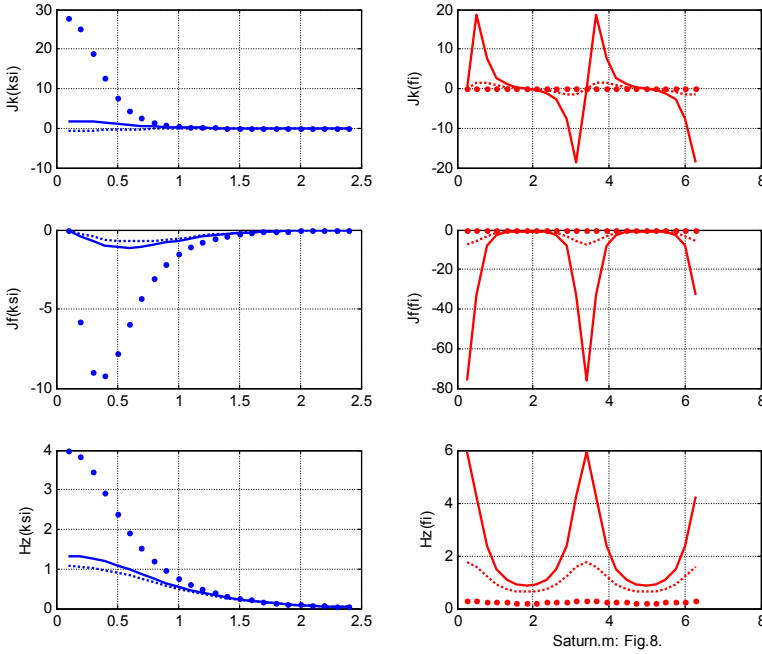
line show these functions under $\varphi = 1.05,\ 1.83,\ 3.67$ respectively.

The right column in Fig. 7 states functions $H_\xi(\varphi),\ H_\varphi(\varphi),\ H_z(\varphi)$ under the stated value of $\xi$. Furthermore, a solid line, dots and a dashed line show these functions under $\xi = 0.4,\ 0.7,\ 1.4$ respectively.

Finally, Fig. 8 states functions $J_\xi(\xi),\ J_\varphi(\xi),\ J_z(\xi)$ and $J_\xi(\varphi),\ J_\varphi(\varphi),\ J_z(\varphi)$ in the same way.

Saturn.m: Fig.6a.



Saturn.m: Fig.7.

Saturn.m: Fig.8.
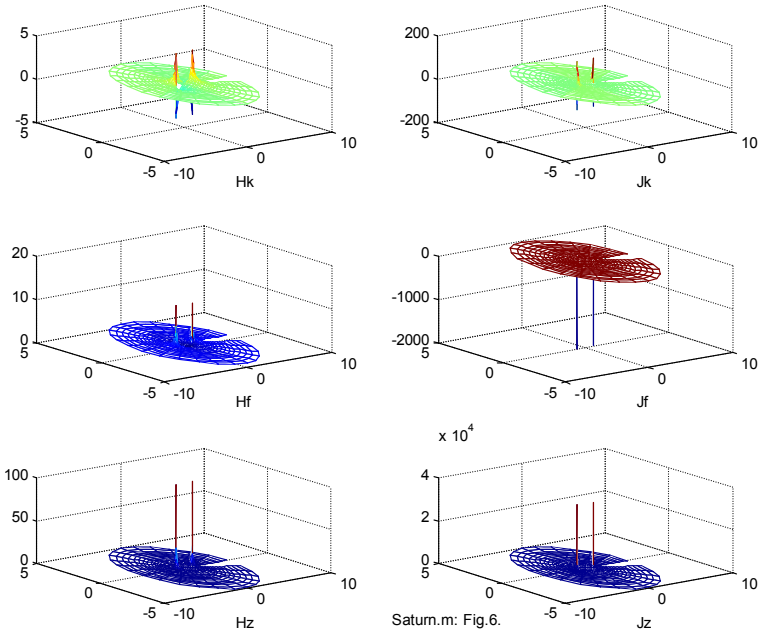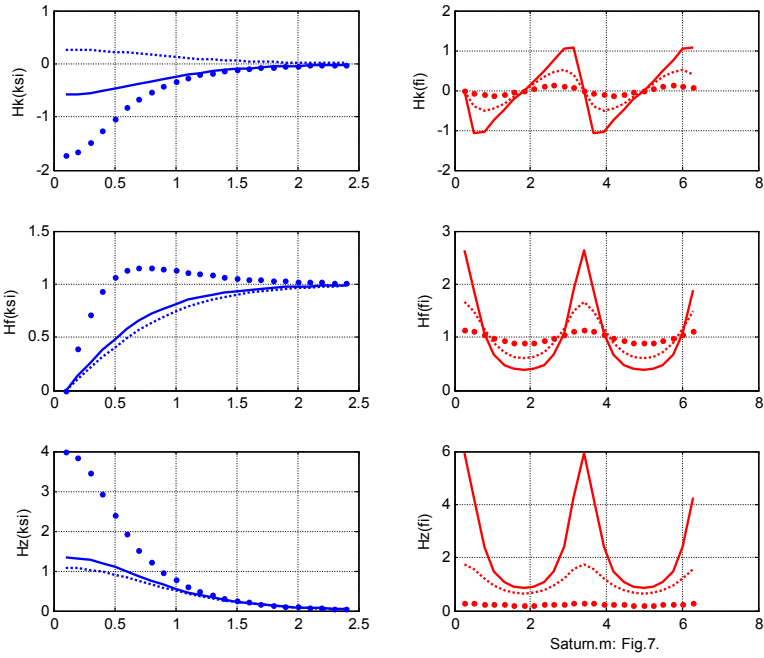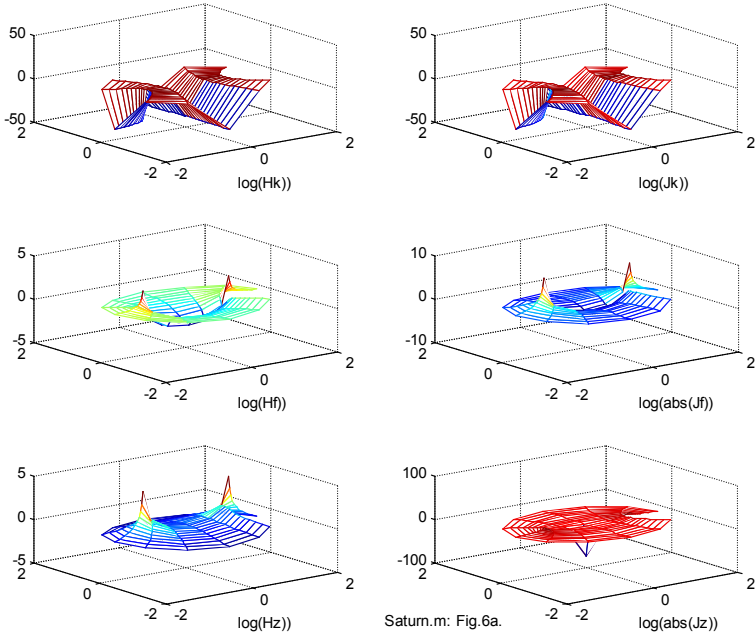
# 4. Mathematical model of hexagonal vortex

The image shown in Fig. 4 is determined by the <u>initial conditions – – massive currents in the bottom of the vortex</u>. In case of several sets of independent initial conditions, several solutions in the specified form occur. As the system of Maxwell's equations is linear, then actual solution is a sum of these several solutions. If the group of initial conditions determines a group of elliptic vortices with a common center, then the common solution will determine the <u>vortex, shaping total ellipses</u>.

It can be shown that the shape of total ellipses represents a closed curve Γ. This means that the locus of points with constant vertical vector of pressure on a free surface differs from a circle of the stated radius having a form of a closed curve Γ. The value of the vertical vector of pressure on this curve Γ will be of the same value. Consequently, in this case the surface of the vortex would be concentric curves Γ instead of concentric circles.

<u>Each closed convex curve Γ can be decomposed into a sum of ellipses</u>. Evidence may be as follows. Any such curve can be represented with two functions of angle $\varphi$ :

$$x = f_x(\varphi), \tag{1}$$
$$y = f_y(\varphi). \tag{2}$$

119

Discrete functions (1, 2) represented in this way can be decomposed into trigonometrical series of the following kind:

$$x = \sum_{n=2}^{N} x_n \,, \tag{3}$$

$$y = \sum_{n=2}^{N} y_n \,, \tag{4}$$

where

$$x_n = \left( \alpha_n \cos\left( \frac{2\pi(n-1)}{N} \varphi \right) + \beta_n \sin\left( \frac{2\pi(n-1)}{N} \varphi \right) \right), \tag{5}$$

$$y_n = \left( \eta_n \cos\left( \frac{2\pi(n-1)}{N} \varphi \right) + \lambda_n \sin\left( \frac{2\pi(n-1)}{N} \varphi \right) \right). \tag{6}$$

Here, each pair of summands $(x_n,\ y_n)$ is an ellipse. Consequently, the curve $\Gamma$ is a sum of ellipses.

Appendix 2 describes expansion of the hexagon into ellipses. The solution for elliptic vortex is stated above. Consequently, there is a possible group of initial conditions for a hexagonal vortex. Observations of Saturn and the Bermuda triangle proved existence of the above-mentioned combination of initial conditions.

## Appendix 1. Solution of Maxwell's equations in cylindrical coordinates

Section 3 describes Maxwell's equations in elliptic coordinates $\xi,\ \varphi,\ z$ (3.4- 3.7a).

Let's find the solution of these equations assuming that all variables are unchanged along axis $z$. In this case, equations (2, 11-13, 14) will be as follows:

$$\frac{1}{\Delta^2}\left(sh(\xi)ch(\xi)H_\xi + \sin(\varphi)\cos(\varphi)H_\varphi\right) + \left(\frac{\partial H_\xi}{\partial \xi} + \frac{\partial H_\varphi}{\partial \varphi}\right) = 0, \tag{1}$$

$$\frac{1}{a\Delta}\frac{\partial H_z}{\partial \varphi} = J_\xi, \tag{2}$$

$$-\frac{1}{a\Delta}\frac{\partial H_z}{\partial \xi} = J_\varphi, \tag{3}$$

$$\left(\frac{1}{a\Delta^3}\left(ch(\xi)sh(\xi)H_\varphi - \cos(\varphi)\sin(\varphi)H_\xi\right) + \frac{1}{a\Delta}\left(\frac{\partial H_\varphi}{\partial \xi} - \frac{\partial H_\xi}{\partial \varphi}\right)\right) = J_z, \tag{4}$$

$$\frac{1}{\Delta^2}\left(\text{sh}(\xi)\text{ch}(\xi)J_\xi + \sin(\varphi)\cos(\varphi)J_\varphi\right)+\left(\frac{\partial J_\xi}{\partial \xi}+\frac{\partial J_\varphi}{\partial \varphi}\right)=0. \tag{5}$$

From (3.7b) we find that

$$\frac{\partial(\Delta^{-2})}{\partial \xi}=\frac{\partial\left(\left(\text{ch}^2(\xi)-\cos^2(\varphi)\right)^{-1}\right)}{\partial \xi}=2\Delta^{-4}\text{sh}(\xi)\text{ch}(\xi), \tag{6}$$

$$\frac{\partial(\Delta^{-2})}{\partial \varphi}=\frac{\partial\left(\left(\text{ch}^2(\xi)-\cos^2(\varphi)\right)^{-1}\right)}{\partial \xi}=2\Delta^{-4}\sin(\varphi)\cos(\varphi). \tag{7}$$

Let

$$H_\xi. = h_\xi\Delta^{-2}\sin(\varphi)\cos(\varphi), \tag{8}$$

$$H_\varphi. = h_\varphi\Delta^{-2}\text{sh}(\xi)\text{ch}(\xi). \tag{9}$$

Then

$$\frac{\partial H_\xi}{\partial \xi}=h_\xi\sin(\varphi)\cos(\varphi)\frac{\partial(\Delta^{-2})}{\partial \xi}=2\Delta^{-4}h_\xi\sin(\varphi)\cos(\varphi)\text{sh}(\xi)\text{ch}(\xi), \tag{10}$$

$$\frac{\partial H_\xi}{\partial \varphi}=h_\xi\sin(\varphi)\cos(\varphi)\frac{\partial(\Delta^{-2})}{\partial \varphi}=2\Delta^{-4}h_\xi\sin^2(\varphi)\cos^2(\varphi), \tag{11}$$

$$\frac{\partial H_\varphi}{\partial \varphi}=h_\varphi\text{sh}(\xi)\text{ch}(\xi)\frac{\partial(\Delta^{-2})}{\partial \varphi}=2h_\varphi\Delta^{-4}\text{sh}(\xi)\text{ch}(\xi)\sin(\varphi)\cos(\varphi), \tag{12}$$

$$\frac{\partial H_\varphi}{\partial \xi}=h_\varphi\text{sh}(\xi)\text{ch}(\xi)\frac{\partial(\Delta^{-2})}{\partial \xi}=2\Delta^{-4}h_\varphi\text{sh}^2(\xi)\text{ch}^2(\xi). \tag{13}$$

From (1, 8-13) we find that

$$\frac{1}{\Delta^2}\left(\begin{array}{c}\text{sh}(\xi)\text{ch}(\xi)h_\xi\Delta^{-2}\sin(\varphi)\cos(\varphi)+\\\sin(\varphi)\cos(\varphi)h_\varphi\Delta^{-2}\text{sh}(\xi)\text{ch}(\xi)\end{array}\right)+\left(\begin{array}{c}2\Delta^{-4}h_\xi\sin(\varphi)\cos(\varphi)\text{sh}(\xi)\text{ch}(\xi)+\\2\Delta^{-4}h_\varphi\text{sh}(\xi)\text{ch}(\xi)\sin(\varphi)\cos(\varphi)\end{array}\right)=0$$

or

$$3h_\xi\sin(\varphi)\cos(\varphi)\text{sh}(\xi)\text{ch}(\xi)+3h_\varphi\text{sh}(\xi)\text{ch}(\xi)\sin(\varphi)\cos(\varphi)=0$$

or

$$h_\xi + h_\varphi = 0. \tag{14}$$

From (4, 8-13) we find that

$$\left(\begin{array}{c}\frac{1}{a\Delta^3}\left(\text{ch}(\xi)\text{sh}(\xi)h_\varphi\Delta^{-2}\text{sh}(\xi)\text{ch}(\xi)-\cos(\varphi)\sin(\varphi)h_\xi\Delta^{-2}\sin(\varphi)\cos(\varphi)\right)+\\\frac{1}{a\Delta}\left(2\Delta^{-4}h_\varphi\text{sh}^2(\xi)\text{ch}^2(\xi)-2\Delta^{-4}h_\xi\sin^2(\varphi)\cos^2(\varphi)\right)\end{array}\right)=J_z$$

or

$$\begin{pmatrix} \left(h_\varphi \text{ch}(\xi)\text{sh}(\xi)\text{sh}(\xi)\text{ch}(\xi) - h_\xi \cos(\varphi)\sin(\varphi)\sin(\varphi)\cos(\varphi)\right) + \\ \left(2h_\varphi \text{sh}^2(\xi)\text{ch}^2(\xi) - 2h_\xi \sin^2(\varphi)\cos^2(\varphi)\right) \end{pmatrix} = a\Delta^{-5}J_z$$

or

$$3h_\varphi \text{sh}^2(\xi)\text{ch}^2(\xi) - 3h_\xi \sin^2(\varphi)\cos^2(\varphi) = a\Delta^{-5}J_z$$

or

$$J_z = \frac{3}{a\Delta^5}\left(h_\varphi \text{sh}^2(\xi)\text{ch}^2(\xi) - h_\xi \sin^2(\varphi)\cos^2(\varphi)\right) \tag{15}$$

By substitution of (2, 3) into (4), we will obtain the following

$$\frac{1}{\Delta^2}\left(\text{sh}(\xi)\text{ch}(\xi)\frac{1}{a\Delta}\frac{\partial H_z}{\partial \varphi} - \sin(\varphi)\cos(\varphi)\frac{1}{a\Delta}\frac{\partial H_z}{\partial \xi}\right) +$$

$$+\left(\frac{1}{a\Delta}\frac{\partial^2 H_z}{\partial \varphi \partial \xi} - \frac{1}{a\Delta}\frac{\partial^2 H_z}{\partial \varphi \partial \xi}\right) = 0$$

or

$$\left(\text{sh}(\xi)\text{ch}(\xi)\frac{\partial H_z}{\partial \varphi} - \sin(\varphi)\cos(\varphi)\frac{\partial H_z}{\partial \xi}\right) = 0. \tag{16}$$

From (6, 7) we find that

$$\left(\text{sh}(\xi)\text{ch}(\xi)\frac{\partial(\Delta^{-2})}{\partial \varphi} - \sin(\varphi)\cos(\varphi)\frac{\partial(\Delta^{-2})}{\partial \xi}\right) = 0. \tag{17}$$

Comparing (16, 17), we can notice that

$$H_z = \Delta^{-2}. \tag{18}$$

From (2, 3, 18), we obtain:

$$J_\xi = \frac{1}{a\Delta}\frac{\partial(\Delta^{-2})}{\partial \varphi}, \tag{19}$$

$$J_\varphi = -\frac{1}{a\Delta}\frac{\partial(\Delta^{-2})}{\partial \xi}. \tag{20}$$

or, taking (6, 7) into account,

$$J_\xi = \frac{2}{a\Delta^5}\sin(\varphi)\cos(\varphi), \tag{21}$$

$$J_\varphi = -\frac{2}{a\Delta^5}\text{sh}(\xi)\text{ch}(\xi). \tag{22}$$

Thus, if variables $H_\xi$ and $H_\varphi$ are determined according to (8, 9), respectively, then variables $H_z$, $J_\xi$, $J_\varphi$, $J_z$ are determined according to (18, 21, 22, 15), respectively, and condition (14) is satisfied.

# Appendix 2. Decomposition of hexagon into ellipses.

Let's consider a hexagon shown in Fig. 1. It can be represented by two functions of angle $\varphi$:

$$x = f_x(\varphi), \tag{1}$$
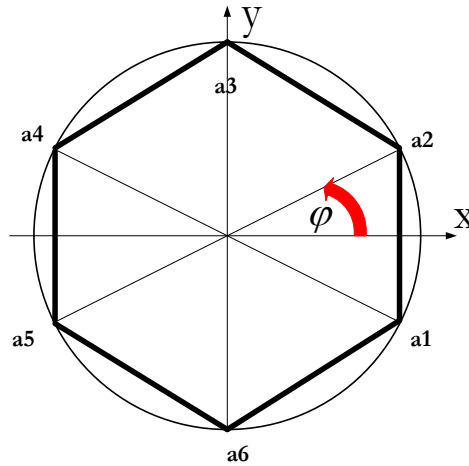
$$y = f_y(\varphi). \tag{2}$$



Fig. 1.

These functions are shown in Fig. 2. Let's represent these functions as a set of points. In Fig. 2 each line section is represented by three points: $n = 3$, and line section [a1, a2] is duplicated. In this case each function is described by $N = 7n$ points. Discrete functions (1, 2) determined in such a way can be decomposed into the trigonometric series of the form (4.1, 4.2).
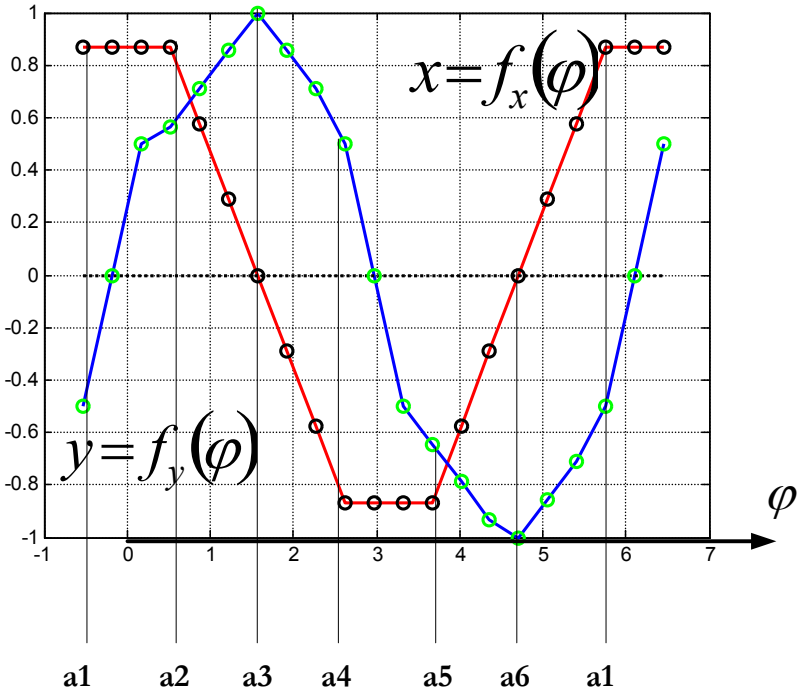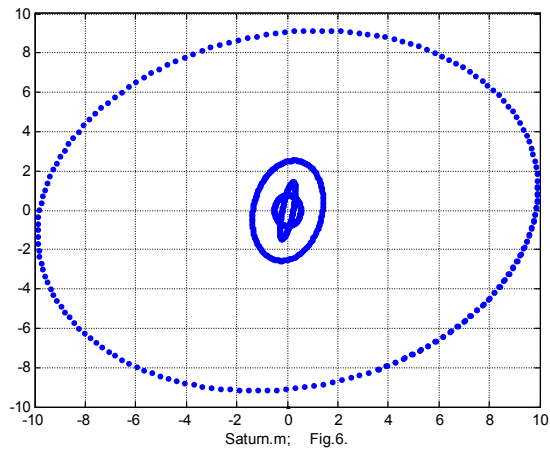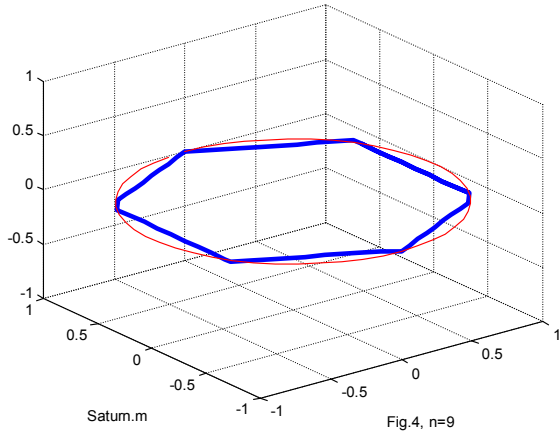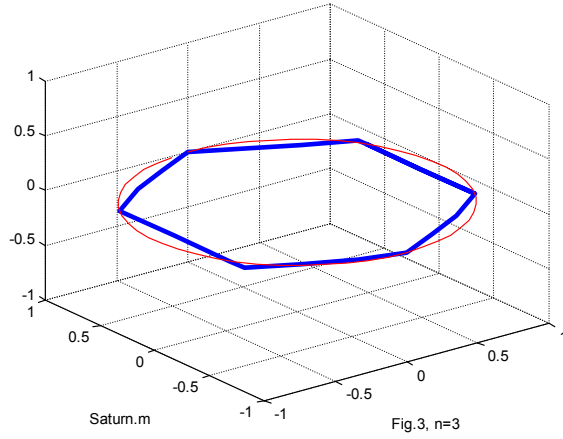
Рис. 2.

Modeling showed that for $n = 1$ the constant values of first components can be neglected. Therefore, functions (1, 2) in polar and cylindrical coordinates can be approximated by $(N-1)$ functions, which describe **ellipses**. The sum of these functions represents a hexagon. For example, Fig. 3 and Fig. 4 show geometric objects obtained as a result of such approximation for $n = 3$ and $n = 9$, respectively. Fig. 6 shows the first 4 ellipses in the decomposition of the hexagon for $n = 3$. The first ellipse is shown in dots.

Saturn.m                             Fig.3, n=3



Saturn.m                             Fig.4, n=9



Saturn.m;   Fig.6.

# References

1. Saturn's hexagon, http://naucaitechnika.ru/blog/43524663032/10-strannyih-obektov-Solnechnoy-sistemyi,-o-kotoryih-nam-malo-ch (in Russian)
2. Saturn's hexagon, http://fishki.net/1592643-krupnye-inoplanetnye-buri-i-uragany.html (in Russian)
3. Saturn's hexagon, https://en.wikipedia.org/wiki/Saturn%27s_hexagon
4. It disclosed the secret of the Bermuda Triangle, https://lenta.ru/news/2016/10/24/bt/ (in Russian)
5. Khmelnik S.I. The Equation of Whirlpool, http://vixra.org/abs/1506.0157.
6. Khmelnik S.I. Experimental Clarification of Maxwell-Similar Gravitation Equations, http://vixra.org/abs/1311.0023; and «The Papers of Independent Authors», publ. «DNA», printed in USA, ISSN 2225-6717, Lulu Inc., ID 14794393, 2014, №28, ISBN 978-1-312-23676-9, http://lib.izdatelstwo.com/Papers/28.104.pdf
7. Andre Ango. Mathematics for Electrical and Radio Engineers, publ. "Nauka", Moscow, 1964, 772 p. (in Russian).
8. S.I. Khmelnik. Hexagonal Storm on Saturn, http://vixra.org/abs/1611.0313, 2016-11-23

# Series: **PHYSICS and ASTRONOMY**

**Solomon I. Khmelnik**

# Mathematical model of a plasma crystal

## Abstract

A mathematical model of the plasma crystal built using Maxwell's equations is given.

## Content

## 1. Problem statement

Dusty plasma (see the [1]) is a set of charged particles. These "particles can arrange in space in a certain way and form the so-called plasma crystal" [2]. The mechanism of formation, behavior and form of such crystals is difficult to predict. Observation of these processes and forms under low gravity conditions sets at the gaze – see illustration (Fig 1.) of the experiments in space in the [3].

Therefore, they were simulated on computer in 2007. The results surprised even greater, which was reflected in the name of a corresponding article [4]: "From plasma crystals and helical structures towards inorganic living matter". The [5] gives a summary and discussion of the simulation results.

I like such comparisons too. But, nevertheless, it should be noted that the method used by the authors of the molecular dynamics simulations does not fully take into account all the features of the dusty plasma. To describe the motion of the particles this method uses classical mechanics and considers only electrostatic forces between the charged particles. In fact, the charged particles motion causes occurrence of charge currents – electrical currents and electromagnetic fields as a consequence. They should be considered during simulation.
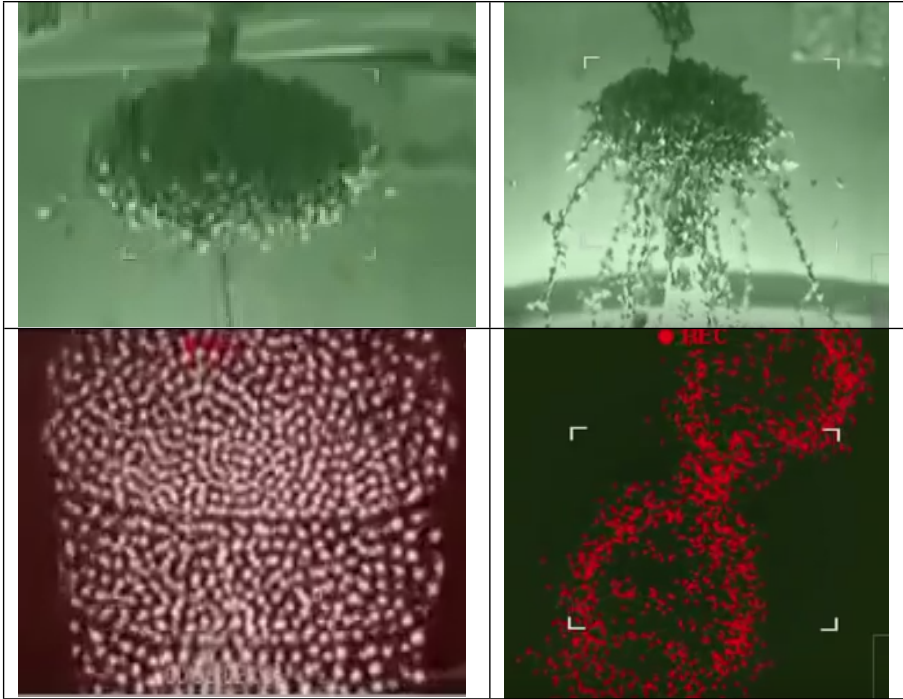
Fig. 1.

In absence of gravity the plasma particles are not affected by gravitational forces. If we exclude radiation energy, then it can be said that the dusty plasma is electric charges, electric currents and electromagnetic fields. Moreover, at its formation (filling a vessel with a set of charged particles) the plasma receives some energy. This energy may be only electromagnetic and kinetic energy of the particles, since there is no mechanical interaction between the particles: they are charged with like charges. Thus, the dusty plasma should meet the following conditions:

- to meet the Maxwell's equations,
- to maintain the total energy as a sum of electromagnetic and kinetic energy of the particles,
- to become stable in terms of the particles structure and motion in some time; it follows, for example, from the said experiments in space – see fig. 1.

The charged particles obviously push off from each other by Coulomb forces. However, the experiments show that these forces do

not act on the periphery of a particles cloud. Consequently, they are compensated by other forces. It will be shown below that these forces are Lorentz forces arising during charged particles motion (although it seems strange at first sight that these forces direct into the cloud, opposing the Coulomb forces). The particles cannot be fixed, since then the Coulomb forces will prevail. But then these forces will move the particles, which causes the Lorentz forces, etc.

In the mathematical model shown below we will not take into account the Coulomb forces, believing that their role is only to ensure that the particles are isolated from each other (just as these forces are not considered in electrical engineering problems).

Thus, we will consider the dusty plasma as an area with flowing electrical currents and analyze it using the Maxwell's equations. Since the particles are in vacuum and are always isolated from each other, there is no ohmic resistance and no electrical voltage proportional to the current – it should not be taken into account in the Maxwell's equations. In addition, in the first stage, we will assume that the currents change slowly – they are constant currents. Considering these remarks, the Maxwell's equations are as follows:

$$\mathrm{rot}(H) - J = 0,\tag{1}$$
$$\mathrm{div}(J) = 0,\tag{2}$$
$$\mathrm{div}(H) = 0,\tag{3}$$

where the $J$, $H$ is the current and magnetic intensity, respectively. In addition, we need to add to these equations an equation uniting the plasma energy $W$ with the $J$, $H$:

$$W = f(J,\ H).\tag{4}$$

In this equation, the energy $W$ is known since the plasma receives this energy at its formation.

In scalar form, the system of equations (1-4) is a system of 6 equations with 6 unknowns and should have only one solution. However, there is no regular algorithm for solving such a system. Therefore, below we propose another approach:

1. Search for analytical solutions of underdetermined system of equations (1-3) with this plasma cloud form. There can be multiple solutions.
2. Calculation of energy $W$ using the (4). If the solution of the system (1-4) is the only one then this solves the system (1-4) with the data of the $W$ and cloud form.

## 2. System of equations

In the cylindrical coordinates $r, \varphi, z$, as is well-known [6], the divergence and curl of the vector H are as follows:

$$\operatorname{div}(H) = \left( \frac{H_r}{r} + \frac{\partial H_r}{\partial r} + \frac{1}{r} \cdot \frac{\partial H_\varphi}{\partial \varphi} + \frac{\partial H_z}{\partial z} \right), \tag{a}$$

$$\operatorname{rot}_r(H) = \left( \frac{1}{r} \cdot \frac{\partial H_z}{\partial \varphi} - \frac{\partial H_\varphi}{\partial z} \right), \tag{b}$$

$$\operatorname{rot}_\varphi(H) = \left( \frac{\partial H_r}{\partial z} - \frac{\partial H_z}{\partial r} \right), \tag{c}$$

$$\operatorname{rot}_z(H) = \left( \frac{H_\varphi}{r} + \frac{\partial H_\varphi}{\partial r} - \frac{1}{r} \cdot \frac{\partial H_r}{\partial \varphi} \right). \tag{d}$$

Considering the equations (a-d) we rewrite the equations (1.1-1.3) as follows:

$$\frac{H_r}{r} + \frac{\partial H_r}{\partial r} + \frac{1}{r} \cdot \frac{\partial H_\varphi}{\partial \varphi} + \frac{\partial H_z}{\partial z} = 0, \tag{1}$$

$$\frac{1}{r} \cdot \frac{\partial H_z}{\partial \varphi} - \frac{\partial H_\varphi}{\partial z} = J_r, \tag{2}$$

$$\frac{\partial H_r}{\partial z} - \frac{\partial H_z}{\partial r} = J_\varphi, \tag{3}$$

$$\frac{H_\varphi}{r} + \frac{\partial H_\varphi}{\partial r} - \frac{1}{r} \cdot \frac{\partial H_r}{\partial \varphi} = J_z, \tag{4}$$

$$\frac{J_r}{r} + \frac{\partial J_r}{\partial r} + \frac{1}{r} \cdot \frac{\partial J_\varphi}{\partial \varphi} + \frac{\partial J_z}{\partial z} = 0 \tag{5}$$

The system of 5 equations (1-5) with respect to the 6 unknowns $\left( H_r, H_\varphi, H_z, J_r, J_\varphi, J_z \right)$ is overdetermined and may have multiple solutions. It is shown below that such solutions exist and for different cases some of possible solutions can be identified.

We will first look for a solution for this system of equations (1-5) as functions separable relative to the coordinates. These functions are as follows:

$$H_r = h_r(r) \cdot \cos(\chi z), \tag{6}$$

$$H_\varphi = h_\varphi(r) \cdot \sin(\chi z), \tag{7}$$

$$H_z = h_z(r) \cdot \sin(\chi z), \tag{8}$$

$$J_r. = j_r(r) \cdot \cos(\chi z), \tag{9}$$

$$J_\varphi. = j_\varphi(r) \cdot \sin(\chi z), \tag{10}$$

$$J_z = j_z(r) \cdot \sin(\chi z), \tag{11}$$

where the $\chi$ is a constant, while the $h_r(r), h_\varphi(r), h_z(r), j_r(r), j_\varphi(r), j_z(r)$ are the functions of the coordinate $r$; derivatives of these functions will be denoted by strokes.

By putting the (6-11) into the (1-5) we get:

$$\frac{h_r}{r} + h'_r + \chi h_z = 0, \tag{12}$$

$$-\chi h_\varphi = j_r, \tag{13}$$

$$-\chi h_r - h'_z = j_\varphi \tag{14}$$

$$\frac{h_\varphi}{r} + h'_\varphi = j_z, \tag{15}$$

$$\frac{j_r}{r} + j'_r + \chi j_z = 0. \tag{16}$$

Let's put the (13) and (15) into the (16). Then we get:

$$\frac{-\chi h_\varphi}{r} - \chi h'_\varphi + \chi \left( \frac{h_\varphi}{r} + h'_\varphi \right) = 0. \tag{17}$$

The expression (17) is an identity 0=0. Therefore, the (16) follows from the (13, 15) and can be excluded from the system of equations (12-16). The rest of the equations can be rewritten as:

$$h_z = -\frac{1}{\chi} \left( \frac{h_r}{r} + h'_r \right), \tag{18}$$

$$j_z = \frac{h_\varphi}{r} + h'_\varphi, \tag{19}$$

$$j_r = -\chi h_\varphi, \tag{20}$$

$$j_\varphi = -\chi h_r - h'_z \tag{21}$$

## 3. The first mathematical model

In this system of 4 differential equations (18-21) with 6 unknown functions we can define two functions arbitrarily. For further study we define the following two functions:

$$h_\varphi = q \cdot r \cdot \sin(\pi \cdot r / \chi), \tag{22}$$

$$h_r = h \cdot r \cdot \sin(\pi \cdot r / \chi), \tag{23}$$

where the $q, h$ are some constants. Then using the (18-23) we find:

$$h_z = -\frac{h}{\chi}\left(2\sin(\pi \cdot r/\chi) + \frac{\pi \cdot r}{\chi}\cos(\pi \cdot r/\chi)\right), \qquad (24)$$

$$j_z = q\left(2\sin(\pi \cdot r/\chi) + \frac{\pi \cdot r}{\chi}\cdot\cos(\pi \cdot r/\chi)\right), \qquad (25)$$

$$j_r = -\chi \cdot q \cdot r \cdot \sin(\pi \cdot r/\chi) \qquad (26)$$

$$j_\varphi = h\cdot\left(\frac{\pi^2}{\chi R^2} - \chi\right)\cdot r \cdot \sin(\pi \cdot r/\chi) + \frac{h}{\chi}\left(2 - \frac{\pi}{\chi}\right)\cdot\cos(\pi \cdot r/\chi). \quad (27)$$

Thus, the functions $j_r(r)$, $j_\varphi(r)$, $j_z(r)$, $h_r(r)$, $h_\varphi(r)$, $h_z(r)$ can be defined using the (26, 27, 25, 23, 22, 24), respectively.
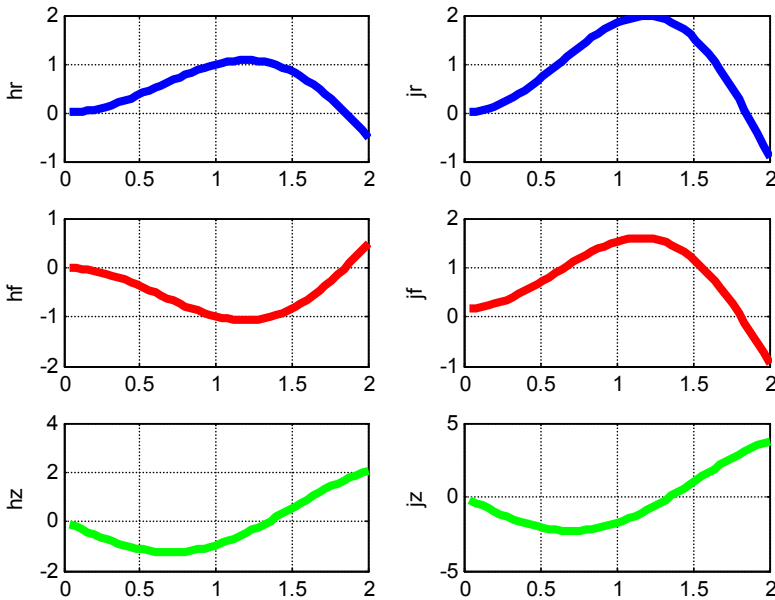


FIG. 2 (figPlazma.m)

**Example 1.**

Fig. 2 shows function graphs $j_r(r)$, $j_\varphi(r)$, $j_z(r)$, $h_r(r)$, $h_\varphi(r)$, $h_z(r)$. These functions can be calculated with data $\chi = 2$, $h = 1$, $q = -1$. The first column shows the functions $h_r(r)$, $h_\varphi(r)$, $h_z(r)$, the second column shows the functions $j_r(r)$, $j_\varphi(r)$, $j_z(r)$.

It is important to note that there is a point in the function graph $j_r(r)$, $j_\varphi(r)$ where $j_r(r) = 0$ and $j_\varphi(r) = 0$. Physically, this means that

there are radial currents $J_r(r)$ in the area $r < \chi$ directed from the center (with $\chi q < 0$). There are no currents $J_r(r)$, $J_\varphi(r)$, in the point $r = \chi$. Therefore, the value $R = \chi$ is the radius of a crystal. The specks of dust outside this radius experience radial currents $J_r(r)$ directed towards the center. This creates a stable boundary of the crystal.

The built model describes a cylindrical crystal of infinite length, which, of course, is inconsistent with reality. Let's now consider a more complex model.

## 4. The second mathematical model

The root of the equation $j_r(r) = 0$ determines the value $R = \chi$ of the cylindrical crystal radius. Let's now change the value $\chi$. If the value $\chi$ is dependent on the $z$, then the radius $R$ will depend on the $z$. But this very dependence is observed in the experiments – see, for example, the first fragment in Fig. 1.

With this in mind, let's consider the mathematical model which differs from the above used by the fact that the function $\chi(z)$ is used instead of the constant $\chi$. Let's rewrite the (6-11) with this in mind:

$$H_r = h_r(r) \cdot \cos(\chi(z)), \tag{28}$$
$$H_\varphi = h_\varphi(r) \cdot \sin(\chi(z)), \tag{29}$$
$$H_z = h_z(r) \cdot \sin(\chi(z)), \tag{30}$$
$$J_r = j_r(r) \cdot \cos(\chi(z)), \tag{31}$$
$$J_\varphi = j_\varphi(r) \cdot \sin(\chi(z)), \tag{32}$$
$$J_z = j_z(r) \cdot \sin(\chi(z)). \tag{33}$$

The system of equations (1-6) differs from the system (2.9-2.14) only by the fact that instead of the constant $\chi$ we use the derivative $\chi'(z)$ along the $z$ of the function $\chi(z)$. Consequently, the solution of the system (28-33) will be different from that of the previous system only by using the derivative $\chi'(z)$ in instead of the constant $\chi$. Thus, the solution in this case will be as follows:

$$j_r = -\chi'(z) \cdot q \cdot r \cdot \sin(\pi \cdot r / \chi'(z)), \tag{34}$$

$$j_\varphi = \left( \begin{array}{l} h \cdot \left( \dfrac{\pi^2}{\chi'(z)R^2} - \chi'(z) \right) \cdot r \cdot \sin(\pi \cdot r / \chi'(z)) + \\ + \dfrac{h}{\chi'(z)} \left( 2 - \dfrac{\pi}{\chi'(z)} \right) \cdot \cos(\pi \cdot r / \chi'(z)) \end{array} \right), \tag{35}$$

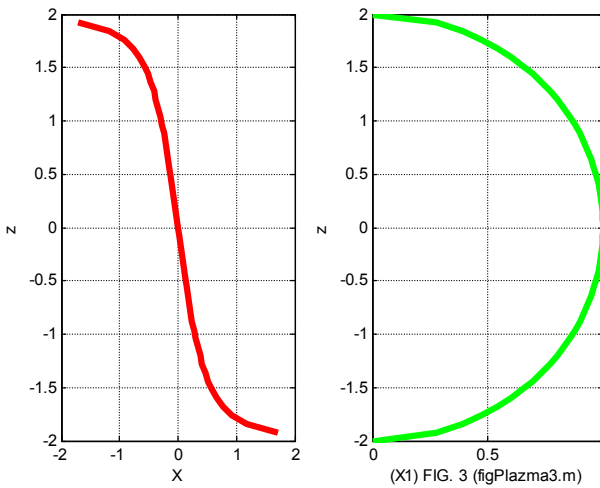$$j_z = q\left(2\sin(\pi \cdot r/\chi'(z)) + \frac{\pi \cdot r}{R} \cdot \cos(\pi \cdot r/\chi'(z))\right), \tag{36}$$

$$h_r = h \cdot r \cdot \sin(\pi \cdot r/\chi'(z)), \tag{37}$$

$$h_\varphi = q \cdot r \cdot \sin(\pi \cdot r/\chi'(z)), \tag{38}$$

$$h_z = -\frac{h}{\chi'(z)}\left(2\sin(\pi \cdot r/\chi'(z)) + \frac{\pi \cdot r}{R}\cos(\pi \cdot r/\chi'(z))\right). \tag{39}$$

The said functions will depend on the $\chi'(z)$. With the $\chi(z) = \eta z$ the equations (34-39) are transformed into the equations (22-27).

For example, Fig. 3 shows the functions $\chi(z)$ and $\chi'(z)$ where the $\chi'(z)$ is an equation of ellipse.



(X1) FIG. 3 (figPlazma3.m)

We can suggest that the current of the specks of dust is such that their average speed does not depend on the current direction. In particular, the path covered by a speck of dust per a unit of time in a circumferential direction and the path covered by it in a vertical direction are equal with a fixed radius. Consequently, in this case with a fixed radius we may assume that

$$\Delta\varphi \equiv \Delta z. \tag{40}$$

The dust trajectory in the above considered system is described by the following formulas

$$co = \cos(\chi(z)), \tag{41}$$

$$si = \sin(\chi(z)). \tag{42}$$

Thus, there is a point trajectory described by the formulas (40-42) in such system on the rotation figure with a radius of $r = \chi'(z)$. This

trajectory is a <u>helix</u>. All the tensions and densities of currents do not depend on the $\varphi$ in this trajectory.

Based on this assumption, we can construct a movement trajectory for specks of dust in accordance with the functions (1-3). Fig. 4 shows the two helices described by the current functions $j_r(r)$ and $j_z(r)$: with $r_1 = \chi'(z)$ with $r_2 = 0.5\chi'(z)$, where the $\chi'(z)$ is defined in Fig. 3.



Fig 4                                                    (Plazma4.m)
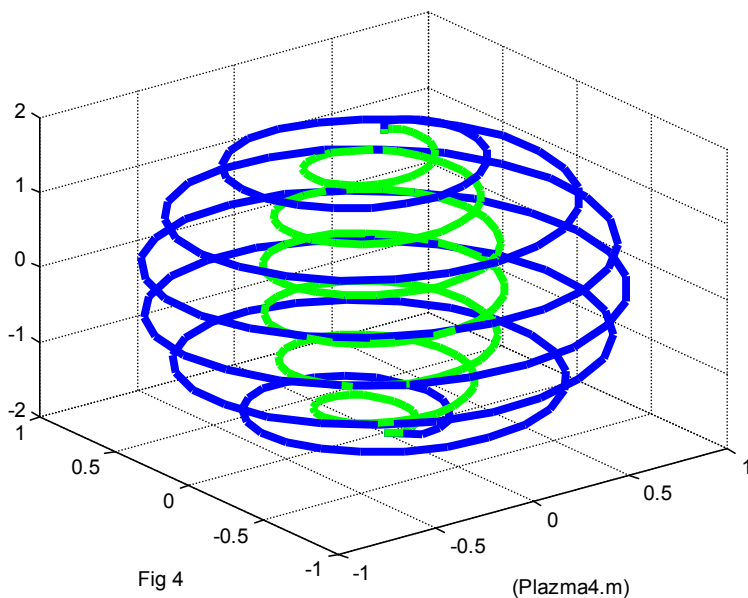
## 5. The plasma crystal energy

Under certain magnetic strengths and current densities we can find the plasma crystal energy. The magnetic field energy density

$$W_H = \frac{\mu}{2}\left(H_r^2 + H_\varphi^2 + H_z^2\right). \tag{43}$$

The specks of dust kinetic energy density $W_J$ can be found in the assumption that all the specks of dust have equal mass $m$. Then

$$W_J = \frac{1}{m}\left(J_\varphi^2 + J_\varphi^2 + J_\varphi^2\right). \tag{44}$$

To determine the full crystal energy we need to integrate the (43, 44) by the volume of the crystal, which form is defined. Thus, with a defined form of the crystal and assumed mathematical model we can find all the characteristics of the crystal.

# References

1. V.Ye. Fortov, A.G. Khrapak, S.A. Khrapak, V.I. Molotkov, O.F. Petrov./ Dusty plasma, UFN, May 2004, in Russian, http://ufn.ru/ru/articles/2004/5/b/

2. Dusty plasma, https://en.wikipedia.org/wiki/Dusty_plasma

3. Experiments with plasma in space, in Rusian, https://www.youtube.com/watch?v=SI406HKLYkM

4. V.N. Tsytovich, G.E. Morfill, V.E. Fortov, N.G. Gusein-Zade, B.A. Klumov and S.V. Vladimirov. From plasma crystals and helical structures towards inorganic living matter. New Journal of Physics, Volume 9, August 2007, http://iopscience.iop.org/article/10.1088/1367-2630/9/8/263/meta

5. Dusty plasma hints at a molecule of life, in Russian, http://www.membrana.ru/particle/693.

6. Andre Angot. Mathematics for Electrical and Radio Engineers, ed. "Nauka", Moscow, 1964, p. 772 (in Russian).

7. S.I. Khmelnik. Mathematical Model of a Plasma Crystal, http://vixra.org/abs/1703.0051, 2017-03-06

# Series: **PHYSICS and ASTRONOMY**

**Solomon I. Khmelnik**

# New solution of Maxwell's equations for spherical wave in the far zone

## Contents

## Annotation

It is noted that the known solution for a spherical electromagnetic wave in the far zone does not satisfy the law of conservation of energy (it is retained only on the average), the electric and magnetic intensities of the same name (in coordinate) are in phase, only one of Maxwell's equations is satisfied. A solution is offered that is free from these shortcomings.

## 1. Introduction

In [1], a cylindrical electromagnetic wave is considered. Below we consider a spherical electromagnetic wave far from the vibrator - in the so-called the far zone, where the longitudinal (radial-directed) electric and magnetic intensities can be neglected. The main drawbacks of the known solution (see Appendix 1) are that

1. the law of conservation of energy is fulfilled only on the average (in time),
2. the magnetic and electrical components are in phase,
3. in the Maxwell equations system, in the known solution, only one equation of eight is satisfied.
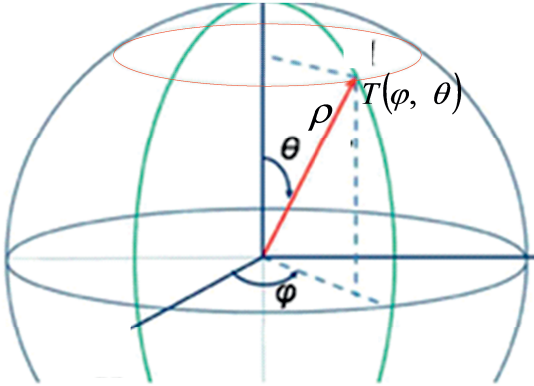
Fig. 1.

## 2. Solution of the Maxwell's equations

Fig. 1 shows the spherical coordinate system ($\rho, \theta, \varphi$). Expressions for the rotor and the divergence of vector E in these coordinates are given in Table 1 [2]. The following notation is used:

E - electrical intensities,

H - magnetic intensities,

$\mu$ - absolute magnetic permeability,

$\varepsilon$ - absolute dielectric constant.

The Maxwell's equations in spherical coordinates in the absence of charges and currents have the form given in Table. 2. Next, we will seek a solution for $E_\rho = 0$, $H_\rho = 0$ and in the form of the functions $E$, $H$ presented in Table 3, where the function $g(\theta)$ and functions of the species $E_{\varphi\rho}(\rho)$ are to be calculated. We assume that the intensities $E$, $H$ do not depend on the argument $\varphi$. Under these conditions, we transform Table 1 in Table 3a. Further we substitute functions from Table 3 in Table 3a. Then we get Table 4.

Substituting the expressions for the rotors and divergences from Table 4 into the Maxwell's equations (see Table 2), differentiating with respect to time and reducing the common factors, we obtain a new form of the Maxwell's equations - see Table 5.

Consider the Table 5. From line 2 it follows:

$$\frac{H_{\varphi\rho}}{\rho} + \frac{\partial H_{\varphi\rho}}{\partial \rho} = 0, \tag{2}$$

$$\chi H_{\varphi\rho} + \frac{\omega\varepsilon}{c} E_{\theta\rho} = 0. \tag{3}$$

Consequently,

$$H_{\varphi\rho} = \frac{h_{\varphi\rho}}{\rho}, \tag{4}$$

$$H_{\varphi\rho} = -\frac{\omega\varepsilon}{\chi c} E_{\theta\rho}, \tag{5}$$

where $h_{\varphi\rho}$ is some constant. Likewise, from lines 3, 5, 5 should be correspondingly:

$$H_{\theta\rho} = \frac{h_{\theta\rho}}{\rho}, \tag{6}$$

$$H_{\theta\rho} = \frac{\omega\varepsilon}{\chi c} E_{\varphi\rho}, \tag{7}$$

$$E_{\varphi\rho} = \frac{e_{\varphi\rho}}{\rho}, \tag{8}$$

$$E_{\varphi\rho} = \frac{\omega\mu}{\chi c} H_{\theta\rho}, \tag{9}$$

$$E_{\theta\rho} = \frac{e_{\theta\rho}}{\rho}, \tag{10}$$

$$E_{\theta\rho} = -\frac{\omega\mu}{\chi c} H_{\varphi\rho}. \tag{11}$$

It follows from (5) that

$$E_{\theta\rho} = -\frac{\chi c}{\omega\varepsilon} H_{\varphi\rho}, \tag{12}$$

and from a comparison of (11) and (12) it follows that

$$\frac{\omega\mu}{\chi c} = \frac{\chi c}{\omega\varepsilon}$$

or

$$\chi = \frac{\omega}{c}\sqrt{\varepsilon\mu}. \tag{13}$$

The same formula follows from a comparison of (7) and (9).
It follows from (5, 13) that

$$H_{\varphi\rho} = -\sqrt{\frac{\varepsilon}{\mu}} E_{\theta\rho}, \tag{14}$$

and it follows from (14, 4, 11, 12) that

$$h_{\varphi\rho} = -e_{\theta\rho}\sqrt{\frac{\varepsilon}{\mu}}, \tag{15}$$

Similarly, it follows from (7, 13) that

$$H_{\theta\rho} = -\sqrt{\frac{\varepsilon}{\mu}} E_{\varphi\rho}, \tag{16}$$

and it follows from (16, 6, 8, 12) that

$$h_{\theta\rho} = -e_{\varphi\rho}\sqrt{\frac{\varepsilon}{\mu}}. \tag{17}$$

From a comparison of (15) and (17) it follows that

$$\frac{h_{\varphi\rho}}{h_{\theta\rho}} = \frac{e_{\theta\rho}}{e_{\varphi\rho}} = q, \tag{18}$$

$$\frac{h_{\varphi\rho}}{e_{\theta\rho}} = \frac{h_{\theta\rho}}{e_{\varphi\rho}} = -\sqrt{\frac{\varepsilon}{\mu}}. \tag{19}$$

Further we notice that lines 1, 4, 7 and 8 coincide, from which it follows that the function $g(\theta)$ is a solution of the differential equation

$$\frac{g(\theta)}{tg(\theta)} + \frac{\partial(g(\theta))}{\partial\theta} = 0. \tag{20}$$

In Appendix 2 it is shown that the solution of this equation is the function

$$g(\theta) = \frac{1}{A \cdot |sin(\theta)|}, \tag{20a}$$

where A is a constant. We note that in the well-known solution $g(\theta) = \sin(\theta)$ - see Appendix 1. It is easy to see that such a function does not satisfy equation (20). Consequently,

> **in the known solution 4 Maxwell's equations with expressions** $rot_\rho(E)$, $rot_\rho(H)$, $div(E)$, $div(H)$ **are not satisfied.**

Thus, the solution of the Maxwell's equations for a spherical wave in the far zone has the form of the intensities presented in Table 3, where

$$H_{\varphi\rho} = \frac{h_{\varphi\rho}}{\rho}, \; H_{\theta\rho} = \frac{h_{\theta\rho}}{\rho}, \; E_{\varphi\rho} = \frac{e_{\varphi\rho}}{\rho}, \; E_{\theta\rho} = \frac{e_{\theta\rho}}{\rho} \qquad (21)$$

$$\chi = \frac{\omega}{c}\sqrt{\varepsilon\mu} \quad \text{(see 13)}, \quad \frac{g(\theta)}{\text{tg}(\theta)} + \frac{\partial(g(\theta))}{\partial\theta} = 0 \quad \text{(see 20)}$$

and the constants $h_{\varphi\rho}$, $h_{\theta\rho}$, $e_{\theta\rho}$, $e_{\varphi\rho}$ satisfy conditions

$$\frac{h_{\varphi\rho}}{h_{\theta\rho}} = \frac{e_{\theta\rho}}{e_{\varphi\rho}} = q \quad \text{(см. 18)}, \quad \frac{h_{\varphi\rho}}{e_{\theta\rho}} = \frac{h_{\theta\rho}}{e_{\varphi\rho}} = -\sqrt{\frac{\varepsilon}{\mu}}. \quad \text{(см. 19)}$$

From Table. 3 it follows that

> **the same (with respect to the coordinates $\varphi$ and $\theta$)**
> **electric and magnetic intensities are shifted in phase by a**
> **quarter of the period.**

This corresponds to experimental electrical engineering. In Fig. 2 shows the intensities vectors in a spherical coordinate system.
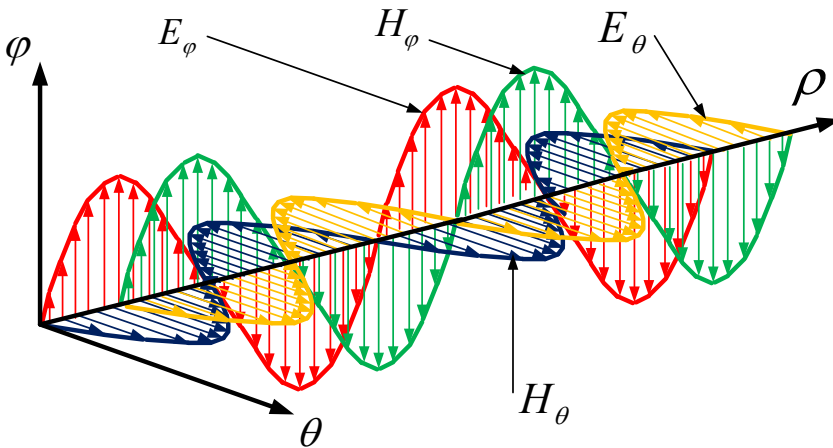


Fig. 2.

## 3. Energy Flows

Also, as in [1], the flow density of electromagnetic energy - the Poynting vector is

$$S = \eta E \times H, \qquad (1)$$

where

$$\eta = c/4\pi. \qquad (2)$$

In spherical coordinates $\varphi, \theta, \rho$ the flow density of electromagnetic energy has three components $S_\varphi$, $S_\theta$, $S_\rho$ directed along

the radius, along the circumference, along the axis, respectively. They are determined by the formula

$$
S = \begin{bmatrix} S_{\varphi} \\ S_{\theta} \\ S_{\rho} \end{bmatrix} = \eta(E \times H) = \eta \begin{bmatrix} E_{\theta}H_{\rho} - E_{\rho}H_{\theta} \\ E_{\rho}H_{\varphi} - E_{\varphi}H_{\rho} \\ E_{\varphi}H_{\theta} - E_{\theta}H_{\varphi} \end{bmatrix}. \tag{4}
$$

From here and from Table 3 it follows that

$$
\begin{aligned}
S_{\varphi} &= 0 \\
S_{\theta} &= 0 \\
S_{\rho} &= \eta \begin{pmatrix} E_{\varphi\rho}H_{\theta\rho}(g(\theta)\sin(\chi\rho + \omega t))^2 - \\ - E_{\theta\rho}H_{\varphi\rho}(g(\theta)\cos(\chi\rho + \omega t))^2 \end{pmatrix}
\end{aligned} \tag{5}
$$

It follows from (2.9, 2.11) that

$$
E_{\varphi\rho}H_{\theta\rho} = \frac{\omega\mu}{\chi c}(H_{\theta\rho})^2, \tag{6}
$$

$$
E_{\theta\rho}H_{\varphi\rho} = -\frac{\omega\mu}{\chi c}(H_{\varphi\rho})^2. \tag{7}
$$

Further from (6, 7, 2.4, 2.6) it follows that

$$
E_{\varphi\rho}H_{\theta\rho} = \frac{\omega\mu}{\chi c}(h_{\theta\rho})^2 \frac{1}{\rho^2}, \tag{8}
$$

$$
E_{\theta\rho}H_{\varphi\rho} = -\frac{\omega\mu}{\chi c}(h_{\varphi\rho})^2 \frac{1}{\rho^2}. \tag{9}
$$

From (5, 8, 9) we obtain:

$$
S_{\rho} = \eta \cdot g^2(\theta)\frac{\omega\mu}{\chi c}\frac{1}{\rho^2}\begin{pmatrix} (h_{\theta\rho})^2(\sin(\chi\rho + \omega t))^2 + \\ + (h_{\varphi\rho})^2(\cos(\chi\rho + \omega t))^2 \end{pmatrix}. \tag{9}
$$

Further from (9, 2.13, 2.18) it follows that

$$
S_{\rho} = \eta \cdot g^2(\theta)\omega\sqrt{\frac{\mu}{\varepsilon}}\frac{1}{\rho^2}\begin{pmatrix} (h_{\theta\rho})^2(\sin(\chi\rho + \omega t))^2 + \\ + (qh_{\theta\rho})^2(\cos(\chi\rho + \omega t))^2 \end{pmatrix}. \tag{10}
$$

where **q** is a previously undefined constant. If we take

$$
q = 1, \tag{10a}
$$

then we get

$$
S_{\rho} = \eta \cdot g^2(\theta)\omega\sqrt{\frac{\mu}{\varepsilon}}\frac{h_{\theta\rho}^2}{\rho^2}. \tag{11}
$$

We also note that the surface area of a sphere with a radius $\rho$ is equal to $4\pi\rho^2$. Then the flow of energy passing through a sphere with a radius $\rho$ is

$$\overline{S_\rho} = 4\pi\eta\omega \cdot g^2(\theta)h_{\theta\rho}^2\sqrt{\frac{\mu}{\varepsilon}}.\qquad(12)$$

It follows from (12) that

> in a spherical electromagnetic wave, the energy flux passing through the spheres along the radius remains constant with increasing radius and does not change with time.

This strictly corresponds to the law of conservation of energy.

It follows from (12) that the <u>energy flow density varies along the meridian</u> in accordance with the law $g^2(\theta)$.

## 4. Conclusion

An exact solution of the Maxwell equations for the far zone, which is presented in the table 3 is obtained, where

$H_{\varphi\rho}(\rho)$, $H_{\theta\rho} = (\rho)$, $E_{\varphi\rho} = (\rho)$, $E_{\theta\rho} = (\rho)$ are functions defined by (2.21, 2.18, 2.19),

$g(\theta)$ is a function defined by (2.20a),

$\chi$ is the constant determined by (2.13).

- The electric and magnetic intensities of the same name (with respect to the coordinates $\varphi$ and $\theta$) are phase shifted by a quarter of a period.
- In a spherical electromagnetic wave, the energy flux passing through the spheres along the radius remains constant with increasing radius and does NOT change with time and this strictly corresponds to the law of conservation of energy.
- The energy density varies along the meridian according to the law $g^2(\theta)$.

Thus, we obtained a rigorous solution of the Maxwell equations in the far zone, free from the drawbacks indicated above. At the same time, it should be noted that in the near zone, where radial electric and magnetic intensities are present, the known solution has an even greater list of disadvantages, in particular [3].

1. the energy conservation law is satisfied only on the average,
2. The solution is inhomogeneous and it is practically necessary to divide it into separate zones (as a rule, near, middle and far), in which the solutions turn out to be completely different,
3. In the near zone there is no flow of energy with the real value
4. The magnetic and electrical components are in phase,
5. In the near zone, the solution is not wave (i.s. the distance is not an argument of the trigonometric function),
6. The known solution does not satisfy Maxwell's system of equations (a solution that satisfies a single equation of the system can not be considered a solution of the system of equations).

These shortcomings are a consequence of the fact that until now Maxwell's equations for spherical coordinates could not be solved. A well-known solution is obtained after dividing the entire domain into so-called near, middle and far zones and after applying a variety of assumptions, different for each of these zones [3, 4].

In practice, these drawbacks of the known solution mean that they (mathematical solutions) do not strictly describe the real characteristics of technical devices. A more rigorous solution, when applied in the design systems of such devices, must certainly improve their quality.

The solution of the Maxwell equations for spherical coordinates in the general case obtained by the author and he seeks for cooperation with organization interested in the practical application of this solution.

## Appendix 1

The known solution has the form [3]:

$$E_\theta = e_\theta \frac{1}{\rho} \sin(\theta) \sin(\omega t - \chi \rho), \tag{1}$$

$$H_\varphi = h_\varphi \frac{1}{\rho} \sin(\theta) \sin(\omega t - \chi \rho), \tag{2}$$

$k_{e\theta} = \dfrac{\chi^2 lI}{4\pi\omega\varepsilon\varepsilon_o}$, $k_{h\varphi} = \dfrac{\chi lI}{4\pi}$, where $l$, $I$ - length and current of the vibrator. We notice, that

$$\frac{e_\theta}{h_\varphi} = \frac{\chi}{\omega\varepsilon} \tag{3}$$

It should be noted that these tensions <u>are in phase</u>, which contradicts practical electrical engineering.

Let us consider how equations (1, 2) relate to Maxwell's system of equations - see Table 2. The intensities (1, 2) enter only in equation (6) from Table 2, which has the form

$$\text{rot}_\varphi E + \frac{\mu}{c}\frac{\partial H_\varphi}{\partial t} = 0 \tag{4}$$

or

$$\frac{E_\theta}{\rho} + \frac{\partial E_\theta}{\partial \rho} + \frac{\mu}{c}\frac{\partial H_\varphi}{\partial t} = 0. \tag{5}$$

We substitute (1, 2) into (5) and obtain:

$$-e_\theta \frac{\chi}{\rho}\sin(\theta)\cos(\omega t - \chi\rho) -$$
$$-h_\varphi \frac{\chi}{\rho}\frac{\mu}{c}\sin(\theta)\cos(\omega t - \chi\rho) = 0 \tag{6}$$

or

$$\frac{e_\theta}{h_\varphi} + \frac{\mu}{c} = 0. \tag{7}$$

From a comparison of (3) and (7) it follows that the intensities (1, 2) satisfy equation (4). The remaining 7 Maxwell equations are violated. In the equations (2, 3, 5) from Table 2 one of the terms differs from zero, and the other is equal to zero. The violation of equations (1, 4, 7, 8) from Table. 2 is shown above in Section 2. So,

> **the known solution does not satisfy Maxwell's system of equations.**

## Appendix 1

We consider (2.20):

$$\frac{g(\theta)}{\text{tg}(\theta)} + \frac{\partial(g(\theta))}{\partial \theta} = 0 \tag{1}$$

or

$$\frac{\partial(g(\theta))}{\partial \theta} = -\text{ctg}(\theta)\cdot g(\theta) \tag{2}$$

or

$$\ln(g(\theta)) = -\int_\theta \text{ctg}(\theta)\partial\theta. \tag{4}$$

It is known that

$$\int_\theta \operatorname{ctg}(\theta)\partial\theta = \ln\left(A \cdot |\sin(\theta)|\right). \tag{5}$$

where $A$ is a constant. From (4, 5) we obtain:

$$\ln(g(\theta)) = -\ln\left(A \cdot |\sin(\theta)|\right) \tag{6}$$

or

$$g(\theta) = \frac{1}{A \cdot |\sin(\theta)|}. \tag{8}$$

## Tables

Table 1.

| 1 | 2 | 3 |
|---|---|---|
| 1 | $\operatorname{rot}_\rho(E)$ | $\dfrac{E_\varphi}{\rho \operatorname{tg}(\theta)} + \dfrac{\partial E_\varphi}{\rho \partial \theta} - \dfrac{\partial E_\theta}{\rho \sin(\theta)\partial\varphi}$ |
| 2 | $\operatorname{rot}_\theta(E)$ | $\dfrac{\partial E_\rho}{\rho \sin(\theta)\partial\varphi} - \dfrac{E_\varphi}{\rho} - \dfrac{\partial E_\varphi}{\partial\rho}$ |
| 3 | $\operatorname{rot}_\varphi(E)$ | $\dfrac{E_\theta}{\rho} + \dfrac{\partial E_\theta}{\partial\rho} - \dfrac{\partial E_\rho}{\rho \partial\varphi}$ |
| 4 | $\operatorname{div}(E)$ | $\dfrac{E_\rho}{\rho} + \dfrac{\partial E_\rho}{\partial\rho} + \dfrac{E_\theta}{\rho \operatorname{tg}(\theta)} + \dfrac{\partial E_\theta}{\rho \partial\theta} + \dfrac{\partial E_\varphi}{\rho \sin(\theta)\partial\varphi}$ |

Table 2.

| 1 | 2 |
|---|---|
| 1. | $\operatorname{rot}_\rho H - \dfrac{\varepsilon}{c}\dfrac{\partial E_\rho}{\partial t} = 0$ |
| 2. | $\operatorname{rot}_\theta H - \dfrac{\varepsilon}{c}\dfrac{\partial E_\theta}{\partial t} = 0$ |
| 3. | $\operatorname{rot}_\varphi H - \dfrac{\varepsilon}{c}\dfrac{\partial E_\varphi}{\partial t} = 0$ |
| 4. | $\operatorname{rot}_\rho E + \dfrac{\mu}{c}\dfrac{\partial H_\rho}{\partial t} = 0$ |
| 5. | $\operatorname{rot}_\theta E + \dfrac{\mu}{c}\dfrac{\partial H_\theta}{\partial t} = 0$ |
| 6. | $\operatorname{rot}_\varphi E + \dfrac{\mu}{c}\dfrac{\partial H_\varphi}{\partial t} = 0$ |

| 7. | $\text{div}(E)=0$ |
|----|-------------------|
| 8. | $\text{div}(H)=0$ |

Table 3.

| 1 | 2 |
|---|---|
| | $E_\theta = E_{\theta\rho}(\rho)g(\theta)\cos(\chi\rho+\omega t)$ |
| | $E_\varphi = E_{\varphi\rho}(\rho)g(\theta)\sin(\chi\rho+\omega t)$ |
| | $E_\rho = 0$ |
| | $H_\theta = H_{\theta\rho}(\rho)g(\theta)\sin(\chi\rho+\omega t)$ |
| | $H_\varphi = H_{\varphi\rho}(\rho)g(\theta)\cos(\chi\rho+\omega t)$ |
| | $H_\rho = 0$ |

Table 3a.

| 1 | 2 | 3 |
|---|---|---|
| 1 | $\text{rot}_\rho(E)$ | $\dfrac{E_\varphi}{\rho \text{tg}(\theta)}+\dfrac{\partial E_\varphi}{\rho\partial\theta}$ |
| 2 | $\text{rot}_\theta(E)$ | $-\dfrac{E_\varphi}{\rho}-\dfrac{\partial E_\varphi}{\partial\rho}$ |
| 3 | $\text{rot}_\varphi(E)$ | $\dfrac{E_\theta}{\rho}+\dfrac{\partial E_\theta}{\partial\rho}$ |
| 4 | $\text{div}(E)$ | $\dfrac{E_\theta}{\rho \text{tg}(\theta)}+\dfrac{\partial E_\theta}{\rho\partial\theta}$ |

Table 4.

| 1 | 2 | 3 |
|---|---|---|
| 1 | $\text{rot}_\rho(E)$ | $\dfrac{E_\varphi}{\rho \text{tg}(\theta)}+\dfrac{\partial E_\varphi}{\rho\partial\theta}$ |
| 2 | $\text{rot}_\theta(E)$ | $-\left(\dfrac{E_{\varphi\rho}}{\rho}\sin(...)+\dfrac{\partial E_{\varphi\rho}}{\partial\rho}\sin(...)+\chi E_{\varphi\rho}\cos(...)\right)g(\theta)$ |
| 3 | $\text{rot}_\varphi(E)$ | $\left(\dfrac{E_{\theta\rho}}{\rho}\cos(...)+\dfrac{\partial E_{\theta\rho}}{\partial\rho}\cos(...)-\chi E_{\theta\rho}\sin(...)\right)g(\theta)$ |

| 4 | $\mathrm{div}(E)$ | $\dfrac{E_\theta}{\rho\,\mathrm{tg}(\theta)} + \dfrac{\partial E_\theta}{\rho\,\partial\theta}$ |
|---|---|---|
| 5 | $\mathrm{rot}_\rho(H)$ | $\dfrac{H_\varphi}{\rho\,\mathrm{tg}(\theta)} + \dfrac{\partial H_\varphi}{\rho\,\partial\theta}$ |
| 6 | $\mathrm{rot}_\theta(H)$ | $-\left(\dfrac{H_{\varphi\rho}}{\rho}\cos(...) + \dfrac{\partial H_{\varphi\rho}}{\partial\rho}\cos(...) - \chi H_{\varphi\rho}\sin(...)\right)g(\theta)$ |
| 7 | $\mathrm{rot}_\varphi H$ | $\left(\dfrac{H_{\theta\rho}}{\rho}\sin(...) + \dfrac{\partial H_{\theta\rho}}{\partial\rho}\sin(...) + \chi H_{\theta\rho}\cos(...)\right)g(\theta)$ |
| 8 | $\mathrm{div}(H)$ | $\dfrac{H_\theta}{\rho\,\mathrm{tg}(\theta)} + \dfrac{\partial H_\theta}{\rho\,\partial\theta}$ |

Table 5.

| 1 | 2 |
|---|---|
| 1. | $\dfrac{g(\theta)}{\mathrm{tg}(\theta)} + \dfrac{\partial(g(\theta))}{\partial\theta} = 0$ |
| 2. | $-\dfrac{H_{\varphi\rho}}{\rho}\cos(...) - \dfrac{\partial H_{\varphi\rho}}{\partial\rho}\cos(...) + \chi H_{\varphi\rho}\sin(...) + \dfrac{\omega\varepsilon}{c}E_{\theta\rho}\sin(...) = 0$ |
| 3. | $\dfrac{H_{\theta\rho}}{\rho}\sin(...) + \dfrac{\partial H_{\theta\rho}}{\partial\rho}\sin(...) + \chi H_{\theta\rho}\cos(...) - \dfrac{\omega\varepsilon}{c}E_{\varphi\rho}\cos(...) = 0$ |
| 4. | $\dfrac{g(\theta)}{\mathrm{tg}(\theta)} + \dfrac{\partial(g(\theta))}{\partial\theta} = 0$ |
| 5. | $-\dfrac{E_{\varphi\rho}}{\rho}\sin(...) - \dfrac{\partial E_{\varphi\rho}}{\partial\rho}\sin(...) - \chi E_{\varphi\rho}\cos(...) + \dfrac{\omega\mu}{c}H_{\theta\rho}\sin(...) = 0$ |
| 6. | $\dfrac{E_{\theta\rho}}{\rho}\cos(...) + \dfrac{\partial E_{\theta\rho}}{\partial\rho}\cos(...) - \chi E_{\theta\rho}\sin(...) - \dfrac{\omega\mu}{c}H_{\varphi\rho}\sin(...) = 0$ |
| 7. | $\dfrac{g(\theta)}{\mathrm{tg}(\theta)} + \dfrac{\partial(g(\theta))}{\partial\theta} = 0$ |
| 8. | $\dfrac{g(\theta)}{\mathrm{tg}(\theta)} + \dfrac{\partial(g(\theta))}{\partial\theta} = 0$ |

# References

1. S.I. Khmelnik. Inconsistency Solution of Maxwell's Equations, publ. "MiC", Israel, Printed in USA, Lulu Inc., ID 19043222, ISBN 978-1-365-23941-0, seventh edition, 2017, 190 p.
2. Andre Ango. Mathematics for Electrical and Radio Engineers, publ. "Nauka", Moscow, 1964, 772 p. (in Russian).
3. Wen Geyi. Foundations of Applied Electrodynamics. Waterloo, Canada, 2010.
4. Neganov V.A., Tabakov D.P., Yarovoi D.P. Modern theory and practical applications of antennas. Editor Neganov V.A. Publ. «Radio engineering», Moscow, 2009, 720 pages (in Russian).
5. S.I. Khmelnik. New Solution of Maxwell's Equations for Spherical Wave in the Far Zone, http://vixra.org/abs/1711.0243, 2017-11-08

# Series: **PHYSICS and ASTRONOMY**

**Solomon I. Khmelnik**

# New solution of Maxwell's equations for spherical wave

## Contents

## Annotation

It is noted that the known solution for a spherical electromagnetic wave does not satisfy the law of conservation of energy (it is retained only on the average), the electric and magnetic intensities of the same name (by coordinates) are in phase, only one from system of Maxwell's equations is satisfied, the solution is not wave solution, there is no flow of energy with real value. A solution is offered that is free from these shortcomings.

## 1. Introduction

In [1] a solution of the Maxwell equations for a spherical wave in the far field was proposed. Next, we consider the solution of Maxwell's equations for a spherical wave in the entire region of existence of a wave (without splitting into bands). Such a problem arises in the solution of the equations of electrodynamics for an elementary electric dipole-vibrator. The solution of this problem is known and it is on the basis of this solution that the antennas are constructed. However, this solution has a number of shortcomings, in particular [2],

1. the energy conservation law is satisfied only on the average,
2. The solution is inhomogeneous and it is practically necessary to divide it into separate zones (as a rule, near, middle and far), in which the solutions turn out to be completely different,

3. In the near zone there is no flow of energy with the real value
4. The magnetic and electrical components are in phase,
5. In the near zone, the solution is not wave (i.s. the distance is not an argument of the trigonometric function),
6. The known solution does not satisfy Maxwell's system of equations (a solution that satisfies a single equation of the system can not be considered a solution of the system of equations).

In practice, these drawbacks of the known solution mean that they (mathematical solutions) do not strictly describe the real characteristics of technical devices. A more rigorous solution, when applied in the design systems of such devices, must certainly improve their quality.

## 2. Solution of the Maxwell's equations

So, we will use spherical coordinates. Fig. 1 shows the spherical coordinate system $(\rho, \theta, \varphi)$. Next, we will place the formulas in tables and use the following notation:

T (table_number) - (column_number) - (line_number)

Table 1-3 lists the expressions for the rotor and the divergence of the vector E in these coordinates [3]. Here and below

E - electrical intensities,

H - magnetic intensities,

$\mu$ - absolute magnetic permeability,

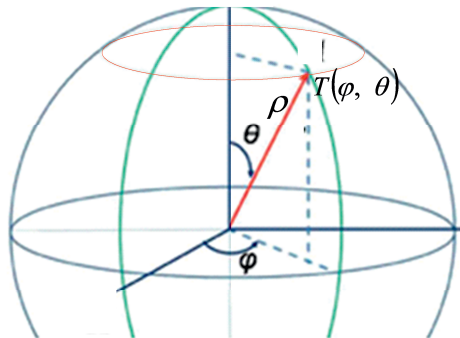$\varepsilon$ - absolute dielectric constant.



Fig. 1.

Next, we will look for the solution in the form of the functions $E, H$, presented in Table 2-2, where the actual functions of the form

$g(\theta)$ and the complex functions of the form $e(\rho)$, $h(\rho)$ are to be calculated, and the coefficients $\chi$, $\alpha$, $\omega$ are known.

Under these conditions, we transform the formulas (T1-3) into (T1-4), where the following notations are adopted:

$$e'_\rho = \frac{\partial(e_\rho(\rho))}{\partial\rho}, \tag{1}$$

$$\hat{g} = \frac{\partial(g(\theta))}{\partial\theta}, \tag{2}$$

$$\Psi(E_\rho) = \psi(e_\rho(\rho)) \cdot g(\theta) \cdot \exp(...), \tag{3}$$

$$T(E_\rho) = \Gamma_\rho(\theta) \cdot e_\rho(\rho) \cdot \exp(...), \tag{4}$$

where

$$\psi(e_\rho(\rho)) = \left(\frac{e_\rho}{\rho} + e'_\rho + i\chi e_\rho\right), \tag{5}$$

$$\Gamma_\rho(\theta) = \left(\frac{g(\theta)}{tg(\theta)} + \hat{g}(\theta)\right). \tag{6}$$

The function (3) is formed from a function of the form $\left(\dfrac{E_\rho}{\rho} + \dfrac{\partial(E_\rho)}{\partial\rho}\right)$

The Maxwell equations in spherical coordinates in the absence of charges and currents have the form given in Table 3-2. Next, we substitute the rotors and divergences from Table 2-4 and the functions $E$, $H$ from Table 2 (after differentiation with respect to time) in Table 3-3. Next, we rewrite the equations from Table 3-3 in Table 4-2. In this case, we also reduce the common factors of the form $\exp(...)$ and use the formulas (1-6).

As a result of these transformations, we obtained an **over**determined system of 8 partial differential equations with respect to 6 unknown functions with two arguments $\rho$ and $\theta$.

The solution of the system of Maxwell equations, in addition to the natural requirement of the feasibility of all equations of the system, must satisfy the basic physical laws:

1. the law of conservation of energy (not on average in time, but at each moment of time),
2. The phase shift experimentally established in electrical engineering between electric and magnetic intensities,

3. experimentally established wave character of the propagation of electric and magnetic intensities in space,

4. The solution should not allow the existence of an infinite value of any intensity.

Mathematically, these patterns should not be a consequence of solving the system of Maxwell equations, but additional conditions that transform the overdetermined system of Maxwell's equations into a strictly defined system. However, a solution can also be found without taking these conditions into account, since even a certain (and even more so, overdetermined) system of partial differential equations can have many solutions. In this set of solutions, there is only one that satisfies the above laws. The greatness of Maxwell's system of equations is that there is always a solution that describes reality. But how does nature find such a solution? The answer, perhaps, lies in the fact that there exists a functional (with a saddle point) relative to the intensities, in which the first variations in the intensities, when converted to zero, coincide with the Maxwell equations. The descent along the functional in the direction of these variations is equivalent to the solution of these equations [5].

The wave character of the solution is provided by the factors $\exp(...)$ of the species in the determination of the electric and magnetic intensities in Table 2. Sufficient conditions for phase displacement between electric and magnetic strains are the following:

$$E_{\rho} = -iH_{\rho}, H_{\rho} = iE_{\rho} \tag{7}$$

$$E_{\varphi} = iH_{\varphi}, H_{\varphi} = -iE_{\varphi} \tag{8}$$

$$E_{\theta} = -iH_{\theta}, H_{\theta} = iE_{\theta} \tag{9}$$

Denote by:

$$E_{\rho,\varphi,\theta}^{sumH} = E_{\rho,\varphi,\theta} + H_{\rho,\varphi,\theta} \tag{11}$$

$$E_{\rho,\varphi,\theta}^{\min H} = E_{\rho,\varphi,\theta} - H_{\rho,\varphi,\theta} \tag{12}$$

First we will seek a solution for vacuum, where in the CGS system

$$\varepsilon = \mu = 1. \tag{13}$$

and denote by

$$q = \omega/c \tag{14}$$

We summarize the equations from Table T4-2 in pairs and write the resulting equations into Table T4-3, using the notation (11, 12, 14). As a result of these transformations, we obtained an **under**definished system of 4 partial differential equations with respect to 6 unknown functions with two arguments $\rho$ and $\theta$.

It follows from (7-12):

$$E_\rho^{sumH} = e_\rho + h_\rho = e_\rho(1+i) = -ih_\rho(1+i) = h_\rho(1-i) \tag{15}$$

$$E_\rho^{minH} = e_\rho - h_\rho = e_\rho(1-i) = -ih_\rho(1-i) = -h_\rho(1+i) \tag{16}$$

$$E_\varphi^{sumH} = e_\varphi + h_\varphi = e_\varphi(1-i) = ih_\varphi(1-i) = h_\varphi(1+i) \tag{17}$$

$$E_\varphi^{minH} = e_\varphi - h_\varphi = e_\varphi(1+i) = ih_\varphi(1+i) = h_\varphi(-1+i) \tag{18}$$

$$E_\theta^{sumH} = e_\theta + e_\theta = e_\theta(1+i) = -ih_\theta(1+i) = h_\theta(1-i) \tag{19}$$

$$E_\theta^{minH} = e_\theta - h_\theta = e_\theta(1-i) = -ih_\theta(1-i) = -h_\theta(1+i) \tag{20}$$

$$E_{r,f,\theta}^{sumH} + E_{r,f,\theta}^{minH} = 2e_{r,f,\theta}, \quad H_{r,f,\theta}^{sumH} + H_{r,f,\theta}^{minH} = 2h_{r,f,\theta} \tag{21}$$

We now rewrite the equations from Table T4-3 into Table T5-2, replacing variables $E_{\rho,\varphi,\theta}^{sumH}$, $E_{\rho,\varphi,\theta}^{minH}$ with variables $e_{\rho,\varphi,\theta}$ according to (15-20).

It is seen that the equations T6-2-2 and T6-2-3 are compatible only if the following two conditions are met:

$$\alpha = 0 \tag{22}$$

$$e_\theta = i \cdot e_\varphi \tag{23}$$

$$g_\theta = g_\varphi \tag{23a}$$

Taking these conditions into account, we rewrite the equations from Table T6-2 in Table T6-3. It is seen that the equations T6-3-2 and T6-3-3 are the same, and the term $\dfrac{e_\varphi}{\rho}\hat{g}_\varphi$ can be deleted from the equations T6-3-1 and T6-3-4. The two equations that we got are written in Table T-7-2. After simple transformations, these equations are rewritten in Table T-7-3. We now write these equations with allowance for the formula (2.5):

$$\frac{e_\rho g_\rho}{\rho} + e'_\rho g_\rho + i\chi e_\rho g_\rho + iq e_\rho g_\rho + \frac{\cos}{\rho\sin}(1+i)e_\varphi g_\varphi = 0 \tag{24}$$

$$\frac{e_\varphi}{\rho} + e'_\varphi + i\chi e_\varphi + iq e_\varphi = 0 \tag{25}$$

Equation (25) splits into two equations:

$$\frac{e_\varphi}{\rho} + e'_\varphi = 0 \tag{26}$$

$$i\chi e_\varphi + iq e_\varphi = 0 \tag{27}$$

from which it follows that

$$\chi = -q \tag{28}$$

$$e_\varphi = \frac{A}{\rho} \tag{29}$$

where A is a constant. Substituting (28, 29) into (24), we find:

$$e'_\rho g_\rho = -\frac{e_\rho g_\rho}{\rho} - \frac{\cos}{\sin}\frac{A(1+i)}{\rho^2} g_\varphi \tag{30}$$

or

$$e'_\rho = -\frac{e_\rho}{\rho} - \frac{\cos}{\sin}\frac{A(1+i)}{\rho^2}\frac{g_\varphi}{g_\rho} \tag{31}$$

Let

$$g_\varphi = \sin, \quad g_\rho = \cos \tag{32}$$

From (31, 32) we find:

$$e'_\rho = -\frac{e_\rho}{\rho} - \frac{A\cdot(1+i)}{\rho^2} \tag{33}$$

An analysis of this equation is given in Section 4.

As a result of the above calculations, complex functions $e_\rho(\rho)$, $e_\varphi(\rho)$, $e_\theta(\rho)$ are defined. For these functions $g(\theta)$, the functions $E_\rho$, $E_\varphi$, $E_\theta$ are determined from Table 2.

For these functions $E_\rho$, $E_\varphi$, $E_\theta$ the functions $H_\rho$, $H_\varphi$, $H_\theta$ are determined from (7-8), from which it follows that

$$h_\rho = ie_\rho \tag{34}$$

$$h_\varphi = -ie_\varphi \tag{35}$$

$$h_\theta = ie_\theta \tag{36}$$

The functions $H_\rho$, $H_\varphi$, $H_\theta$ are also listed in Table 2.

## 3. Energy Flows

Density of electromagnetic energy flow - Poynting vector

$$S = \eta E \times H, \tag{1}$$

where

$$\eta = c/4\pi .\tag{2}$$

In the SI system formula (1) takes the form:

$$S = E \times H .$$

(3)

In spherical coordinates $\varphi$, $\theta$, $\rho$ the flux density of electromagnetic energy has three components $S_\varphi$, $S_\theta$, $S_\rho$, directed along the radius, along the circumference, along the axis, respectively. It was shown in [4] that they are determined by the formula

$$S = \begin{bmatrix} S_\varphi \\ S_\theta \\ S_\rho \end{bmatrix} = \eta(E \times H) = \eta \begin{bmatrix} E_\theta H_\rho - E_\rho H_\theta \\ E_\rho H_\varphi - E_\varphi H_\rho \\ E_\varphi H_\theta - E_\theta H_\varphi \end{bmatrix} .\tag{4}$$

Taking into account (2.7-2.9) from (4) we find:

$$S_\rho = E_\varphi H_\theta - E_\theta H_\varphi = E_\varphi i E_\theta + E_\theta i E_\varphi \tag{4a}$$

or

$$S_\rho = 2i E_\theta E_\varphi ,\tag{5}$$

$$S_\theta = E_\rho H_\varphi - E_\varphi H_\rho = i H_\rho H_\varphi - i H_\varphi H_\rho = 0 \tag{6}$$

$$S_\varphi = E_\theta H_\rho - E_\rho H_\theta = -i H_\theta H_\rho + i H_\rho H_\theta = 0 .\tag{7}$$

It follows from (6, 7) that there is no flow of energy along the circles of the sphere.

In Appendix 1 it is shown that the energy flux density, passing through a sphere with a radius $\rho$,

$$\overline{S_\rho} = 8\eta\pi^2 A^2 .\tag{8}$$

and does not depend on time, i.e. this flux has the same value on a spherical surface of any radius at any instant of time. In other words, the energy flux directed along the radius retains its value with increasing radius and does not depend on time, which corresponds to the law of conservation of energy.

## 4. About the longitudinal wave

We consider in more detail the equation (2.33). It has a solution of the following form [8, p. 12]:

$$e_\rho = -A \cdot (1+i)\frac{\ln(\rho)}{\rho^2}\tag{1}$$

It determines the electric intensities of the longitudinal electromagnetic field - see Table 2. The magnetic intensities of the longitudinal electromagnetic field also follows from Table 2. The electric intensity of

the longitudinal electromagnetic field is also present in the known solution for a spherical wave in the near zone, but there is no magnetic intensity of the longitudinal electromagnetic field, which (of course) contradicts Maxwell's equations. In addition, in the proposed solution, the electric intensity has a different description. In general, the solution does not exist in the absence of longitudinal intensities - one can easily verify that the equations of T6-3 are not compatible, when $e_\rho(\rho) = 0$.

In [1] a solution was given for the far zone, where $e_\rho(\rho) = 0$. But in solution from [1] there are cases when there are infinite values of any intensity - this makes that decision practically inapplicable.



r    Fig. 2 (AntObr.m)
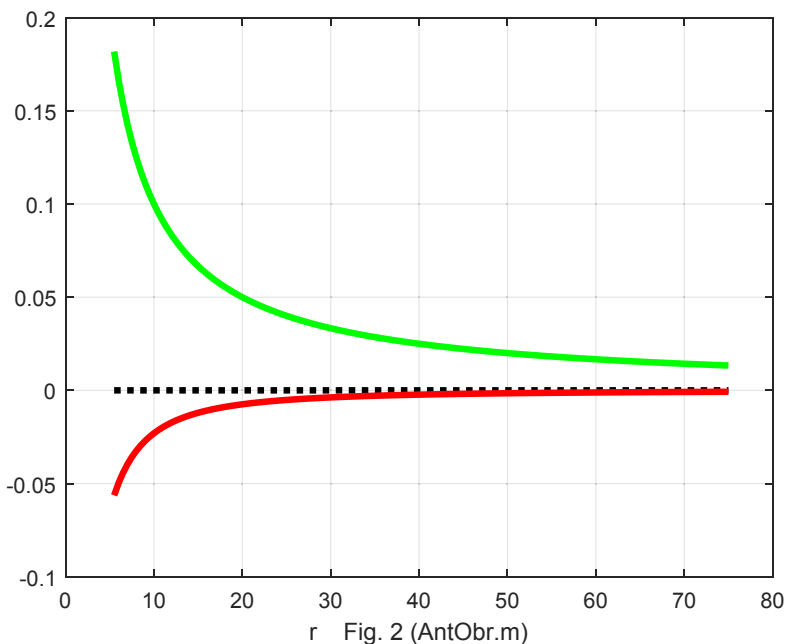
In Fig. 2 shows the form of the solution of equation (1) at $A = 1$, where the real part $e_\rho$ of the function (1) is shown (see the lower curve) and the function (2.29) $e_\varphi = A/\rho$ (see the upper curve). It is important to note that the function (1) always has a negative value (with respect to the constant A). When $A = -1$ the longitudinal wave is directed away from the source, i.e. coincides in the direction of the energy flow. The energy from the main energy flux of the transverse wave (3.8) is transmitted to the longitudinal wave. In this case, the main energy flux decreases (a comparative estimate of the energy of the longitudinal and transverse waves is not given here). Thus, the energy of the transverse wave is

converted into the energy of the longitudinal wave. Simultaneously, the intensity of the transverse wave decreases and the propagation of the wave stops (indeed, it is difficult to imagine an unbounded spherical wave in space).

## 5. Conclusion

1. A rigorous solution of Maxwell's equations, shown in Table. 1 and free from the above disadvantages, is presented in Table. 2, where

$$\varepsilon = \mu = 1. \tag{1}$$

$$q = \omega/c \tag{2}$$

$$\chi = -q \tag{3}$$

$$\alpha = 0 \tag{4}$$

$$E_\rho = -iH_\rho, H_\rho = iE_\rho \tag{5}$$

$$E_\varphi = iH_\varphi, H_\varphi = -iE_\varphi \tag{6}$$

$$E_\theta = -iH_\theta, H_\theta = iE_\theta \tag{7}$$

$$g_\rho = \cos(\theta) \tag{8}$$

$$g_\theta(\theta) = g_\varphi(\theta) = \sin(\theta) \tag{9}$$

$$e_\varphi = \frac{A}{\rho} \tag{10}$$

$$e_\theta = i \cdot e_\varphi \tag{11}$$

$$e_\rho = -A \cdot (1+i)\frac{\ln(\rho)}{\rho^2} \tag{12}$$

$$h_\rho = ie_\rho \tag{13}$$

$$h_\varphi = -ie_\varphi \tag{14}$$

$$h_\theta = ie_\theta \tag{15}$$

2. The solution found is complex. It is known that the real part of the complex solution is also a solution. Therefore, as a solution, instead of the functions presented in Table. 2, you can take their real parts. Taking into account this remark and the above formulas, we rewrite Table 2 in Table 8, where the real values of the intensities are shown. In Fig. 3 shows the intensities vectors in a spherical coordinate system.

3. The electric and magnetic intensities of the same name (according to coordinates $\rho$, $\varphi$, $\theta$) are phase shifted by a <u>quarter of a period</u>.

4. There is a longitudinal electromagnetic wave having electric and magnetic components.

5. In a transverse electromagnetic wave, the energy flux passing through the spheres along the radius remains constant with increasing radius and <u>does NOT change with time</u>.

6. The energy of the transverse wave is converted into the energy of the longitudinal wave. In this case, the intensity of the transverse wave decreases and the wave propagation ceases.
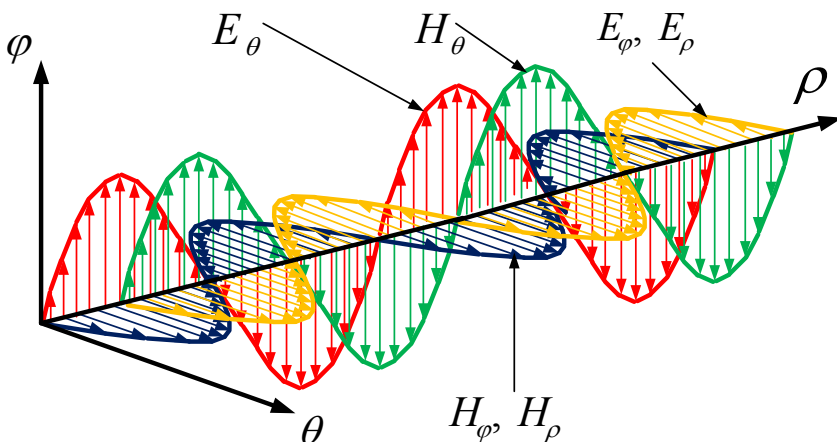


Fig. 3.

## Appendix 1

Рассматривая табл. 2 и формулы (2.22, 2.23, 2.23а, 29, 32) находим:

$$E_\varphi = \frac{A}{\rho}\sin(\theta)\exp(i\cdot(\chi\rho+\omega t)) = \frac{A}{\rho}\sin(\theta)[\cos((\chi\rho+\omega t))+i\sin((\chi\rho+\omega t))] \tag{1}$$

$$E_\theta = i\cdot E_\varphi = i\frac{A}{\rho}\sin(\theta)\exp(i\cdot(\chi\rho+\omega t)) = \frac{A}{\rho}\sin(\theta)\exp\left(i\cdot\left((\chi\rho+\omega t)+\frac{\pi}{2}\right)\right) =$$

$$= \frac{A}{\rho}\sin(\theta)\left[\cos\left((\chi\rho+\omega t)+\frac{\pi}{2}\right)+i\sin\left((\chi\rho+\omega t)+\frac{\pi}{2}\right)\right] = \tag{2}$$

$$= \frac{A}{\rho}\sin(\theta)[-\sin(\chi\rho+\omega t)-i\cos(\chi\rho+\omega t)]$$

From (1, 2, 4.5) we find:

$$S_\rho = 2iE_\theta E_\varphi = \frac{2iA^2}{\rho^2}\sin^2(\theta)[\cos(...)+i\sin(...)][-\sin(...)-i\cos(...)] =$$

$$= \frac{2iA^2}{\rho^2}\sin^2(\theta)[-i\cos^2(...)-i\sin^2(...)] = \frac{2iA^2}{\rho^2}\sin^2(\theta)(-i)$$

or

$$S_\rho = \frac{2A^2}{\rho^2}\sin^2(\theta).$$

(3)

Note also that the surface area of a sphere with a radius $\rho$ is $4\pi\rho^2$. Then the flow of energy passing through a sphere with a radius $\rho$ is

$$\overline{S_\rho} = \eta\int_\theta 4\pi\rho^2 S_\rho\, d\theta = \eta 4\pi\rho^2\frac{2A^2}{\rho^2}\int_\theta \sin^2(\theta)\, d\theta$$

or

$$\overline{S_\rho} = 8\eta\pi^2 A^2.$$

(4)

# References

1. Khmelnik S.I. New solution of Maxwell's equations for spherical wave in the far zone, http://vixra.org/abs/1711.0243, 2017-11-13.
2. Pimenov Yu.V., Volman V.I., Muravtsov A.D. Technical electrodynamics. Edited by Yu.V. Pimenov, Moscow, 2002 г., 536 p. (in Russian).
3. Andre Ango. Mathematics for Electrical and Radio Engineers, publ. "Nauka", Moscow, 1964, 772 p. (in Russian).
4. S.I. Khmelnik. Inconsistency Solution of Maxwell's Equations, publ. "MiC", Israel, Printed in USA, Lulu Inc., ID 19043222, ISBN 978-1-365-23941-0, sixth edition, 2017, 190 p., http://vixra.org/abs/1607.0423, 27.07.2017.
5. Khmelnik S.I. Variational Principle of Extremum in Electromechanical and Electrodynamic Systems, Publisher by "MiC", printed in USA, Lulu Inc., ID 1142842, ISBN 978-0-557-08231-5, Fourth Edition, 2014, 347 c. http://vixra.org/abs/1402.0026, 2014-11-10.
6. Near and far zones of the electromagnetic field, http://lib.izdatelstwo.com/Papers2/BIZ.pdf (in Russian).
7. Neganov V.A., Tabakov D.P., Yarovoi D.P. Modern theory and practical applications of antennas. Editor Neganov V.A. Publ. «Radio engineering», Moscow, 2009, 720 pages (in Russian).
8. Zaitsev VF, Polyanin AD Handbook of ordinary differential equations. Moscow, FIZMATLIT, 2001, 576 p. (in Russian).
9. S.I. Khmelnik. New solution of Maxwell's equations for spherical wave. The Papers of independent Authors, ISSN 2225-6717, 2018, volume 41, http://dna.izdatelstwo.com/ (in Russian).

**10.** S.I. Khmelnik. New Solution of Maxwell's Equations for Spherical Wave, http://vixra.org/abs/1801.0348, 2018-01-25

# Tables

Table 1.

| 1 | 2 | 3 | 4 |
|---|---|---|---|
| 1 | $\mathrm{rot}_\rho(E)$ | $\dfrac{E_\varphi}{\rho\,\mathrm{tg}(\theta)}+\dfrac{\partial E_\varphi}{\rho\partial\theta}-\dfrac{\partial E_\theta}{\rho\sin(\theta)\partial\varphi}$ | $\dfrac{T(E_\varphi)}{\rho}-\dfrac{i\alpha E_\theta}{\rho\sin(\theta)}$ |
| 5 | $\mathrm{rot}_\rho(H)$ | $\dfrac{H_\varphi}{\rho\,\mathrm{tg}(\theta)}+\dfrac{\partial H_\varphi}{\rho\partial\theta}-\dfrac{\partial H_\theta}{\rho\sin(\theta)\partial\varphi}$ | $\dfrac{T(H_\varphi)}{\rho}-\dfrac{i\alpha H_\theta}{\rho\sin(\theta)}$ |
| 2 | $\mathrm{rot}_\theta(E)$ | $\dfrac{\partial E_\rho}{\rho\sin(\theta)\partial\varphi}-\dfrac{E_\varphi}{\rho}-\dfrac{\partial E_\varphi}{\partial\rho}$ | $\dfrac{i\alpha E_\rho}{\rho\sin(\theta)}-\psi(E_\varphi)$ |
| 3 | $\mathrm{rot}_\varphi(E)$ | $\dfrac{E_\theta}{\rho}+\dfrac{\partial E_\theta}{\partial\rho}-\dfrac{\partial E_\rho}{\rho\partial\varphi}$ | $\psi(E_\theta)-\dfrac{i\alpha E_\rho}{\rho}$ |
| 6 | $\mathrm{rot}_\theta(H)$ | $\dfrac{\partial H_\rho}{\rho\sin(\theta)\partial\varphi}-\dfrac{H_\varphi}{\rho}-\dfrac{\partial H_\varphi}{\partial\rho}$ | $\dfrac{i\alpha H_\rho}{\rho\sin(\theta)}-\psi(H_\varphi)$ |
| 7 | $\mathrm{rot}_\varphi H$ | $\dfrac{H_\theta}{\rho}+\dfrac{\partial H_\theta}{\partial\rho}-\dfrac{\partial H_\rho}{\rho\partial\varphi}$ | $\psi(H_\theta)-\dfrac{i\alpha H_\rho}{\rho}$ |
| 4 | $\mathrm{div}(E)$ | $\dfrac{E_\rho}{\rho}+\dfrac{\partial E_\rho}{\partial\rho}+\dfrac{E_\theta}{\rho\,\mathrm{tg}(\theta)}+$ $+\dfrac{\partial E_\theta}{\rho\partial\theta}+\dfrac{\partial E_\varphi}{\rho\sin(\theta)\partial\varphi}$ | $\psi(E_\rho)+\dfrac{T(E_\theta)}{\rho}+\dfrac{i\alpha E_\varphi}{\rho\sin(\theta)}$ |
| 8 | $\mathrm{div}(H)$ | $\dfrac{H_\rho}{\rho}+\dfrac{\partial H_\rho}{\partial\rho}+\dfrac{H_\theta}{\rho\,\mathrm{tg}(\theta)}+$ $+\dfrac{\partial H_\theta}{\rho\partial\theta}+\dfrac{\partial H_\varphi}{\rho\sin(\theta)\partial\varphi}$ | $\psi(H_\rho)+\dfrac{T(H_\theta)}{\rho}+\dfrac{i\alpha H_\varphi}{\rho\sin(\theta)}$ |

Table 2.

| 1 | 2 |
|---|---|
| | $E_\theta = e_\theta(\rho)g_\theta(\theta)\exp(i\cdot(\chi\rho+\alpha\varphi+\omega t))$ |
| | $E_\varphi = e_\varphi(\rho)g_\varphi(\theta)\exp(i\cdot(\chi\rho+\alpha\varphi+\omega t))$ |
| | $E_\rho = e_\rho(\rho)g_\rho(\theta)\exp(i\cdot(\chi\rho+\alpha\varphi+\omega t))$ |
| | $H_\theta = h_\theta(\rho)g_\theta(\theta)\exp(i\cdot(\chi\rho+\alpha\varphi+\omega t))$ |
| | $H_\varphi = h_\varphi(\rho)g_\varphi(\theta)\exp(i\cdot(\chi\rho+\alpha\varphi+\omega t))$ |
| | $H_\rho = h_\rho(\rho)g_\rho(\theta)\exp(i\cdot(\chi\rho+\alpha\varphi+\omega t))$ |

Table 3.

| 1 | 2 | 3 |
|---|---|---|
| 1. | $\operatorname{rot}_\rho E + \dfrac{\mu}{c}\dfrac{\partial H_\rho}{\partial t} = 0$ | $\dfrac{T(E_\varphi)}{\rho} - \dfrac{i\alpha E_\theta}{\rho\sin(\theta)} + \dfrac{i\omega\mu}{c}H_\rho = 0$ |
| 5. | $\operatorname{rot}_\rho H - \dfrac{\varepsilon}{c}\dfrac{\partial E_\rho}{\partial t} = 0$ | $\dfrac{T(H_\varphi)}{\rho} - \dfrac{i\alpha H_\theta}{\rho\sin(\theta)} - \dfrac{i\omega\varepsilon}{c}E_\rho = 0$ |
| 2. | $\operatorname{rot}_\theta E + \dfrac{\mu}{c}\dfrac{\partial H_\theta}{\partial t} = 0$ | $\dfrac{i\alpha E_\rho}{\rho\sin(\theta)} - \Psi(E_\varphi) + \dfrac{i\omega\mu}{c}H_\theta = 0$ |
| 3. | $\operatorname{rot}_\varphi E + \dfrac{\mu}{c}\dfrac{\partial H_\varphi}{\partial t} = 0$ | $\Psi(E_\theta) - \dfrac{i\alpha E_\rho}{\rho} + \dfrac{i\omega\mu}{c}H_\varphi = 0$ |
| 6. | $\operatorname{rot}_\theta H - \dfrac{\varepsilon}{c}\dfrac{\partial E_\theta}{\partial t} = 0$ | $\dfrac{i\alpha H_\rho}{\rho\sin(\theta)} - \Psi(H_\varphi) - \dfrac{i\omega\varepsilon}{c}E_\theta = 0$ |
| 7. | $\operatorname{rot}_\varphi H - \dfrac{\varepsilon}{c}\dfrac{\partial E_\varphi}{\partial t} = 0$ | $\Psi(H_\theta) - \dfrac{i\alpha H_\rho}{\rho} - \dfrac{i\omega\varepsilon}{c}E_\varphi = 0$ |
| 4. | $\operatorname{div}(E) = 0$ | $\Psi(E_\rho) + \dfrac{T(E_\theta)}{\rho} + \dfrac{i\alpha E_\varphi}{\rho\sin(\theta)} = 0$ |
| 8. | $\operatorname{div}(H) = 0$ | $\Psi(H_\rho) + \dfrac{T(H_\theta)}{\rho} + \dfrac{i\alpha H_\varphi}{\rho\sin(\theta)} = 0$ |

Table 4.

| 1 | 2 | 3 |
|---|---|---|
| 1 | $\dfrac{e_\varphi g_\varphi}{\rho tg} + \dfrac{e_\varphi \hat{g}_\varphi}{\rho} - \dfrac{i\alpha}{\rho\sin} e_\theta g_\theta + \dfrac{i\omega\mu}{c} h_\rho g_\rho = 0$ | $\dfrac{E_\varphi^{sumH}}{\rho tg} g_\varphi + \dfrac{E_\varphi^{sumH}}{\rho} \hat{g}_\varphi -$ |
| 5 | $\dfrac{h_\varphi g}{\rho tg} + \dfrac{h_\varphi \hat{g}_\varphi}{\rho} - \dfrac{i\alpha}{\rho\sin} h_\theta g_\theta - \dfrac{i\omega\varepsilon}{c} e_\rho g_\rho = 0$ | $-\dfrac{i\alpha}{\rho\sin} E_\theta^{sumH} g_\theta -$ $-iqE_\rho^{\min H} g_\rho = 0$ |
| 2 | $\dfrac{i\alpha}{\rho\sin} e_\rho g_\rho - \psi(e_\varphi) g_\varphi + \dfrac{i\omega\mu}{c} h_\theta g_\theta = 0$ | $\dfrac{i\alpha}{\rho\sin} E_\rho^{sumH} g_\rho - \psi(E_\varphi^{sumH}) g_\varphi$ |
| 6 | $\psi(e_\theta) g_\theta - \dfrac{i\alpha}{\rho} e_\rho g_\rho + \dfrac{i\omega\mu}{c} h_\varphi g_\varphi = 0$ | $-iqE_\theta^{\min H} g_\theta = 0$ |
| 3 | $\dfrac{i\alpha}{\rho\sin} h_\rho g_\rho - \psi(h_\varphi) g_\varphi - \dfrac{i\omega\varepsilon}{c} e_\theta g_\theta = 0$ | $\psi(E_\theta^{sumH}) g_\theta - \dfrac{i\alpha}{\rho} E_\rho^{sumH} g_\rho -$ |
| 7 | $\psi(h_\theta) g_\theta - \dfrac{i\alpha}{\rho} h_\rho g_\rho - \dfrac{i\omega\varepsilon}{c} e_\varphi g_\varphi = 0$ | $-iqE_\varphi^{\min H} g_\varphi = 0$ |
| 4 | $\psi(e_\rho) g_\rho + \dfrac{e_\theta}{\rho tg} g_\theta + \dfrac{e_\theta \hat{g}_\theta}{\rho} + \dfrac{i\alpha}{\rho\sin} e_\varphi g_\varphi = 0$ | $\psi(E_\rho^{sumH}) g_\rho + \dfrac{E_\theta^{sumH}}{\rho tg} g_\theta +$ |
| 8 | $\psi(h_\rho) g_\rho + \dfrac{h_\theta g}{\rho tg} + \dfrac{h_\theta \hat{g}_\theta}{\rho} + \dfrac{i\alpha}{\rho\sin} h_\varphi g_\varphi = 0$ | $+\dfrac{E_\theta^{sumH}}{\rho} \hat{g}_\theta + \dfrac{i\alpha}{\rho\sin} E_\varphi^{sumH} g_\varphi = 0$ |

Table 5.

| 1 | 2 |
|---|---|
| 1. | $\dfrac{(1-i)e_\varphi}{\rho tg} g_\varphi + \dfrac{(1-i)e_\varphi}{\rho} \hat{g}_\varphi - \dfrac{i\alpha}{\rho\sin}(1+i)e_\theta g_\theta - (1-i)\dfrac{i\omega\mu}{c} e_\rho g_\rho = 0$ |
| 2. | $\dfrac{i\alpha}{\rho\sin}(1+i)e_\rho g_\rho - (1-i)\psi(e_\varphi) g_\varphi - (1-i)\dfrac{i\omega\mu}{c} e_\theta g_\theta = 0$ |
| 3. | $(1+i)\psi(e_\theta) g_\theta - (1+i)\dfrac{i\alpha}{\rho} e_\rho g_\rho - (1-i)\dfrac{i\omega\mu}{c} e_\varphi g_\varphi = 0$ |
| 4. | $(1+i)\psi(e_\rho) g_\rho + (1+i)\dfrac{e_\theta}{\rho tg} g_\theta + (1+i)\dfrac{e_\theta}{\rho} \hat{g}_\theta + (1-i)\dfrac{i\alpha}{\rho\sin} e_\varphi g_\varphi = 0$ |

Table 6.

| 1 | 2 | 3 |
|---|---|---|
| 1 | $\dfrac{1}{\rho\sin}\left(e_\theta\alpha g_\theta - e_\varphi g_\varphi\cos\right) + iqe_\rho g_\rho - \dfrac{e_\varphi}{\rho}\hat{g}_\varphi = 0$ | $\dfrac{e_\varphi}{\rho}\hat{g} = \dfrac{g\cos}{\rho\sin}e_\varphi + iqe_\rho g_\rho$ |
| 2 | $\psi\left(e_\varphi\right)g_\varphi + qe_\theta g_\theta + \dfrac{\alpha}{\rho\sin}e_\rho g_\rho = 0$ | $\psi\left(e_\varphi\right)g_\varphi + iqe_\rho g_\varphi = 0$ |
| 3 | $\psi\left(e_\theta\right)g_\theta - qe_\varphi g_\varphi - \dfrac{i\alpha}{\rho}e_\rho g_\rho = 0$ | $i\cdot\psi\left(e_\varphi\right)g_\varphi - qe_\varphi g_\varphi = 0$ |
| 4 | $\psi\left(e_\rho\right)g_\rho + \dfrac{1}{\rho\sin}\left(e_\theta g_\theta\cos + e_\varphi\alpha g_\varphi\right) + \dfrac{e_\theta}{\rho}\hat{g}_\theta = 0$ | $\psi\left(e_\rho\right)g_\rho + \dfrac{ig_\varphi\cos}{\rho\sin}e_\varphi + \dfrac{ie_\varphi}{\rho}\hat{g}_\varphi = 0$ |

Table 7.

| 1 | 2 |
|---|---|
| 1. | $-\psi\left(e_\rho\right)g_\rho - \dfrac{i\cos}{\rho\sin}e_\varphi g_\varphi - \dfrac{\cos}{\rho\sin}e_\varphi g_\varphi - iqe_\rho g_\rho = 0$ |
| 2. | $\psi\left(e_\varphi\right)g_\varphi + iqe_\varphi g_\varphi = 0$ |

Table 8.

| 1 | 2 |
|---|---|
| | $E_\theta = e_\varphi(\rho)\sin(\theta)\sin(\chi\rho + \omega t)$ |
| | $E_\varphi = e_\varphi(\rho)\sin(\theta)\cos(\chi\rho + \omega t)$ |
| | $E_\rho = e_\rho(\rho)\cos(\theta)\cos(\chi\rho + \omega t)$ |
| | $H_\theta = -e_\varphi(\rho)\sin(\theta)\cos(\chi\rho + \omega t)$ |
| | $H_\varphi = e_\varphi(\rho)\sin(\theta)\sin(\chi\rho + \omega t)$ |
| | $H_\rho = e_\rho(\rho)\cos(\theta)\sin(\chi\rho + \omega t)$ |

# Series: PHYSICS and ASTRONOMY

**Ruben G. Kojamanyan**

# Physics of light

## Abstract

A new concept of electromagnetic radiation is exposed in the article. First of all it shall be said that the following concept is a revolutionary one. But I urge you not to start blaming it too quickly for this reason, because the very approach may lead us to vast explanations.

The following hypothesis is based on rather spare but canonical and still quotable materials. The Michelson–Morley experiment using interferometer is the core. Besides, not a single new formula has been discovered ever since – well, there were no calls for it. However, the new idea of semi-inertance is introduced for the first time in this work; explanation of the phenomenon's origin is apprehensible. The mathematics here although simple, still meets all the strictest requirements, which is the only possible way.

Electromagnetic wave, in particular when it comes to the postulate of its independent propagation velocity, is deemed a fundamental concept developed as early as in classic era. It seems everything is as clear as a day here. But we have discovered a crack in this foundation, thus it needs troubleshooting. Modern representations of such concepts as dualism, invariant mass (zeroing for some reason), energy differences in an isolated system (and photon is such a system) violating the law of conservation – this all sounds lame and inconsistent. Interestingly, the first inconsistency can be seen in the construction of Michelson–Morley experiment conducted more than 120 years ago. But the problem of parallel formation on the basis of Euclidean axioms is even older and is solvable. No future without a past, and no brandnew theory of electromagnetic radiation would have appeared without pains of ancient scientist to their glory. The concept of relativeness, Einstein's postulates, and Lorentz transformations are predominant in the modern theory of matter and spacetime. However ,its the objective of science to reflect upon any concept to either turn it over or leave it be. I must say I anticipate this text would sound horrible to some experts because I appeal approach rather complex concepts with undue simplicity. I can do nothing with it, so I'm afraid the only thing I may suggest here is to take it as it is. Our ambitions however minor they are, or scientific search for truth– everyone is up to judge on its own which one is more important. Thank you.

So, I am to start with the starting points of the hypothesis.

First – I believe that the absolute space is yet a reality. If one had observed the gravitational attraction of two commensurable masses – of the Earth and the Moon, for instance – from a distant star, then he would have found three relative gravity accelerations (g). A man from Earth, and later from the Moon would obtain equal approaching (gravity) accelerations – the same distance and the same time. However, according to the Newton's law, the acceleration should be dependent from mass of an attracting object and independent from the mass of an object being attracted. The famous formula is lawful exclusively if related to stars, i.e. in the absolute space.

The conclusions deduced from the experiments comparing g's of various objects are inconsistent since such experiments were held using objects incommensurably small against the Earth. It's worthless trying to detect the difference using wooden or lead balls. Existence of the absolute space follows from existence of the Universe itself. The formula of gravity in the relative space is as follows:

$$F = m_3 g = [m(m+M)/r^2]G_3 = M_\Lambda g = [m(m+M)/r^2]G_\Lambda$$

where

$G_3$ – relative to the Earth

$G_\Lambda$ – relative to the Moon as a sum of two countering accelerations when travelling the same distance.

Mass of the Earth measured from the Moon equals mass of the Moon measured from the Earth, is we consider mass as a force gaining a specific acceleration. For this to become valid, we need a base such as friction or spring tension; in both cases dependant from gravity. We obtain an non-relative value when employing the comparison method (using scales) independent from gravity, i.e. beyond the relativity. That's all subject to conditions, of course. The gravity constant is just another relative value itself – we get another value when measuring from the Moon. The unconditional this here is that the real value is possible to measure only in conditions free of gravity. Thus, if start measuring objects' masses gaining them up gradually, there would come to a point from which mass and weight would grow inequally, i.e. we would find inequality between inert mass and gravity mass. The formula above shall be of significant practical importance since no motionless support points exist in the Universe. As for the absolute space, two fundamental properties of matter are essential: existence of the universal gravity center, and inertia.

That's all simple with Time. Time is an interval between events; and it's not Time's fault that no constant intervals (to be used as measurement units) exist in nature. Time is not a train one can speed up or down, stop or reverse.

Next, I shall say I can not perceive the space curvature resulting from the presence of a mass; if it had existed, it would have been easier to enter an orbit considering there is no gravity. Inertial motion implies no speed changes in space. However, if the Moon had not been speeding up or down, it would not have rotated about the Earth. Gravity is the only possible cause of such alterations of speed.

Next, I don't believe Lorentz transformations are viable. Let us consider three space vehicles, each of them moving self-sufficiently. Now, if Lorentz transformations happen inside one of them in relation to another, then what kind of transformations happen in relation to the third vehicle? Nonsense. If however, we understand speeds in relation to the absolute space, then we speak off the subject.

Now, let us consider the Michelson–Morley experiment. If electromagnetic wave would have been inertial, then would have been no doubts regarding the experiment outcomes. However, the postulate claims independence and invariability of light speed, not its inertance. Is seems as if Nature conceals the movement from us in the outer space. Yet the non-inertance of light is not the only reason of the interference displacement. When studying this case the incorrectness of the very idea of the experiment was surprisingly revealed. In cross direction the beam must reach the mirror earlier, forming an angle to the straight line which is from glass to mirror. This fact is described in every guidance, but the fact is omitted that this angle remains the same after revolving the assembly – during revolving they do not displace it. Both directions are always negligently described simultaneously and independently presuming that the situations is balanced after the revolving is completed. However, it is imperative to examine each of the two beams in one direction and subsequently in the other. A beam heading along with the Earth's direction remains its direction after the assembly was revolved, and it's the mirror now that displaces aside.

As the result the interference displacement should have happened in any case. Lorentz transformations of time and distance don't remedy the situation. But this just does not happen!

It is hard to escape the conclusion that the two things – the postulate of light speed relativity and the Michelson–Morley experiment outcomes – do not live together.

Being devoted to experiment-based approach, I have developed the hypothesis.

The idea emerged from the Einstein's law, i.e. the equivalence of mass and energy. It is a common place nowadays that an elementary particle is able to transform to field energy and vice versa, and also to other particles. Or– one type of field, the symbolic for instance, is transformable to a neutral type, and so on. Transformations, being the permanent state of particles and energy, are universally widespread in Nature.

Then what if the light yet bears the property of the rest mass $mo=/=0$, if passing with time, thus kind of pulsating constantly. It means photon has a habit of constant transformation (annihilation and emergence) from particle to energy and vice versa. The moment after the atomic electronic shell swells up from excess of energy the photon emerges within its action area. Simultaneously the decline of the shell –of its level– takes place. The particle annihilates instantly, thus forming its own field which emerges from the opposite edge of

the field but still within its borders. After living extremely short while the photon particle transforms again – so getting further and further away from the atom where it was initially born. Thus the photon remains literally motionless in relation to its source, but the shortness of its life allows for independent and constant expansion with its wild speed until it reaches another atom. Based on the unity of the universal energy, the space limited by every phase (period) of the transformation process is adopted simultaneously. No forward movement of energy or particle ever happens – but it is the redistribution (transformation) of their forms, types and intensities towards the direction of the emission; unity of matter interaction forces, for short. In general, where the energy field is found, the particle shall present, and vice versa – the particle is always followed by the energy. Thus, electromagnetic radiation is in physical terms motionless in a coordinate system referenced to the source but it expands by transforming. It is hard to imagine what a 'mayhem' the electromagnetic wave –this Mistress of the Universe– would have done to us (in any cases – with or without particle) would that all have been structured otherwise. Besides, according to the theory, the mobile mass of photon should be increasing to almost an infinite scale, isn't it? And regarding the pressure which the light yet exhibits – it results from photon particles aggregations impacting the matter with their inertia when their fields (of particles and matter) mutually interfere.
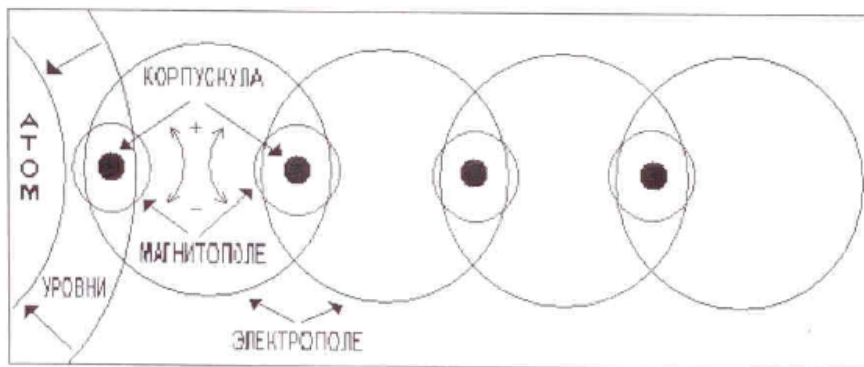


Variable intensity of existence of mass and field – represented by a sine wave graph – should me mentioned as well. The graph below shows that the energy sine in form of electric and magnetic fields acts against the law of conservation of energy. Existence of the corpuscle eliminates the contradiction, since it makes the sum of the three energy types constant at any point of time given.

This concept does not go against any discovered properties of the electromagnetic wave, but it gives feasibility to introduce a very important property – semi-inertance, i.e. the light speed nevertheless bears  half of the source speed!
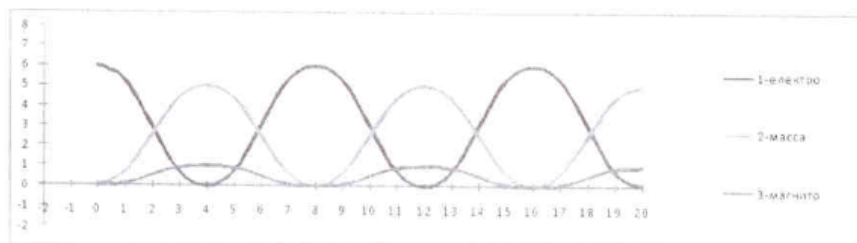
Not we are able to interpret the interferometer experiment outcomes. After the assembly is displaced the beams have no effect on the interference travelling different distances with different speeds but for one and the same time. The waves are found in the right place in the right time. But these waves belong not to vibration but to the photon. Furthermore, it does not matter whether the assembly arms are of the same length, or which is the angle between them. The same principle as with an inert object – only the trajectories differ. These are the outcomes we get in this famous and historic experiment when making allowance for the semi-inertance of light.

Let us address to the beam reflection from the side mirror. The reflection angle differs like a ball bouncing from wall which keeps moving relative to the viewer. The only difference here is that the photon particle, unlike the ball, makes no forward movement along the beam direction, and the reflection angle may be calculated using a somewhat different principle – still in full accordance with this concept. Presumably we deal hear with mechanical interaction of fields, which influences the wave direction.

Now, if we measure lengths, time intervals and masses in different labs, we obtain different values, i.e. apparent change. Let us note that the values received in keeping with semi-inertance principle are very close to those received by employing Lorenz transformations based on trigonometric calculations. For example, when observing the star during eclipse (mentioned earlier) the flexure appeared to be 2 times more than anticipated. In the guidances this fact is considered accordant to the relativity theory. But the semi-inertance concept allows for a specific explanation. The inertia mass of the photon is twice as small as the gravity mass since the field energy – aspect of the photon – has gravity mass but no inertia mass.

It is possible to detect inertance of the light – or, rather, its semi-inertance – by making experiments employing the Earth movement both directional and axial, if we register positions of the fixed beam on the screen every hour or two over a period of 24 hours. Inertance of the beam is revealed by presenting the major diameter of the resulting ellipse. Another possible method – we direct the beam towards revolving disk, the edge surface of which is mirror-polished. Any deflection of the reflected beam happening along with change of revolving speed would speak for inertance. The photon particle may be also discovered by smashing the beam with a bundle of elementary particles (e.g. electrons) from a distance divisible by the wave length.

The concept provided explanation to my own following observance. The bright side of the Moon is slightly directed towards the Sun. It is well seen even by unaided eye when the Moon and the Sun appear together within the field of sight. Optical (lens) effect of atmosphere comes not in play here due to its insignificance.

The explanation is the following – axial rotation of the Sun and the resulting corpuscle shifting across vector direction 'falls down' subject to gravity leads to trajectory curvature. The further from the Sun the weaker gravity is, and the beam straightens , but the trajectory distortion remains (due to inertance) thus reflecting from the Moon. The direction is radial, it is not the space curvature caused by a massive object  that matters.

Now, briefly about the parallel postulate. It Is deemed impossible to be proved based on the foregoing axioms. Yet, it possible owing to the present concept – concept of movement within one and only coordinate system with no place for any forward  movement at all, and where the minimal distance between two points of a line exists since the geometric locus exists. Employing the triangle strength one can build a line, all and every single points of which are equally distanced from the initial line.  Such building is considered a terminated cycle, i.e. we may continue building it endlessly in cycles. These two lines can not cross over, which means they are parallel to each other. When transferring this principle to a spherical surface we suddenly face an invincible obstacle. According to Euclidean axioms, any geometrical shape can be duplicated, then shifted, flipped, rotated, and then applied again to the surface, and it shall remain the same as the initial shape. However this principles does not work with a sphere. We cannot chip off a bit of an egg shell and put it back to the egg by its external side keeping the initial shape perfectly. Such an element is involved in the mentioned building. But if we assume change of curvature tensor to the reversed sign, we get lines approaching each other, thus violating the parallelism. Interestingly, any two straight lines surfaced on sphere cross over each other in two points, and yet these lines are deemed parallel. Besides, *at most one line parallel to the given line can be drawn through the point not on it* since another line, if possible, shall present either a tangent line or transverse – a third is not given. But in the first case (tangent) the line will be directed not along the largest circle thus may not be deemed a straight line of the given surface i.e. sphere. In the second case (transverse), the line forms angles in the cross point, thus the sum of unilateral angles at the line crossing both parallel lines in the mentioned point shall not be equal to $180°$ – which conflicts with the definition of parallelism. Displacement by transformation process of material points aggregates 'molded' by other forces (i.e. displacement of objects) due to partial lack of forward movement may resolve the paradoxes of such ancient Pythagorean philosophers as Zeno and others (the paradox of Achilles overrunning the turtle). The track where they run (as well as any other object) is also the geometric locus. Expanding the concept, there is no other forward movement of matter than inertial one corrected for gravity against semi-time.

The variety of directions (vectors) and intensities are resulted from interaction of material points, and then the same scenario comes in play. Yet the initial impulse was given at the moment of initial explosion in the same way is the light pressure works. The directional lines of the explosion I believe had a spiral configuration due to spinning. All the rest are radiations (transformations) of the corresponding direction within the second semi-period. Yet another thing – material transformations may be both external (radiations) and internal. The Brownian motion may be explained by this fact. Molecules are not bees in a hive, and haze is not energy which activates the bees. But the transformations are totally dependant from energy absorption by levels of electrons. The energy is partially re-absorbed, partially appears in inertial clashes when the fields interact.

What shall I say in conclusion? Infinity of the Universe looks nonsense, just as its finiteness. I am the physicist, not a philosopher. I believe the Universe keeps its mysteries not in the far-far galaxies, rather in its yet uncovered properties. What if antimatter, just like matter, is dissipated not uniformly, and there are vast anti-agglomerations able to transform entire stellar systems by creating the illusion of infinity, and its finiteness is lost in endless variety of transformation types?

# Series: **PHYSICS and ASTRONOMY**

**Solovyev A.A., Chekarev K.V., Solovyev D.A.**

# Low-Grade Heat in Production of Electricity

## Abstract

Several technical solutions of using low-grade heat for cooling heat engines of power plants are considered. The methods of computer modeling of heat and mass transfer and aerodynamics and hydrodynamics were used to calculate the efficiency coefficient for cooling circulating water of power plants for two types of evaporative cooling towers with a natural drought and different classes of configuration of water and air flows: counter flow and cross flow. The growth of the efficiency coefficient was established for natural drought towers with external heat transfer compared to conventional cooling towers where the heat transfer occurs inside the tower.

## Contents

## 1. Introduction

The low-grade heat is one of the types of renewable sources of energy and is used for different purposes by different ways [1]. The most common use is the heat conversion from low to high temperature with the help of heat pump [2]. There have been and continue efforts to use geothermal and ocean resources of low-grade heat to produce electricity with the help of heat engines, but these attempts are in the experimental stage [3]. One way to use low-grade heat is its conversion into electrical energy by creating inside the tower a rising convective flow of warm air which rotates a turbine of a power generator [4]. With the growth of the

power of heat engines there has been required a need to cool them. The cooling with cold water turned to be the most promising way of doing that. In the absence of a permanent source of cold water, the warm water, which had passed through the heat engine, was cooled by the flow of cold air in devices called cooling towers [5]. The aim of the research presented in this article was the finding of the technical solutions that improve the efficiency of cooling towers with a natural drought and the assessment of their efficiency with the help of computer modeling.

## 2. The use of low-grade heat in natural drought towers

The configuration of natural drought tower is shown in the figure 1. A typical natural draught cooling tower comprises a hyperbolic shell structure mounted on leg supports over a circular pond. The circulating warm water enters the tower and cascades over a slatted structure, referred to as the 'packing', mounted above the pond. The packing is considered to be the primary heat transfer surface in the tower, where the warm water transfers its heat to the cold air entering the tower. The drought is driven by the difference of the density of the warm moist air inside the tower compared with the cooler air outside the shell. The figure 1 illustrates the counter-flow configuration where the flow of circulating warm water in the tower is in the opposite direction to the flow of air in the packing.

This type of cooling towers has several disadvantages. Some of them can be relatively easily removed. The efficiency of the cooling of the warm water depends on the intensity of the flow of the incoming cold air and its distribution inside the tower. Since in this type of cooling towers the cold air flow is horizontal flow that is directed along the radius of the base of the tower and then turns into the vertical air flow, so in the towers there are areas which the cold air misses. To achieve a more even distribution of the incoming flow of cold air inside the tower it was proposed to insert in the construction of the cooling tower the shields directing the flow of incoming air [6]. They were placed in the area between leg supports at an angle to the radius of the base of the tower. In cooling towers with such shields the incoming flow of cold air is directed not along the radius to the center of the tower base, but at an angle to it [7]. As a result, there were created conditions for reducing dead zones which cold air missed and conditions for increasing the time of the heat transfer. Automatic rotation of the shields gave the possibility to adjust the incoming flow of cold air under different weather

conditions. The possibility of such adjustment is of particular importance for achieving the optimal temperature of cooling of circulating water as under extremely low temperatures of the air in the winter as under the high temperatures in the summer. Upgraded cooling tower with the system of air adjusting devices has been successfully working for several years and shows a reliable work both in the summer and in the winter [8].
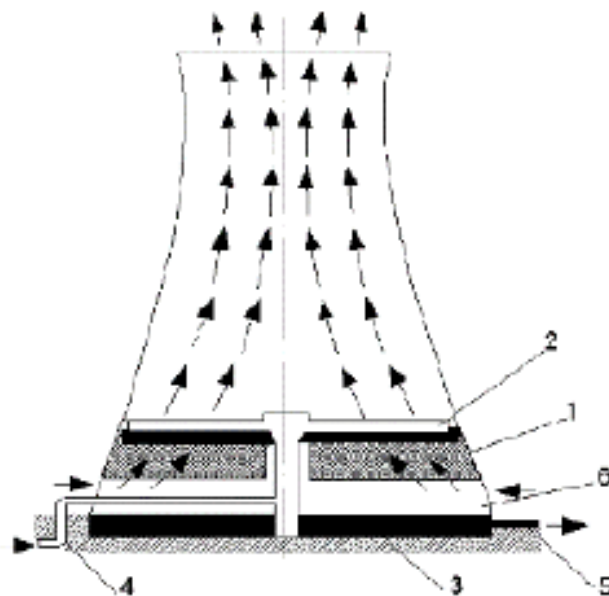


Fig.1. Configuration of natural draught cooling tower with counter-flow. 1-water-catcher; 2-water distribution system; 3-cold water pond; 4-hot water inlet; 5-cold water output; 6-air feeding.

Despite the efficiency of proposed technical solutions there are some disadvantages in existing cooling towers that can be explained by the fact that hydrodynamic processes defining the heat and mass transfer of warm water and incoming cold air were not taken into account. The heat and mass transfer is organized like following. Firstly the warm circulating water is turning above the packing into little droplets which are falling on the packing and in the form of thin films they are flowing down and are streaming into the pond. In the area between the surface of the pond and the bottom of the packing the streams of warm water come into contact with flow of the cold air entering the tower at the right angle to the streams of the water. Here they transfer their heat to the cold air by contact and evaporation. As the result the cold air becomes very fast warm and moist and begins to rise in the tower passing through the

packing, which is considered to be the primary heat transfer. But it is not so, because at this time the cold air has already interacted with the streams of warm water falling down from the packing and at the moment when it comes into contact with the thin films of water in the packing it is warm and moist and its capacity to cool the water is very low. Thus the packing placed inside the cooling tower dose not fully perform its function of heat transfer. In addition to that the packing almost completely fills the space of the tower which creates a big aerodynamic resistance to the air flow inside the tower and reduces its velocity and hence the efficiency of the cooling tower.

The elimination of this disadvantage is possible by the division of functions of the tower which are to create a vertical flow of warm air in it and to be an area where the heat and mass transfer between warm water and incoming cold air is taking place. In order to divide these functions it has been proposed a construction of cooling towers with external heat and mass transfer [9]. The packing in this cooling towers is placed around the base of the tower ( fig.2).
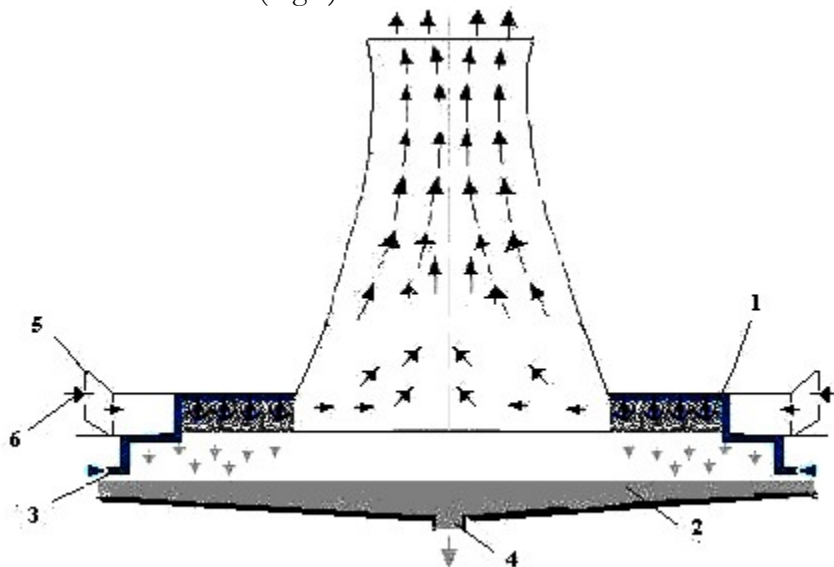


Fig .2. Configuration of natural draught cooling tower with cross - flow.
1 –packing ; 2- pond;3- entrance of warm water ; 4 output chilled water; 5 air adjustment boards; 6 - entrance of outside air.

In this construction of cooling towers the warm water is running down the packing in the form of thin films and the flow of the air is coming at a right angle to them. This construction is called cross-flow.

The cooling towers with the packing placed inside the tower are mistakenly called counter-flow because the flow of circulating water in the packing is in the opposite direction to the flow of the air in them. In fact these cooling towers are mixed constructions because in the space between the pond and the packing the incoming flow of air is entering the tower at the right angle to the streams of water falling from the packing. To improve the intensity of the process of heat and mass exchange in the cooling towers with external transfer it has been proposed the packing consisted of shields arranged around the tower at an angle to the radius to the tower base which direct the flow of incoming air [10]. This construction of the packing increases the air path length, and consequently, the time of the contact of the cold air and warm water which increases the heat transfer intensity.

## 3. Mathematical model of the physical processes in cooling towers with internal and external heat and mass transfer

To compare the effectiveness of the cooling capacity of natural drought towers with internal and external heat and mass transfer there has been used a mathematical model describing physical processes of evaporation and contact heat transfer between air flow and water vapor-air mixture. As an object of the model there have been chosen two natural drought towers with the packing inside and outside the tower and air directing shields with vertical axis of rotation placed between supporting legs of the tower h. Mathematical model of flows in the cooling towers represents a boundary problem for the system of ordinary differential equations describing the heat and mass transfer between phase states of the air-water-vapor in the process of the aerodynamic and hydrodynamic interactions of heat carriers. The differential equations of conservation of mass and energy for contacting flows and equations of heat-mass transfer between phases are included in the heat transfer part of the mathematical model [11].

$$\frac{dG_w(x_3)}{dx_3} = -\gamma B \cdot \left[\rho_s(x_3) - \rho_v(x_3)\right]$$

$$\frac{dG_v(x_3)}{dx_3} = \gamma B \cdot \left[\rho_s(x_3) - \rho_v(x_3)\right]$$

$$\frac{d}{dx_3} J_a(x_3) = \alpha b \cdot \left[T_w(x_3) - T_a(x_3)\right]$$

$$\frac{d}{dx_3}\overset{\text{\textbardbl}}{J}_v(x_3) = -b \cdot \begin{Bmatrix} \alpha \cdot [T_w(x_3) - T_a(x_3)] \\ -r \cdot \gamma \cdot [\rho_s(x_3) - \rho_v(x_3)] \end{Bmatrix}$$

where T – temperature, (°C); $\rho$ - density, (kg/m³); J - specific enthalpy (heat content), (kcal/ kg); Q is mass flow rate (kg/s); b - the height of the sprinkler, (m); B - width of the sprinkler, (m); r - latent heat of vaporization, (kJ/kg); $\alpha$ - heat transfer coefficient, (Wt/(m² °C)); $\gamma$ - mass transfer coefficient, (kg/(m³/s)). Indices: a - air; s - saturated; v - vapor; w - water; coordinate system $Ox_1$, $Ox_2$, $Ox_3$.

Aerodynamics and contact heat transfer in the model of the cooling tower are presented by a system of equations of motion, continuity, thermal conductivity and the equation of the state.

$$\frac{\partial \overset{\shortmid}{U}_a}{\partial t} + (\vec{U}_a \nabla)\vec{U}_a = -\frac{1}{\rho_a}\nabla p_a + \nu \Delta \vec{U}_a + g\vec{k} - 2\left[\vec{\Omega}_a \times \vec{U}_a\right],$$

$$\frac{\partial \rho_a}{\partial t} + \text{div}(\rho_a \vec{U}_a) = 0,$$

$$\frac{\partial T_a}{\partial t} + (\vec{U}_a \nabla)T_a = \kappa \Delta T_a,$$

$$\rho_a = \rho_a(T_a)$$

Here $\overset{\shortmid}{U}$ - velocity vector, m/s; T - temperature, °C; p pressure, Pa; $\rho$ - density, kg /m³; g - acceleration due to gravity, m/s²; t - time s; $\nu$ and $\kappa$ - respectively, viscosity and thermal conductivity, m² /s; $\overset{\shortmid}{\Omega}$ - vector angular velocity, s⁻¹.

The boundary conditions for the system of equations are presented in the following form:

* At the entrance of the tower they are : set outdoor temperature $T_{1a}$, its humidity $\varphi$ and pressure- $P_a$ , heat flow $-C_a\rho_a\lambda_a\frac{\partial T_a}{\partial x_3} = Q(x_2)$, air enthalpy $J_{a1}$, the velocity of incoming flows into the tower $U_1 = U_1^{in}$, $U_2 = U_2^{in}$, air consumption- $G_a$ , twist of flow $\Omega = (U^{in}/R)\sin\chi$ with the angle of entrance $\chi$, measured between directions of shields and direction of the radius of the tower base;

* For the upper part of the packing conditions are: the initial flow rate $G_w$ , water temperature $T_{1w}$ enthalpy of steam $J_{a1}$ initial water temperature.

Implementation of mathematical models of the cooling tower was made in Matlab mathematical package.

## Discussion

To compare the effectiveness of two types of natural drought towers with internal and external heat transfer there has been used the thermal coefficient of cooling capacity of the cooling tower.

$$\eta = \frac{T_{1w} - T_{2w}}{T_{1w} - \tau}$$

Where $T_{1w}$ - the temperature of water entering the tower; $T_{2w}$ - water outlet temperature; $\tau$ -wet - bulb temperature. In the analysis of the thermal efficiency of coolers the dependence of the thermal efficiency $\eta$ on the relative mass flow of air $Q_a$ and water flow $Q_w$.
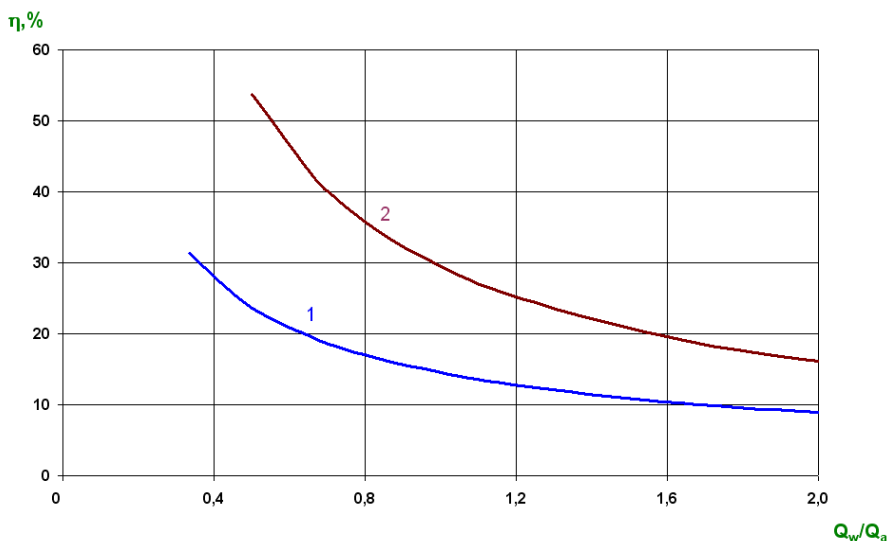


Fig. 3. Thermal efficiency of the use of low-grade heat in cooling towers with an inner (1) and external deployment (2) of the packing depending on the ratio of the intensity of water $Q_w$ and $Q_a$ of air flows.

To discuss the influence of heat and mass transfer and aerodynamics and hydrodynamics on the efficiency of the use of low-grade heat in two types of natural drought towers with internal and external disposition of the packing here are presented the results of numerical model calculations of the thermal coefficient of efficiency at different relative consumptions of air and water flows. The calculations were carried out for the same standard conditions of the work of cooling

towers: at a flow rate of water supplied to the cooling tower water distribution system - $Q_w$ = 100m³/h; inlet water temperature $T_{w1}$, = 40 ° C; outdoor air temperature $T_a$ = 25 ° C; relative humidity of the air f = 50% and the mass air flow values within Qa = (30-400) m³/h, with variable angles of air directing shields $X$ in the range (10 ° ÷ 70 °) (see Fig.3).

The results of calculations illustrated in the Fig.3 show very clearly the advantage of using of the low-grade heat for cooling the circulating water in the natural drought towers with the external packing. In the cooling towers with internal heat transfer a noticeable increase of cooling capacity begins to appear only at a sufficiently high rate of air flow entering the tower. In conditions of high temperatures of the air close to the temperature of circulating water entering the tower it is possible to achieve a higher temperature difference of incoming and outgoing water in the cooling towers with external heat transfer than with internal heat transfer. This is clearly illustrated by the curves of the rate of increase of thermal efficiency depending on the change of the air flow entering the tower (Fig.4).
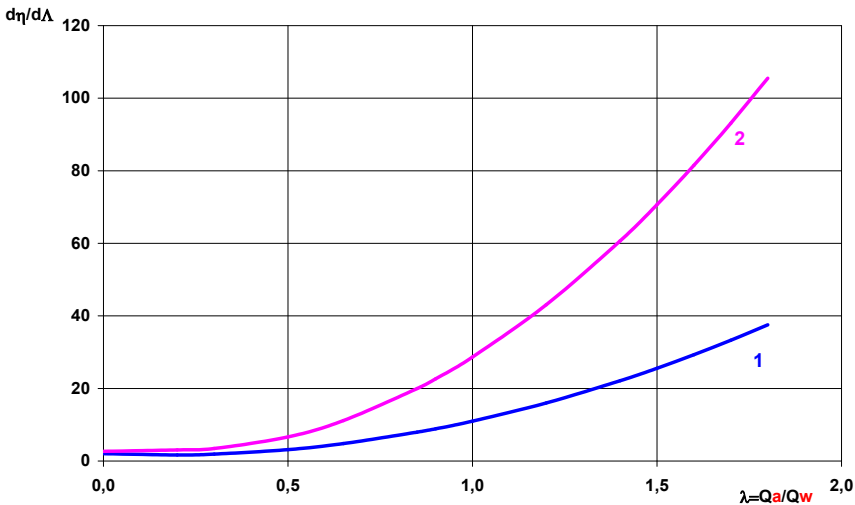


Fig. 4. The rate of increase of thermal efficiency $d\eta/d\Lambda$ ($\Lambda = Q_w/Q_a$) in the two cooling towers - with an inner (1) and outer (2) heat transfer when the relative flow configuration is changed.

It should be noted that under standard working conditions the relative rate of air and water flow is close to the $\Lambda$ = 1. The difference of values of thermal efficiencies of cooling towers with internal and external

heat transfer is 15%. For large heat engines of big atomic power stations such a level of cooling of turbine condensers corresponds to an increase in electric power generation in the range of 2-3 MW. It is essential that the difference of the rates of change of thermal efficiency of the value of decimal fraction of relative rates of thermal curriers in the two compared towers reaches a significant value of 17,7% (Fig.4 ).

# Conclusion

At present time a large percentage of world's electricity is produced by heat engines and regardless of used fuel there is a need to remove the heat that is a by-product of creating high pressure inside engines for making them work. In this process a low-grade heat is produced in large quantities. Thus atomic power plants create 2000MW of low-grade heat per 1000MW of produced electricity. Therefore it is very important to develop new methods to increase efficiency of existing ways of using low-grade heat for electricity production as well as to search new areas where these methods can be used. From presented description of natural drought towers with external heat transfer and results of modeling of processes of aerodynamic and hydrodynamic and heat-mass interaction of air and water flows it was established that the heat transfer outside the tower can be used to increase efficiency of electricity production and utilization of low-grade heat. Some of proposed above technical solutions have already been successfully implemented in production and now the task is to increase their use in existing power plants. Creating aerodynamic devices on the base of natural drought towers with external heat transfer should be the next step in the use of low-grade heat to generate electricity.

## Literature

1. Zakirov D.G. The use of low-grade heat  M .: Rusayns, 2015- 158 pp.
3.  Berman   L.D.   Evaporative   cooling   circulating   water.   M  .: Gosenergoizdat 1957.-440 pp.
2. Alhasov A.B. The development of low-grade geothermal heat. M.: Fizmatgiz,2012.-280 pp.

3. Renewable energy sources: terms and definitions /edited by A.A. Solovyev, N.A. Rustamov . M: Frantera, 2014.

4. Solovyev A.A. Vortice convettivo di energia solare // Italian Science Review, 2014, V. 6, N 15, P. 91-94.

5. Berman L.D. Evaporative cooling circulating water. M .: Gosenergoizdat 1957.- 440 pp.

6. Solovyev A.A., Nigmatulin R.I., Gusinskaya N.V. Malyx Y.B. Duct evaporative cooling tower with the agitation of the vortex flow // Rus. Patent № 2196947, 20.01.2003

7. Solovyev A.A., Aksyutin O.E., Nigmatulin R.I., Chekarev K.V., Malyx Y.B. Cooling tower with air adjustment devices // Rus. Patent № 2540127, 10.02.2015

8. Kazarov G.I. Report on the Technical Meeting on Advances in Non-Electric Applications of Nuclear Energy and Efficiency Improvement at Nuclear Power Plants .International Atomic Energy Agency. Oshava, Ontario, Canada, 6-8 Oct., 2014, Ref. No: 622-I3-TM-47233, P.7.

9. Tumpenny A et all Cooling water options for the new generation of nuclear power statinsin the UK / Report SC070015/SR3, Environment Agency, 2010, P.49-55.

10. Solovyev A.A., Chekarev K.V. Natural draught cooling tower with external heat transfer // Rus. Patent № 2527799, 09.10.2014

11. Dobreco K.V., Hemmasian-Kashani M.M., Lasko E.E. Simulation of cooling tower and influence of aerodynamic elements on its work under conditions of wind //Energy. Proceedings of higher educational institutions, 2014, № 6, P. 47-60.

12. Gelfand R.E, Sverdlin B.L., Tikhonov A.V. Thermal calculations of evaporative cooling towers and Merkel equation // Electric stations. 2012, №4.

# Series: **PHYSICS and ASTRONOMY**

**Tafur Perdomo Ivan Humberto**

# Peltier Efect Simplified Theory

In special circumstances it is possible to approximate an idealized model of the Peltier effect making some assumptions: the effect is characterized by the Peltier coefficient as the ratio of the electron energy to the density of current flow [3]:

$$DU / dJ = \prod \qquad (1)$$

The latter formula can serve as a basis for further study of the phenomenon. This way, assuming that the energy flux density can be expressed in the form:

$$U = W .v \qquad (2)$$

It is the energy density and v is the phase velocity of the wave (electrons or phonons). In turn, W is the energy density, the product of the average energy of the particles Ee. the concentration of said particles n [2]:

$$We = Ee. n \qquad (3)$$

The scattering probability of an electron in the unit time is given by:

$$1/\tau = \sigma N v \qquad (4)$$

effective scattering cross-section ($\sigma$). And N concentration of the scattering centers = number of scattering centers in the unit volume.
In the case of phonons (number of normal oscillations in a cubic lattice) for

$$kT \gg h.\nu$$

Because the electron under the influence of an electric field travels in a straight line is always possible to assume, with great generality that is dispersed in a one-dimensional lattice in the network, entirely classical, each standing wave corresponds to a power

$$W = k T r,$$

where

$$r = k T / h. \nu$$

represents an integer, which in turn symbolizes the "tone" that is subject to the respective standing wave. On average

$$W = Ef. r = Wp, \qquad (5)$$

$$\nu. \lambda = c,$$

$^{\gamma}$ - it corresponds to the maximum wavelength, (minimum energy) that can be taken as a basis for the ground state,

$\lambda = L/2$ length or period of the network.

After replacing it obtains

$$U/J = k \, T \, Ee \, /e \, Ef \qquad (6)$$

In the metal, because the most likely level of electron energy is in the same valence band, can be assumed that the energy (electron) is in equilibrium with the crystal lattice

$$Ee. \, r = Wp$$

(average) and as

$$U / J = \alpha \, T, \, \alpha = k / e$$

In the own semiconductor with spherical iso-energy surfaces

$$Ee = h2 \, k2 \, / \, 2m$$

is equal to the difference between the energy of the electrons in the conduction band and the most likely level of energy of the electrons at the given temperature [1]:

$$(Fermi \, level) = Ec\text{-}Ef.$$

It follows, that

$$U \, /J = k \, r \, (Ec\text{-}Ef.)/e \, Wp$$

and finally

$$\alpha = k/e \, ( \, Ec\text{-}Ef.)/ \, Ef. \qquad (7)$$

# References

1. Shalimova, K.V. Semiconductors Physics", Energoatomizdat, 1985.
2. Frenkel, Y.I. "Introduction to the Metal Theory, GTTA, Leningrad, 1950.
3. Ioffe, A.F. Semiconductor Thermoelements, AN USSR, 1960
4. Haywang, W. "Amorphe und plicristaline Halbleiter", Springer – Verlag, 1984.

# Authors

**Chekarev Konstantin V**., *Russia.*
kostya-chekarev@yandex.ru
tel.:+ 79031814331
He graduated from Physical Faculty, Lomonosov Moscow University, Researcher Department of Renewable Sources Energy, Geographical Faculty, Lomonosov Moscow University. The author of a number of patents, inventions and articles about renewable energy, condensation physics, cooling machines.

**Etkin, Valery A.***, Israel.*
v_a_etkin@bezeqint.net
Professor, Dr. Techn. Sc., Member of Internat. Acad. of Creativity (1995); Int. Acad. Bioenerg. Technol. (2002) and Europ. Acad. of Natur. Sc. (2009); ex-head of the Department of Heat Engineering and Hydraulics at Togliatty State University (RF).
Author more than 300 original articles and 10 books including the monograph "Thermokinetics" (1999) issued after the doctoral thesis and recommended by the Ministry of Education of the Russian Federation for a study guide at technical universities and republished in English (2010), as well as the monograph "Energodynamics" (2008), issudednded under the sponsorship of the Russian Fund of Fundamental Investigations and awarded Leibnitz medal by the European Academy of Natural Sciences. Chief director of «Integrative Research Institute» (IRI). Leader of Israel association «Energo-informatics». «The person of year» (Haifa, 2010).

**Khmelnik Solomon I.**, *Israel.*
solik@netvision.net.il
Ph.D. in technical sciences. Author of about 300 patents, inventions, articles, books. Scientific interests – electrical engineering, power engineering, mathematics, computers.

**Kojamanyan Ruben G.,** *Russia.*
kojamanyan@yandex.ru, farn79@rambler.ru
Was born in 1955 in Abkhazia in the village of Pitsunda. He graduated from the Yerevan State Medical Institute. I was interested in physics from the very childhood. Interests: theoretical physics, politics, chess.

**Leshinsky-Altshuller Anya**, *Israel.*
M.Sc. in Kibernetics,
M.Sc. in Chemical Engineering.
Professional activity: Application Development Engineer in KLA-Tencor, Israel. Also worked in the field of mechanical control systems engineering.

**Shatov Vladimir V**., *Russia.*
vladimir@shatov.org
In 1986 had graduated from the theoretical section of the chemical department of Leningrad State University (currently SPSU). Had spent ~ 40 years in chemistry researches. Had been developing methods of caring out measurements: mass spectroscopy, optic and X-ray spectrometry, X-ray structural analysis, physical methods, electrochemistry, "wet chemistry". Hobby – fundamental science ~40 years
Website: www.shatov.org;

**Solovyev Alexander A.**, *Russia.*
geosolmgu@mail.ru
tel.:+79855249084
Professor, Dr. Phys - Matem. Sci.,
Member Acad. of Natur. Sci.( 2003)
Associate Professor, Department of Molecular Physics, Physical Faculty (1968- 1987) Lomonosov Moscow University.
Head Department of Renewable Sources Energy, Geographical Faculty, Lomonosov Moscow University (with 1987-date).
Author more than 150 original articles and 10 books including the monograph: A New Look at the Problem.

**Solovyev Dmitry A.**, *Russia.*
solovev@guies.ru
tel.:+79855249084
He graduated from Physical Faculty, Lomonosov Moscow University, Researcher Sea-Air Interaction and Climate Laboratory (SAIL) Shirshov Institute of Oceanology, Russian Academy of Sciences and Department of distributed energy systems of Joint Institute for High Temperatures, Russian Academy of Sciences. The author of a number of articles focused on the ocean's role in climate variability and change, ocean's renewable energy, Geophysics & technological problem of the Energy sector.

**Sherbaum Valery,** *Israel.*
valerys@technion.ac.il
M. Sc. in Mechanical Engineering,
PhD in Jet Propulsion.
Aerothermodynamics, non-stationary laminar and
turbulent flows, gas turbines cycles.
Since 1989 – till present time: Research
Consultant, Research Engineer. Technion,
Faculty of Aerospace Engineering. Israel Institute
of Technology.

**Tafur Perdomo Ivan Humberto,** *Colombia.*
ivansladki61@mail.ru
REGISTERED WORKS:
1- "What is the problem" (guidelines for the
development of mathematical ability. Neiva, 2001
particular edition).
2- "Investigations in Physics and Mathematics".
Neiva, 2005
3- "International system of units" Neiva, 2000 Series
of the synthesis and resolution of problems in
Physics

**Triger Vitaly,** *Israel.*
vitalytriger@gmail.com
Free Lancer (Electronics, Robotics, Applied
problems of physics)